AB

USAAVLABS TECHNICAL REPORT 69-4

EMULSIFIED FUELS COMBUSTION STUDY

By
T. R. Koblish
R. A. Roberts
H. R. Schwartz
R. D. Gordon
E. A. Ault

February 1969

U. S. ARMY AVIATION MATERIEL LABORATORIES
FORT EUSTIS, VIRGINIA

CONTRACT DAAJO2-67-C-0094
PRATT & WHITNEY AIRCRAFT
DIVISION OF UNITED AIRCRAFT CORPORATION
EAST HARTFORD, CONNECTICUT

141

DISCLAIMERS

The findings in this report are not to be construed as an official Department of the Army position unless so designated by other authorized documents.

When Government drawings, specifications, or other data are used for any purpose other than in connection with a definitely related Government procurement operation, the United States Government thereby incurs no responsibility nor any obligation whatsoever; and the fact that the Government may have formulated, furnished, or in any way supplied the said drawings, specifications, or other data is not to be regarded by implication or otherwise as in any manner licensing the holder or any other person or corporation, or conveying any rights or permission, to manufacture, use, or sell any patented invention that may in any way be related thereto.

DISPOSITION INSTRUCTIONS

Destroy this report when no longer needed. Do not return it to the originator.

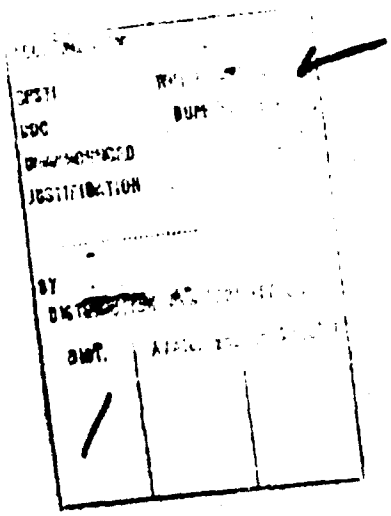

DEPARTMENT OF THE ARMY
U S ARMY AVIATION MATERIEL LABORATORIES
FORT EUSTIS VIRGINIA 23604

This report was prepared by Pratt and Whitney Aircraft Div'sion of United Aircraft Corporation under the terms of Contract DAAJ-02-67-C-0094.

Work under the contract involved a determination of the differences between JP-4 liquid fuel and three Government-supplied emulsified fuels from the standpoint of cold flow, corrosion, and combustion characteristics in a typical turbine engine can-type combustor.

The effect that emulsified fuels produced on six different materials normally used in turbine blade construction was investigated in approximately 600 hours of combustor running at exit temperatures of 1700°F and 2000°F.

The test procedures followed during the conduct of the program and a detailed evaluation of the results obtained are presented in this report.

The conclusions and recommendations made by the contractor are concurred in by this Command. However, this concurrence is based solely on the results obtained with the particular fuels tested and does not imply the acceptance of similar findings with optimized emulsion formulas.

Task 1F162203A15003
Contract DAAJ02-67-C-0094
USAAVLABS Technical Report 69-4
February 1969

EMULSIFIED FUELS COMBUSTION STUDY

Final Report

PWA-3515

By
T. R. Koblish
R. A. Roberts
H. R. Schwartz
R. D. Gordon
E. A. Ault

Prepared by

Pratt & Whitney Aircraft
Division of United Aircraft Corporation
East Hartford, Connecticut

for

U. S. ARMY AVIATION MATERIEL LABORATORIES
FORT EUSTIS, VIRGINIA

SUMMARY

This report describes a research program conducted to determine the cold flow, combustion, and corrosion characteristics of three different Government selected and supplied emulsified JP-4 fuels and to compare them to liquid JP-4 fuel. The program consisted of a study of the emulsified fuel flow and spray characteristics, and an evaluation of the combustion and altitude relight capabilities of emulsified fuels relative to JP-4 fuel using a can-type burner rig that simulates a gas turbine environment. The corrosion characteristics of the emulsified fuels were evaluated relative to liquid JP-4 on several coated and uncoated turbine materials when operating at 1700°F and 2000°F average combustor exit temperatures.

The cold flow test results show that, except for individual deviations due to formulation differences, the flow behavior of two out of the three emulsified fuels through fuel nozzles, lines, and pump of a gas turbine fuel system is nearly identical to the flow of liquid JP-4 fuel. Considerable breakdown of the emulsion occurred as it passed through the gear fuel pump. The degree of breakdown was found to be a function of the pressure rise across the pump as well as emulsified fuel formulation. The spray characteristics of these emulsified fuels flowing through a pressure atomizing fuel nozzle were found to be essentially identical to those of liquid JP-4.

Laboratory testing indicated that the net heat of combustion of the emulsified fuels consistently, except in one instance, fell short of the JP-4 minimum specification value of 18,400 Btu/lb.

The results indicated that only minor differences in combustor performance with respect to combustion efficiency, flame length, or exit gas temperature pattern exist between JP-4 and emulsified fuel under the steady-state conditions tested. The same was found to be true for light-off, transient, and altitude relight conditions. The steady-state corrosion tests have shown that some slight vane surface distress and corrosion were caused by two of the emulsified fuels, whereas the third emulsified fuel caused severe distress.

Although the combustion characteristics of the emulsified fuels are nearly identical to JP-4, it is recognized that additional work on the fuel system to prevent nozzle screen plugging must be done before the emulsified fuel can be effectively utilized in a conventional gas turbine.

Of the three emulsified formulations tested, it is concluded that emulsified fuel A shows superior overall performance relative to the other emulsified fuels.

FOREWORD

This report describes the results of an investigation to determine the combustion characteristics and hot corrosion problems associated with three emulsified fuels compared to liquid JP-4 fuel. This investigation was conducted by Pratt & Whitney Aircraft under the terms of United States Army Aviation Materiel Laboratories, Fort Eustis, Virginia, Contract DAAJ02-67-C-0094 (Task 1F162203A15003). The work was performed during the period 29 June 1967 through 28 September 1968.

TABLE OF CONTENTS

LIST OF ILLUSTRATIONS

LIST OF TABLES

LIST OF SYMBOLS

DAB	Para-dimethylaminobenzaldehyde
ΔT	Temperature rise, ^{o}F
ΔTVR	Temperature-rise variation ratio ($T_{max} - T_{in}/T_{exit} - T_{in}$)
f/a	Fuel air ratio
K	Specific heat ratio
I.D.	Inside diameter, in.
LBO	Lean blowout
MBTH	3-methyl-2-benzathiozolene hydrazone hydrochloride
NEDA	N-(1-naphthyl)-ethylenediamine dihydrochloride
O.D.	Outside diameter, in.
P_s	Static pressure
P_t	Total pressure
T_{exit}	Average burner exit temperature, ^{o}F
SMD	Sauter mean diameter
T_{in}	Average burner inlet temperature, ^{o}F
T_{max}	Maximum burner exit temperature, ^{o}F
W_a	Weight of airflow, lb/hr.
W_f	Weight of fuel flow, lb/hr.

INTRODUCTION

Several practical means of emulsifying JP-4 fuel have been developed by industry. In the emulsified state JP-4 fuel is more easily contained, and if ignited, the flames propagate at a much slower rate than liquid JP-4 fuel. These characteristics of emulsified JP-4 fuel reduce the threat of fire from accidental causes as well as minimize the danger of posterash fire in survivable type aircraft crashes. Although the feasibility of burning emulsified JP-4 fuel has already been successfully demonstrated in a number of gas turbine engines, it has become increasingly desirable to investigate, in more detail, the combustion characteristics and the corrosive properties of the emulsified fuels relative to JP-4 fuel. An experimental program to accomplish the aforementioned investigation was established first to evaluate the performance of two types of fuel injection systems operating with three different emulsified JP-4 fuel formulations (identified herein as fuel A, fuel B, and fuel C) under cold flow conditions and then to evaluate the combustion performance of emulsified JP-4 fuels in a rig typical of a gas turbine burner section. The object of the cold flow tests was to determine the flow behavior and spray characteristics of the emulsified fuels relative to JP-4 fuel. These tests were conducted with both a pressure atomizing and an air-assist fuel nozzle system. In addition, certain laboratory inspections were conducted on the emulsified fuels to determine the fuels' physical properties in order to insure uniformity.

The combustion experiments were conducted in a 5.3-inch-diameter can-type combustor consistent with existing turbine engine design and equipped with suitable instrumentation to determine such combustion characteristics as the following:

1. Relative combustion efficiencies
2. Exit gas temperature patterns
3. Radiant energy level measurements to investigate the possibility that emulsions may require greater combustion length
4. Light-off, transient, and steady-state characteristics
5. Lean and rich blowout limits
6. Gas analysis of combustion products to determine if there are unusual or undesirable combustion products.
7. Altitude relight capability

Upon completion of this portion of the program, the best qualified fuel injector system and emulsified fuel combination was selected to determine the hot corrosion problems which may be associated with emulsified JP-4 fuels. Since the composition of the emulsified fuels was proprietary, their combustion products could not be predicted and their reaction with turbine materials at elevated temperatures could not be anticipated. In the second half of the experimental program, six typical gas turbine materials were exposed to the combustion products of these fuels.

Six hundred hours of material testing was conducted, divided equally between the three emulsified JP-4 fuels and the liquid JP-4 fuel. The combustor was run at an average exit temperature of 1700°F for half of the test hours and at an average exit temperature of 2000°F for half of the test hours. Thus, a complete test consisted of 150 hours of combustor operation with each fuel: 75 hours at 1700°F exit temperature, and 75 hours at 2000°F exit temperature.

The test materials/combustor location relationship was consistent with current engine design practices. The test materials were fabricated in a simulated airfoil shape and were located to provide choked flow at approximately the 80 percent position along the chord of the vane. After testing, the test materials were thoroughly analyzed using standard metallurgical techniques to determine qualitatively (and quantitatively to the extent possible) the existence of any oxidation, sulfidation, or other obvious effects which could be considered detrimental to normal engine operation.

COLD FLOW TEST APPARATUS AND PROCEDURE

Cold Flow Test Apparatus

The schematic diagram in Figure 1 shows the pumping and distribution system used to evaluate the cold flow characteristics of the emulsified fuels and the JP-4 reference fuel. Fuel was pumped and pressures were controlled using a gear pump driven by a variable-speed air-operated motor. A 200-mesh stainless-steel screen filtered the fuel prior to its passage through needle valves which controlled the flow split between primary and secondary nozzle passages. Pressures were measured with bourdon-tube gages. Two types of fuel nozzles were run during the program. One was the standard JT12 engine part, a pressure atomizing dual-orifice nozzle with concentric primary and secondary orifices (Figure 2). The other was a special air-assist nozzle designed and built for this project (Figure 3). It was designed to match the outer envelope dimensions as well as the fuel flow schedule of the standard JT12 engine part.

In the air-assist nozzle, all the fuel passes through the central orifice only. The area of this orifice is relatively large (compared to the dual-orifice fuel nozzle) so that at low fuel flow the fuel pressure drop across the orifice is small, thereby necessitating air-assist for effective fuel atomization.

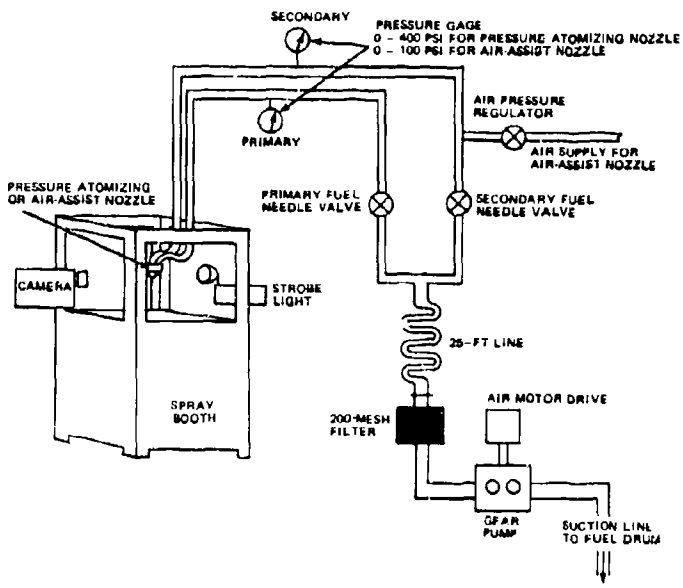

Figure 1. Cold Flow Testing Apparatus.

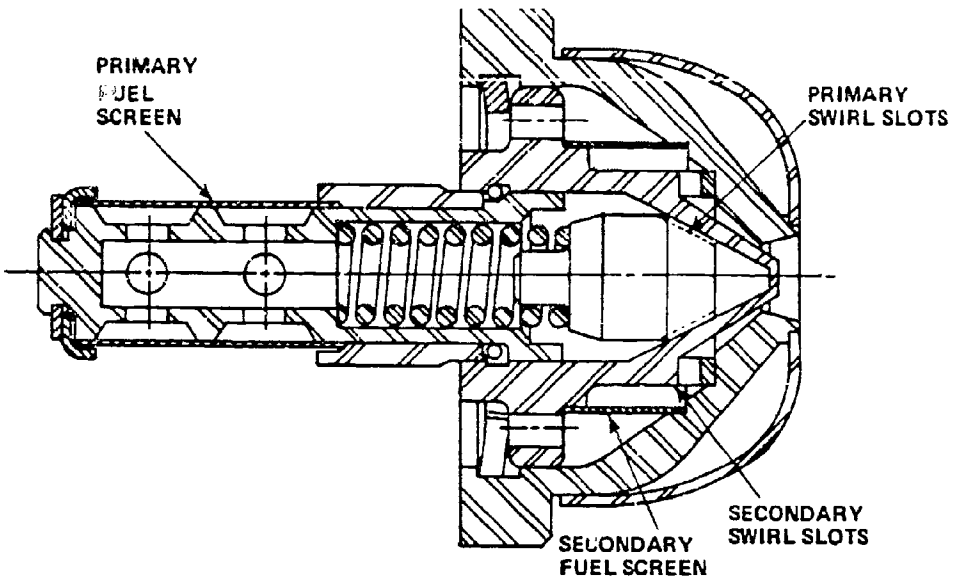

Figure 2. Cross Section of Pressure Atomizing Nozzle.

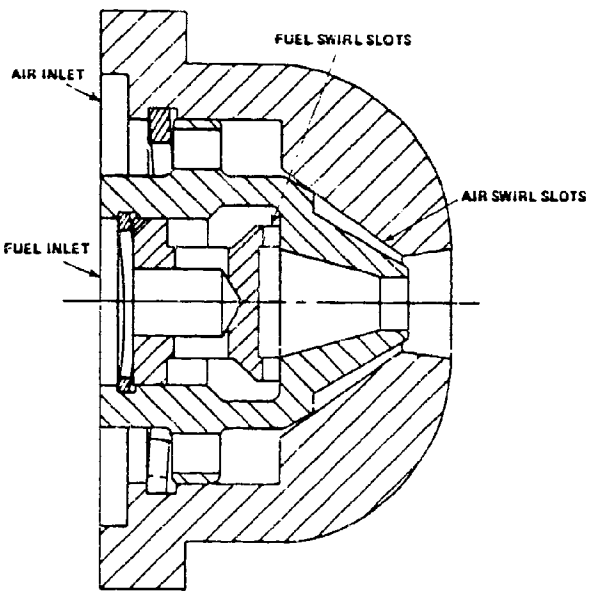

Figure 3. Cross Section of Air-Assist Nozzle.

Cold Flow Test Procedure

Emulsion Breakdown

The procedure followed for the emulsion breakdown tests was as follows: with the primary valve fully open and the secondary valve shut, the gear pump was driven at sufficient speed to produce the desired primary fuel pressure and flow. When running emulsion breakdown tests with the air-assist nozzle, air was supplied at 7.2 psi (2.0 cfm) under all fuel flow conditions, as recommended by the manufacturer.

For points with secondary flow, the secondary valve was opened sufficiently to obtain the desired pressure while pump speed adjustments were made as necessary to maintain primary pressure. After the designed steady-state conditions were achieved, a 1-liter glass graduate was placed directly under the nozzle discharge and removed when filled. After several minutes, the emulsion and liquid phases separated sufficiently to permit visual measurement of the volumes of each phase, i.e., the percentage of emulsion breakdown produced by the fuel transfer system and nozzle. To determine the emulsion breakdown existing before the fuel passed through the nozzle, the pump (with fuel pressure at steady-state conditions) was quickly stopped. The 25-foot line downstream of the filter was disconnected at both ends and held to drain into the graduate. The emulsion breakdown was then visually determined as before. The volume of fuel occupying the 25-foot line was previously measured for comparison.

Fuel Flow/Nozzle Pressure Drop

A volume-time method for measuring fuel flow was used to check out both nozzles. After steady-state conditions were established as outlined above, a 1-liter graduate was quickly placed under the nozzle discharge while a stop watch was started at the same instant. When nearly full, the graduate was removed and the stop watch was stopped at the same time. Three trials were made at each test point. Density determinations were made on each of the fuels collected in the graduate for conversion of data to mass flow rate.

Spray Cone Photography

Spray cone photographs were taken as required at steady-state flow conditions. Fuel was sprayed vertically from nozzles mounted near the top of the spray booth. The camera was aimed through one window, with synchronized strobe flash units aimed through both side windows.

Droplet Size Distribution

Photomicrographs of the fuel sprays were made with a 35mm stop-motion movie camera aimed through a hole in one window of the spray booth. The camera exposures were made at a rate of one frame per second. The camera was synchronized to a strobe unit which was set for a 0.8-microsecond flash duration and positioned behind the opposite window. Before the spray was started, a 2.0-mil-diameter wire was suspended in the spray cone area approximately 3 inches downstream from the orifice and 1 inch

in front of the cone axis. The camera was then positioned and focused on the wire. Several frames of the suspended wire were shot with no fuel spray. These frames provided a reference in the focal plane of the droplets for the subsequent spray pictures. After these frames were exposed, the reference wire was removed without disturbing the rest of the apparatus.

After the initial reference frames had been exposed as described above, the fuel system was started and brought to the desired steady-state condition. Approximately 70 frames were taken of the spray for each fuel and pressure condition. For analysis of the developed film, a frame with a view of the reference wire was projected through a strip projector onto a movie screen. The projector was then moved forward or backward to a position where, when focused, the image of the reference wire on the screen measured exactly 0.250 inch. This provided a precise magnification of 125X. All of the spray droplet frames were then projected, and the diameters of all sharply focused droplets were measured with a scale.

Laboratory Inspection

Upon receipt of the emulsified fuels at Pratt & Whitney Aircraft, each batch was submitted to the materials laboratory for a determination of the following four properties:

1. Yield value – dynes/cm^2
2. Net heat of combustion – Btu/lb
3. Specific gravity at 60°F/60°F
4. Water content weight percent

The yield value of the fuels was measured using a cone penetrometer as described in ASTM Method D217-65T. The initial cone used was a lightweight 15-gram cone attached to a 45-gram shaft. A lightweight shaft (22 grams) arrived in time to measure penetration before the end of the test period. Following the outlined ASTM procedure, the penetration was measured directly in tenths of a millimeter. This figure was then converted to yield value in dynes/cm^2 by use of equations developed at the U.S. Army Fuels and Lubricants Research Laboratory. (Ref. letter progress report for month of August 1967 from U.S. Army Fuels and Lubricants Research Laboratory to USAAVLABS, Fort Eustis, Virginia.)

The net heat of combustion was measured in a Parr Adiabatic Calorimeter following the procedure described in ASTM Method D2382-65.

The specific gravity was measured in a laboratory weighing bottle standardized with distilled water.

The water content of Emulsions A and C was measured by the Karl Fischer Reagent method described in ASTM D-1744. The use of absolute methyl alcohol/chloroform solvent as described in the procedure broke down the emulsion, making analysis of the emulsified fuel no more difficult to perform than that of liquid fuels

Due to the presence of interfering compounds, namely, formamide and urea, in emulsified fuel B, ASTM D-1744 was not applicable to the fuel. In order to determine the water content of this fuel, an alternate course was selected which appears to give satisfactory and repeatable results. The method is outlined below.

The fuel and water were separated by following the procedure outlined in ASTM Method 095-62.

The "aqueous" layer condensed in the trap was then analyzed chromatographically to determine what volume percent of the layer was water. This figure was then converted to weight percent of the whole fuel.

The chromatograph used in this procedure operated under the following conditions:

1. Helium carrier gas - 40 cc/min
2. Poropak Q column
3. Filament current - 180 ma
4. Temperature
    a. Column - 130°C
    b. Detector - 100°C
    c. Injection port - 200°C

COMBUSTION TEST APPARATUS AND PROCEDURE

Combustion Test Apparatus

Test Stand

Figure 4 is an overall plan view and Figure 5 is a side view of the JT12 burner rig installation in a Pratt & Whitney Aircraft burner rig test stand. Figures 6 and 7 show two additional views of the test installation. Combustion air was supplied from an engine-driven turboblower at an adjacent facility. The air was heated by an automatically controlled gas-fired heat exchanger on the roof of the burner test stand. Airflow rate and rig pressure were controlled by manipulation of butterfly valves located fore and aft of the test rig. Both valves were operated from the control panel.

JP-4 from a remote storage area was piped through a filter into a bypass controlled constant-speed gear pump to feed the burner rig. Flow of the JP-4 was metered and controlled by the test operator. The operator also monitored and controlled water and high-pressure air for cooling any rig, stand, or instrumentation hardware where cooling was required. He also controlled N_2 purge gas for the fuel nozzle and manifold.

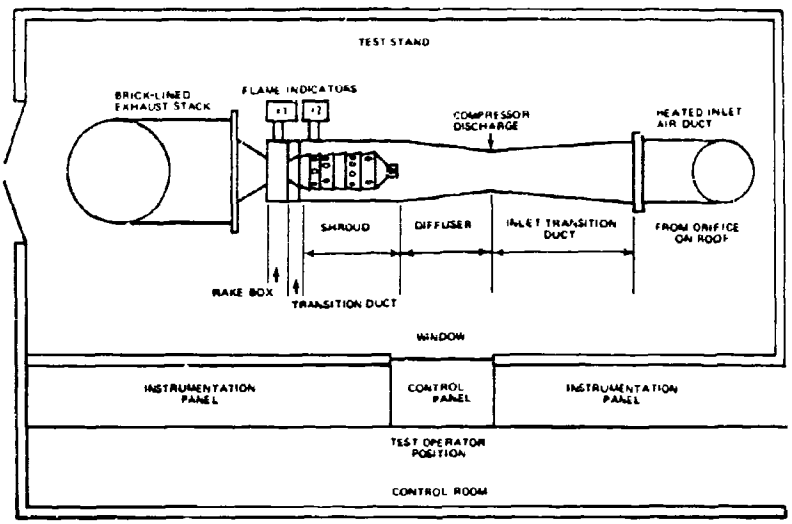

Figure 4. Plan View of JT12 Burner Rig in Test Stand.

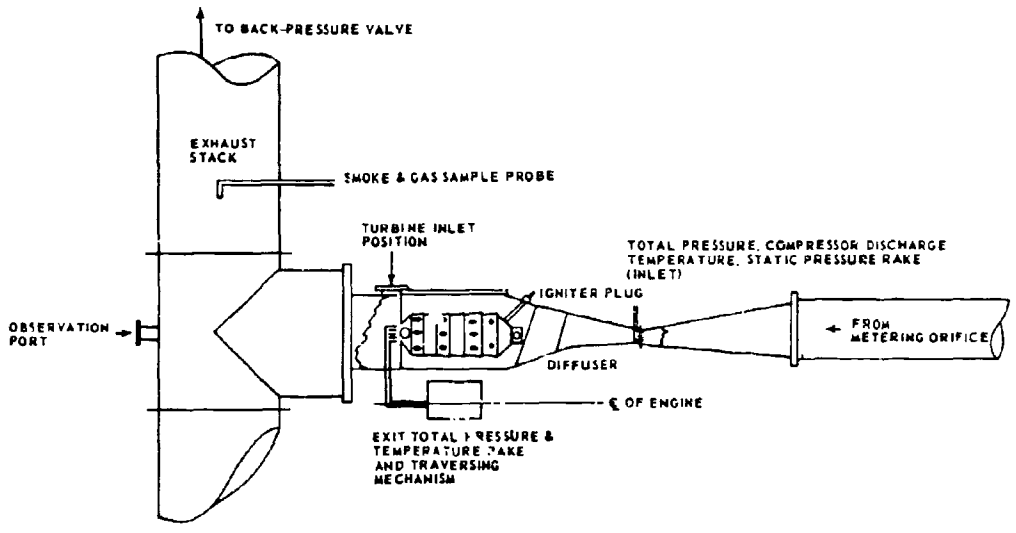

Figure 5. Side View of JT12 Burner Rig in Test Stand.

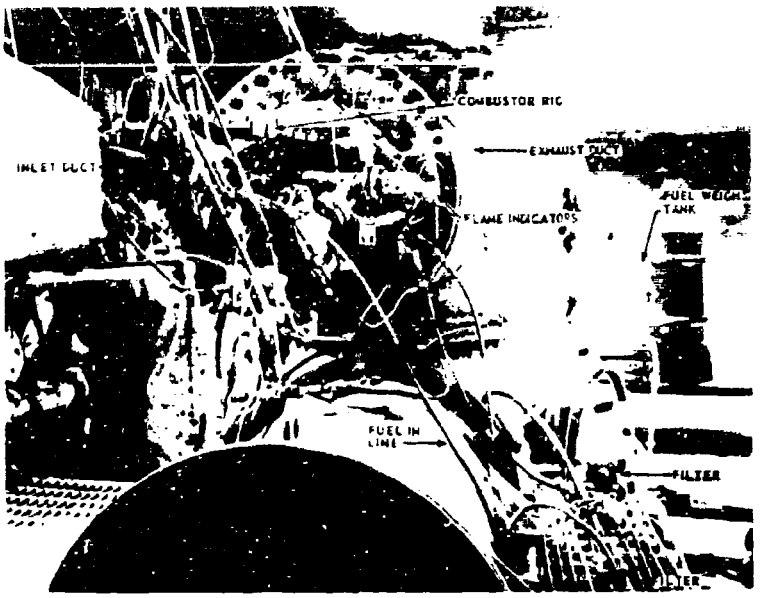

Figure 6. Combustor Rig Installed in Test Stand With Instrumentation.

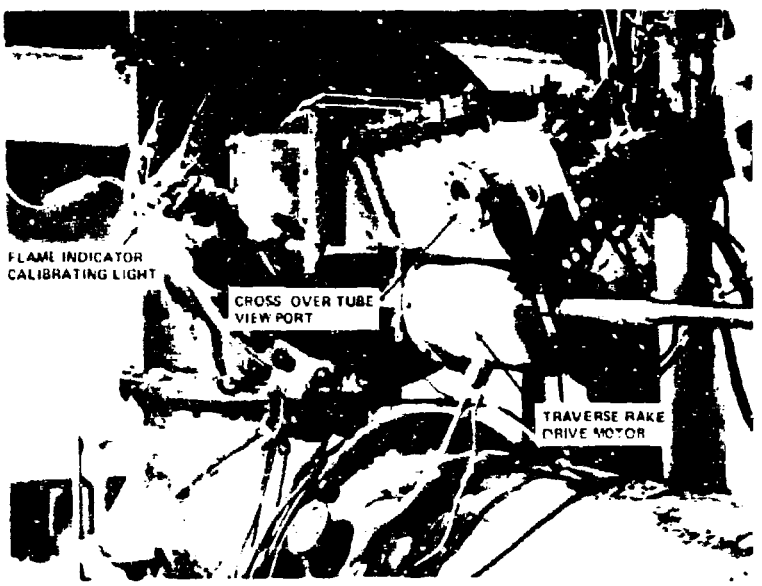

Figure 7. Close-up View of Combustor Rig Installation Showing Traverse Rake Drive Motor.

Burner Rig and Hardware

The burner rig (Figures 4 and 5) was a 1/8 segment full-scale model of the hot section of a JT12 engine. It was the type of rig generally used in can-annular main combustor development since, for one burner can, it provides the best simulation of engine flow passage geometry from the compressor discharge to the turbine inlet. The combustor (Figure 8) was a standard burner can (5.3-inch diameter) of the type used in the current JT12A-8 engine model. The can was supported at the rear by a 1/8 segment exhaust transition duct cut from a standard JT12 engine part. The front was supported by a modified 1/8 segment cut from a standard JT12 engine fuel nozzle manifold assembly. The nozzle manifold segment was modified during initial rig preparation to include a metal heat shield suspended around the concentric fuel transfer tubes leading from the rig wall to the nozzle socket. The intent was to protect the primary fuel circuit (outer concentric tube) from impinging gases, since the 800°F inlet temperature specified for part of the test program was considerably higher than actual engine operating temperatures. Nozzles tested included the standard JT12 pressure atomizing dual-orifice nozzle and the air-assist nozzle previously described.

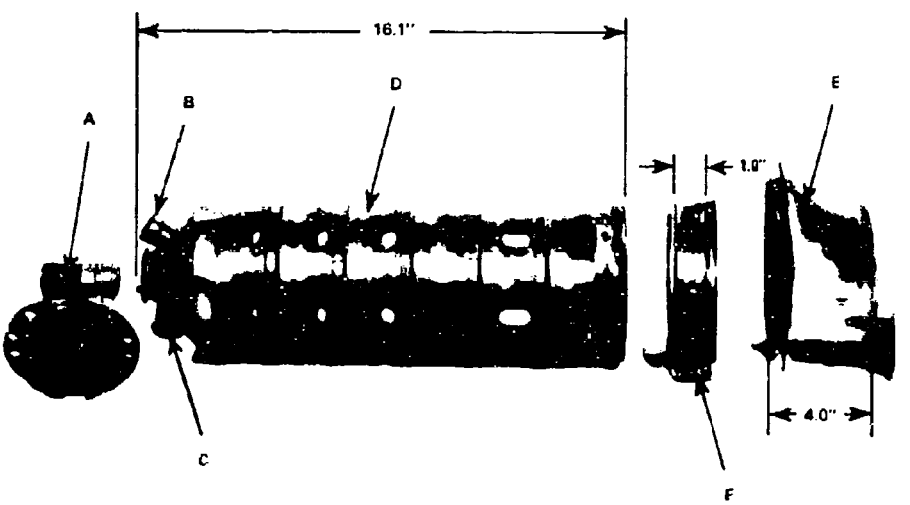

Figure 8. Exploded View of Combustor System Used for Emulsified Fuel Combustion Tests Showing A. Fuel Nozzle and Manifold, B. Ignitor Boss, C. Blanked Off Cross-over Tube, D. JT12 Burner Can, E. Transition Duct, and F. Burner-transition Clamp.

Fuel System

The schematic diagram in Figure 9 shows the basic fuel system used for most of the combustion testing. A rubber-vane-type barrel pump mounted on a 55-gallon emulsified fuel supply drum facilitated the transfer of fuel into a 30-gallon weighing tank. This tank rested on the platform of a 75-pound dial scale, which in turn rested on a table suspending the scale and tank 4 feet from the ground. The fuel drum, scale, and weighing tank were just outside the test stand, as shown in Figure 10.

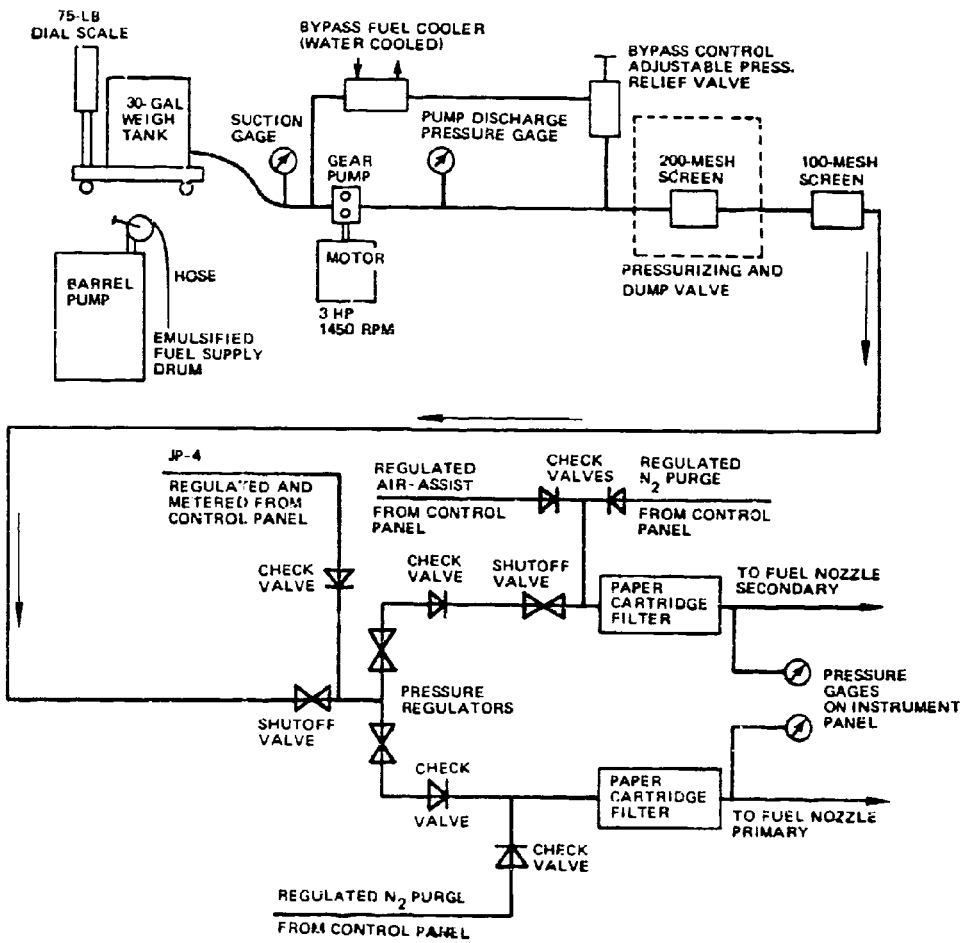

Figure 9. Schematic of Fuel Supply System for Burner Rig Testing.

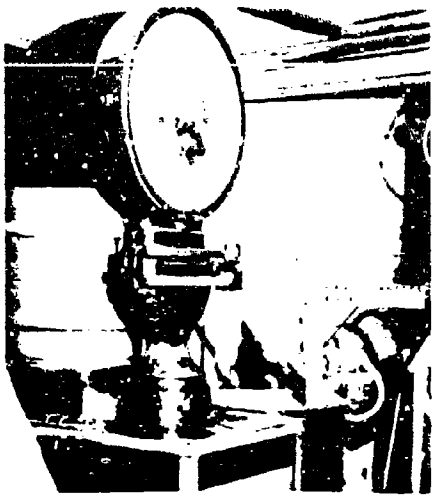

Figure 10. Fuel Weigh Tank System for Emulsified Fuel Tests.

A 3/4-inch I.D. flexible hose, 4 feet long, led from the bottom of the weighing tank to the inlet of the pump resting on the test stand floor. The flexible hose consisted of a stainless-steel wire braid jacket over a tetrafluoroethylene lining. This hose was used for all lines in the system that carried emulsified fuel. The gear pump which was used for emulsified fuel pressurization in combustor rig test stands was rated at 72 gallons/hour at 1500 rpm and 1500-psi pressure rise. It was driven by a 1450-rpm, 3 hp, constant-speed AC motor. A pump return bypass loop, including an adjustable pressure relief valve and a stainless-steel cooler, permitted the setting of any desired pump discharge pressure. The pressurized fuel continued on through an engine pressurizing and dump valve, inside of which was located a 200-mesh stainless-steel screen, then through a 100-mesh stainless-steel thimble screen as a backup. The system then split into the primary and secondary circuits; each circuit incorporated adjustable pressure regulators and a final paper cartridge filter before connecting to a nozzle manifold on the rig. Air regulated at the control panel was delivered into the secondary circuit when running with the air-assist nozzle. Nitrogen purge gas lines were teed into both circuits. The nitrogen gas was used to purge residual emulsified fuel out of the fuel lines, in order to prevent flame torching through the burner or coke build-up in the fuel nozzle when the burner is shut down. JP-4 from the regular test stand fuel system was teed into the emulsified fuel system for baseline running. Sufficient shutoff and check valves were installed in the system to permit any fuel or nozzle combination to be run without line changes.

The system just described and as illustrated in Figure 9 was used for all baseline tests with JP-4, all transient tests, all performance tests with the pressure atomizing nozzle, and all performance tests at 800°F inlet temperature with the air-assist nozzle. The tests with emulsified fuels that were run with the air-assist nozzle at 500°F inlet temperature were conducted with the same system except that a variable-speed motor was substituted for the constant-speed electric motor. This permitted the removal of the bypass return loop in order to minimize breakdown of the emulsified fuels for these tests. All light-off tests with emulsified fuels were conducted with the system as illustrated except the pump was driven by a 1/2-hp motor through an adjustable-speed reduction gear unit, without the pump bypass return loop.

Altitude Relight Test Apparatus

Figure 11 shows the JT12 burner rig installed in the altitude simulation test stand. An exhauster-cooler capable of producing rig inlet total pressures of less than 7 inches of mercury absolute and temperatures below -20°F was used to simulate altitudes approaching 35,000 feet.

The burner rig and fuel system were identical to those used for corrosion testing with emulsified fuel B, except for the removal of the test vanes and vane holder from the burner exit plane for the relight tests.

Figure 11. Altitude Relight JT12 Burner Rig Installed in Test Stand.

Gas Analysis Apparatus

A dual-column, dual-detector instrument was used to determine the percent by volume of N_2, CO_2, O_2 + Ar, and CO in the exhaust stream. The first column was made of aluminum tubing, 30 inches long by 1/4 inch in diameter. It was packed with 30-percent hexamethylphosphoramide on a 60-80 mesh solid support and was used to separate and detect CO_2. The second column, also made of aluminum, was 13 feet long by 3/16 inch in diameter and was packed with 40-60 mesh molecular sieve 13X. The length suggested by the vender for the second column was 6.5 feet; however, by doubling the length of the column, a larger sample volume could be injected into the instrument without a loss of resolution between adjacent peaks on the chromatogram. The larger sample volume greatly increased the sensitivity and lowered the limit of detectability for those gases in the parts-per-million range. The second column was used to separate and detect the percent by volume of O_2 + Ar, N_2, and CO in the low parts-per-million range.

Instrumentation

Airflow Measurement

Mass airflow through the rig was measured using a Verein Deutscher Ingenieure (V.D.I.) orifice. The orifice pressure drop and inlet static pressure were read from vertical manometers. All temperatures except that of the platinum/platinum-rhodium traverse rake were measured with chromel/alumel thermocouples connected through a selector switch to a potentiometric temperature indicator. There were three inlet total pressure probes, two inlet static pressure taps, and two thermocouples at the compressor exit position. Exhaust total pressures and temperatures were measured with a traversing burner exit rake. A chromel/alumel rake head (Rake No. 1) was used for tests at 500°F inlet temperature. A platinum/platinum-rhodium rake head (Rake No. 2 or 2A), similar in design to the chromel/alumel rake head, was used for tests at 800°F as well as some limited tests at 500°F inlet temperature. The head of this rake, with five total pressure probes and five double shielded platinum/platinum-rhodium thermocouples, is illustrated in Figure 12. These thermocouples had a separate selector switch and indicator. All inlet and exit pressures were measured on vertical mercury manometers referenced to atmosphere. Primary fuel temperature entering the nozzle was measured by means of a thermocouple mounted inside the primary passage of the nozzle socket.

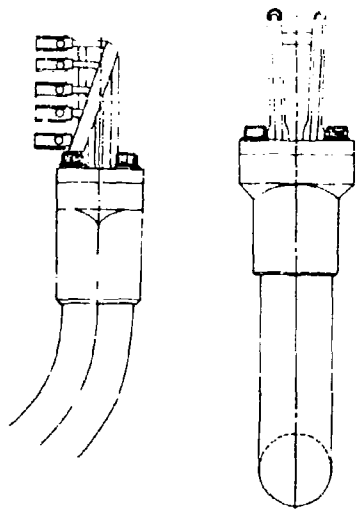

Figure 12. Platinum Temperature/Total Pressure Exhaust Traverse Rake.

Fuel Flow Measurement

JP-4 fuel flow was monitored with a glass tube rotameter. Emulsified fuel flows were measured by the weight/time method using a Toledo scale with 1-ounce graduations and a stop watch. Nozzle primary and secondary pressures were monitored on bourdon-tube pressure gages. When conducting transient and light-off tests, pressure transducers were tied into the fuel lines. These transducers and the exhaust rake thermocouples were tied into a multichannel transient recorder.

Flame Indicator

Flame intensities were measured through quartz windows in the rig at two positions (see Figure 4) with Pratt & Whitney flame indicator units. The positions viewed were (1) at the burner exit (turbine inlet position) and (2) at a position 8.1 inches upstream sighting into a dilution hole in the burner can.

The flame indicator is a tool developed to measure flame levels. It consists of a photoelectric tube sensitive to ultraviolet radiation between 2000 Angstroms and 2400 Angstroms, and an electronic console to measure the tube output. The output is proportional to the intensity level and quantity of flame viewed. When the field of view is limited and filled with flame, the flame indicator signal is linearly proportional to the flame intensity within 5 percent (envelope of 95 percent certainty). The distinguishing characteristics of the flame being analyzed by the flame indicator are the active or reacting CO ions, formed from interactions of the fuel and oxidant. These nonequilibrium species, being very high in energy, tend to emit well above the continuum of thermal radiation.

Two rig-mounted, standardized, ultraviolet sources were used in this program to provide on-stand calibration of the flame indicator units.

Combustion Test Procedure

Steady-State Performance Tests

Steady-state performance tests were conducted with all three emulsified fuels relative to JP-4.

Steady state combustion performance tests were run using the combustor rig shown pictorially in Figures 6 and 7. The test procedures and performance point settings used to determine steady-state combustion performance are outlined in Appendix I.

Transient Tests

Transient tests were conducted with all three emulsified fuels relative to JP-4.

Transient tests were run using the JT12 burner rig shown in Figures 4 through 7. For these tests, the fuel supply system of the JT12 burner test rig, shown schematically in Figure 9, was modified as follows: the secondary fuel system was not used. The primary fuel system was split by inserting a 3-way plug valve just before the primary pressure regulator. The inlet of the primary pressure regulator was connected to one leg of this 3-way valve. The inlet of a second pressure regulator was connected to the other leg of the 3-way valve. The outlet of the second pressure regulator was connected to the outlet of the primary pressure regulator through a tee connection. With this system, the fuel flow to the primary nozzle could instantaneously be switched from one pressure regulator to the other without interrupting the flow.

The tests consisted of rapid acceleration from the flow conditions at point 2 to the flow conditions at point 7 described in Appendix I. When running a test, point 2 conditions were set with fuel flow controlled through one pressure regulator, and point 7 conditions were set with fuel flow controlled through a second pressure regulator. A recorder, with paper feed set at 2 inches per second, was used to record primary fuel pressure and exhaust rake thermocouple readings with the rake in center stream. The 3-way valve was switched several times for each fuel and nozzle combination, producing recordings of acceleration from point 2 to point 7 conditions.

Light-off Tests

Light-off tests were conducted with all three emulsified fuels relative to JP-4.

Light-off tests were run using the JT12 burner rig shown in Figures 4 through 7. For these tests, the fuel supply system of the JT12 burner test rig, shown schematically in Figure 9, was modified as follows: The secondary fuel system was not used. A 3-way plug valve was installed just aft of the primary pressure regulator. The continuation of the primary fuel system was connected to one leg of this 3-way valve. The other leg of

the 3-way valve was connected to a separate nozzle and manifold of the same type that was in the test rig but spraying into an empty drum. With this system, the fuel flow could be instantaneously switched from zero (flow to an empty drum) to sea level light-off conditions (flow to the primary fuel nozzle). When running a test, the nozzle spraying into the drum was used to set sea level light-off conditions. A recorder with paper feed set at 2 inches per second was used to record inlet nozzle pressures and rake thermocouple readings. The ignition, energy level 4 joules, was started (spark rate≈5/sec). The 3-way valve was switched several times from zero to light-off conditions for each fuel and nozzle combination tested, producing recordings which indicated light-off times (i.e., the interval between the appearance of pressure at the nozzle and the start of rapidly rising rake thermocouple readings).

Altitude Relight Test Procedure

Altitude relight tests were conducted with all three emulsified fuels relative to JP-4.

The windmilling relight capability was determined by setting a constant airflow rate through the burner and lowering the burner inlet total pressure until a no-light was encountered. (Failure of the burner to light within 30 seconds of the initiation of fuel flow constitutes a no-light condition.) This procedure was carried out for airflows of 600 pph, 800 pph, 1200 pph, 1600 pph and 2000 pph. The inlet air temperature was maintained at -20°F, and the bulk fuel temperature was essentially equal to the room temperature. The ignition energy was 4 joules. The light-off fuel flow rate was held constant at 37.5 pph.

Test Procedure - Exhaust Gas Sampling

The exhaust gas samples were collected through the smoke sampling probe shown in Figure 5. The probe ram pressure was sufficient for all samples. Fifty feet of heated 3/8 in. I.D. flexible sampling line was used. No attempt was made to obtain isokinetic sampling, as it has been shown that an isokinetic sampling does not affect the results of these tests.

Test Procedure - Exhaust Gas Particulate

Total particulates were collected by a Millipore in-line vacuum filtering unit with Type HA cellulose ester filters having an average pore size of 0.45 micron. Measurements were made gravimetrically, following normal procedures for reducing errors due to water absorption. Relative smoke densities were measured using a Pratt & Whitney Aircraft spot filtering smoke meter. Total gas volume was maintained at 18.3 cubic feet for each smoke reading to provide a constant reference point.

Test Procedure - Gas Analysis

A dual-detector instrument was used to determine the percent by volume of nitrogen, carbon dioxide, oxygen plus argon, and carbon monoxide in the exhaust stream. The operating conditions for the instrument were:

1. Helium carrier gas
2. 40 cc/min flow
3. 4 cc sample loop
4. Ambient column and detector temperature

A recorder equipped with a 5-mv range plug was used to record the chromatograms of O_2 + Ar, N_2, and exhaust CO_2. A second recorder equipped with a 1-mv range plug was used to record the exhaust CO and the intake CO_2 contents.

A total hydrocarbon analyzer was used to measure hydrocarbon emissions as methane. The instrument was calibrated with zero air and with a mixture consisting of 200-parts-per-million methane air.

Test Procedure - Wet Chemical Test

A five-position manifold consisted of four positions including a flow regulating valve, a four-way sampling valve, an absorbing bubbler, a mist trap, and a flow meter, and one position with an oxidizer bubbler between the flow valve and the sampling valve. There was a vacuum meter on the exhaust manifold to monitor vacuum for flow corrections and a fiberglass filter on the inlet to curtail soot contamination.

The first four positions were used for SO_2, olefins (as 1-pentene), aldehydes (as formaldehyde), and NO_2. The last bubbler was for NO_x.

The actual operation of the manifold was as follows:

1. The five bubblers were filled with the following solutions -

   SO_2 - 10 ml of ferric ammonium sulfate solution and 10 ml of o-phenthroline solution

   Olefins - 20 ml of DAB absorber solution

   Aldehydes - 35 ml of MBTH aldehyde absorber

   NO_2 - 10 ml of NEDA NO_2 absorber

   NO_x - first the oxidizer bubbler was filled with 10 ml of acid-permanganate oxidizer, followed by a bubbler with 10 ml of NEDA NO_2 absorber.

   All solutions were pipetted to assure volume control.

2. To sample a gas, the flows were adjusted as shown below with the sampling valves in "flow-adjust" position (this omitted the bubblers from the sampling train).

   SO_2 - 1 liter/min
   Olefins - 1 liter/min
   Aldehydes - 0.5 liter/min
   NO_2 and NO_x - 0.4 liter/min

3. A stop watch was started, and the olefin and SO_2 bubblers were switched into the line. After 1 minute, the aldehyde bubbler was switched in. After an additional 1-1/2 minutes, the NO_2 and NO_x bubblers were switched in. All were shut off after an additional 30 seconds. It should be mentioned that after a new bubbler was put on the line, flows had to be slightly readjusted. This sample procedure afforded the following sensitivities:

   SO_2 - 0.3 ppm
   Olefins - 0.3 ppm
   Aldehydes - 0.5 ppm
   NO_2 and NO_x - 2.0 ppm

   Since there was always sufficient positive pressure coming into the system, a vacuum was not needed.

4. Equivalent volumes of unused solutions were taken to use as blanks in the analysis procedure.

   The absorbance of the various solutions was determined by spectrophotometry. The absorbances were then put into a computer program, and the ppm values were computed.

CORROSION TEST APPARATUS AND PROCEDURE

Corrosion Test Apparatus

Test Materials and Specimen Design

The turbine materials to be subjected to the combustor exhaust gases while burning emulsified JP-4 fuels were selected on the basis that they would represent current as well as advanced gas turbine material applications. The following materials were selected in both a cast and a wrought state as indicated:

1. Wrought U-500 Uncoated
2. W.I. 52 - Chromalloy U.C. Aluminide Coating
3. Wrought U-700 - Uncoated

4. Inco 713C PWA Proprietary Aluminide Coating

5. Inco 713C - Uncoated

6. B-1900 - PWA Proprietary Aluminide Coating

The test materials were shaped into a symmetrical airfoil with no turning. The airfoil selected has the same geometric design as the 1st stage turbine inlet guide vanes in the JT12 engine. That is, the leading and trailing edge radii as well as the chord to vane thickness ratio are the same for the test specimen as for actual engine hardware. Figure 13 shows the leading-edge view of the vane, while Figure 14 shows the side view. The radius of the leading edge is 0.080 ± 0.005 inch, while the radius of the trailing edge is 0.012 ± 0.003 inch. The span at the leading edge is 2.160 ± 0.005 inches, while the span at the trailing edge is 1.500 ± 0.005 inches. The chord of the vane specimen is 1.250 ± 0.005 inches, while the maximum thickness is approximately 0.180 inch. As shown by Figure 14, a converging passage had been designed into the vane geometry in order to provide choked flow along the flow path at approximately the 80 percent chord station. Engine experience has indicated that this is usually the location of sonic flow conditions.

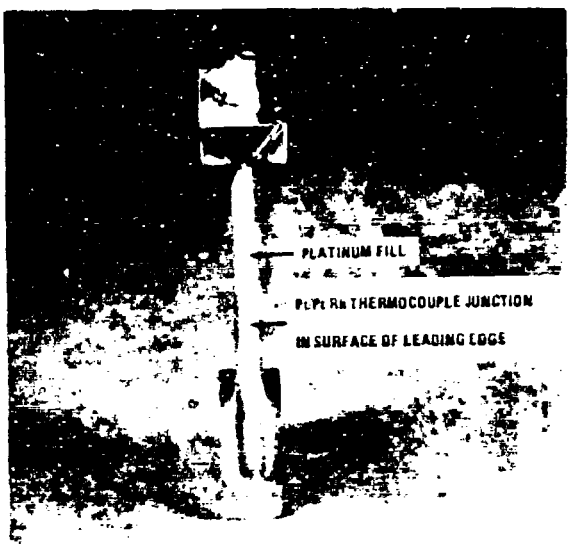

Figure 13. Vane Specimen Showing Installation of Thermocouple for Pre-endurance Calibration Test of the Emulsified Fuel Program.

Figure 14. Side View of Vane Specimen Showing Five Static Pressure Taps Installed in Preparation for Pre-endurance Calibration Test of the Emulsified Fuel Test Program.

Test Material/Burner Installation

The location of the test specimens relative to the burner exit plane is shown in Figure 15. The burner system upstream of the vane test specimens is the same as that used during the combustion experiments with the pressure atomizing fuel nozzle. A fixture designed to hold the test specimens in their proper position relative to the burner exit annulus is shown in Figure 16. This fixture is bolted to the rear section of the burner rig and simulates the first turbine vane support structure of a gas turbine engine. The test samples are retained by the fixture in a manner so as not to impose any stresses in the vane span because of any thermal differences. The installation of the test vane pack in the burner test rig is shown in Figure 17. A cross section view is shown in Figure 18. The construction of the holding fixture enables the vanes to be easily removed for scheduled rotation and inspection and reinstalled without major disassembly. An observation port through the side of the burner rig enables a view of 70 percent of the leading edges of the test specimens when at operating conditions.

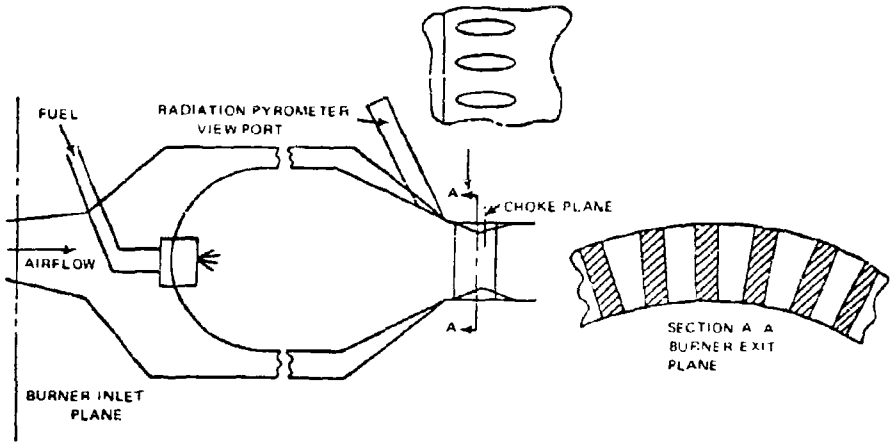

Figure 15. Cross Section Showing Locations of Test Specimens Relative to Burner Exit Plane in Corrosion Tests.

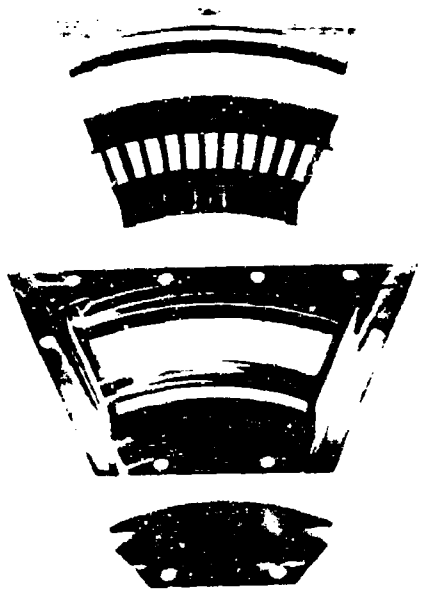

Figure 16. Exploded View of Test Specimen Support Fixture for Emulsified Test Program Showing Cover, Test Specimens, Vane Support Assembly, and Bottom Cover (View Looking Upstream).

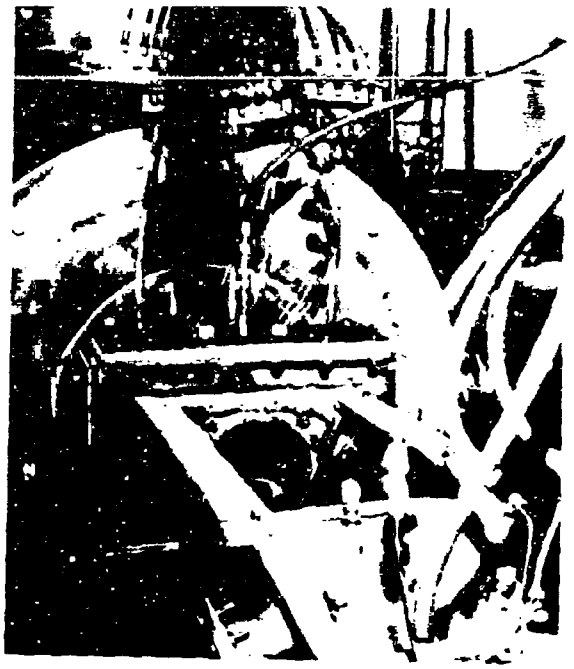

Figure 17. Installation of Instrumented Vane Pack Showing Instrumentation Leads Emerging From Test Rig.

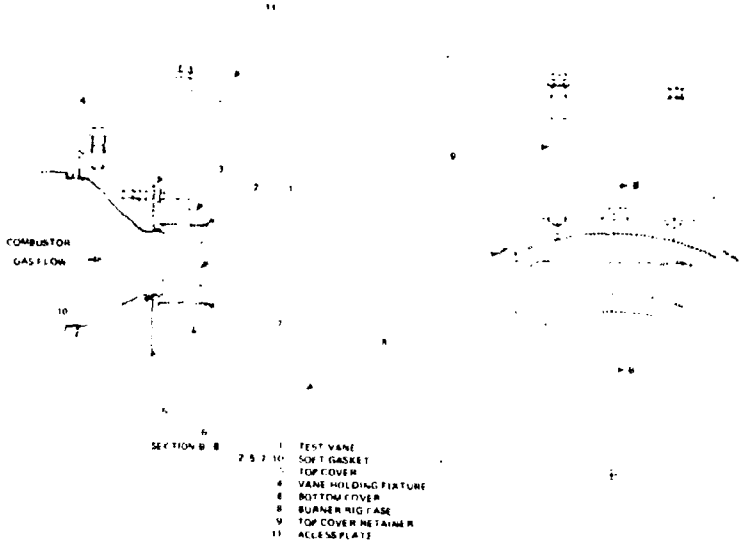

Figure 18. A Cross Section Showing Assembly of Test Vane Pack in Rig.

Test Stand/Instrumentation

The installation of the burner rig in the test stand is shown in Figure 19. A heat exchanger mounted upstream of the airflow measuring venturi provided the heated air to the burner inlet. Total pressure and temperature instrumentation was installed at the burner inlet section. The burner exit gases were exhausted through refractory lined duct work to the atmosphere. Radiation shielded thermocouples mounted in the exhaust duct provided the ability to monitor the exhaust gas temperature in case of operational problems. High and low temperature limits were set by these exhaust thermocouples and were inputted into an automatic alarm system which would alert the test stand operator in the event of trouble.

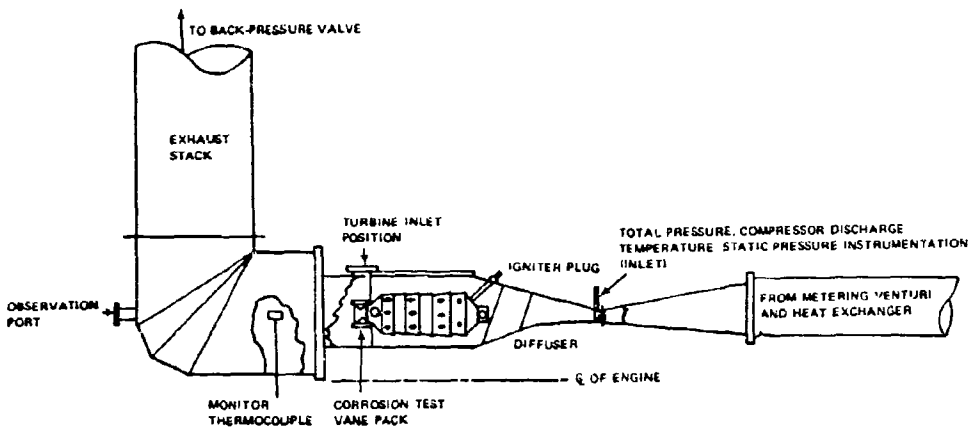

Figure 19. Side View of JT12 Burner Rig Showing Location of Corrosion Test Pack.

Fuel Systems

Figure 20 shows a schematic of the fuel system used to supply emulsified fuels A and C to the burner rig. This fuel system was modified for use with emulsified fuel B by eliminating the bypass loop and replacing the pump constant-speed drive with a variable speed drive. Also, an additional 40-micron filter was installed just upstream of the fuel nozzle. The fuel tank and all fuel line fittings and valves were of stainless-steel material. The flexible fuel lines were lined with tetrafluoroethylene. A 5/8 in. I.D. flexible line size was used on all lines between the fuel supply tank and the inlet to the main fuel pump. A vane pump with a variable-speed drive acted as a boost pump to overcome line pressure loss and to maintain the main fuel pump inlet pressure at approximately 20 psig. The distance between the boost pump and the main fuel pump was approximately 45 feet. Stainless cleanable 40-micron filters were the only type of filters used in the fuel system. The main fuel pump used was a gear type used on a current aircraft auxiliary power unit. It has the capability of running on kerosene as well as aviation gasoline.

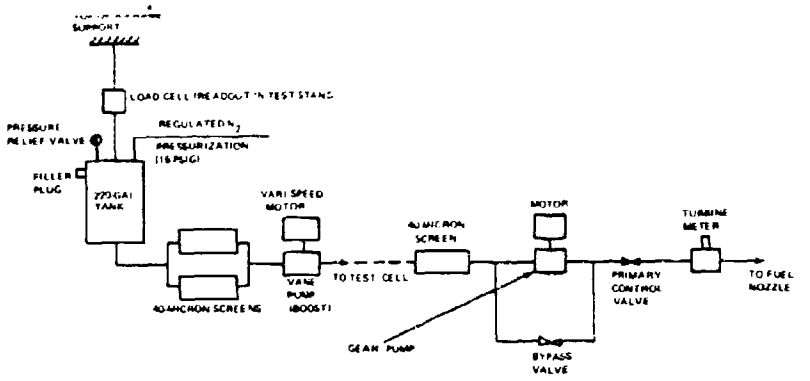

Figure 20. Fuel Transfer System for Emulsified Fuels A and C.

The fuel flow rate was monitored by use of a direct-reading "load cell" which indicated the loss of fuel weight as it was being consumed. Bourdon type pressure gages were installed both before and after the fuel filters as well as at the fuel nozzle to monitor the fuel pressures. This enabled a check in the pressure-flow relationships in order to apprehend any deviations from the previously calibrated fuel flow schedule.

Corrosion Test Procedure

The test conditions for the corrosion experiment were established so that the temperature rise across the burner would be the same for both the 1700°F and the 2000°F burner exit gas temperatures. That is, the temperature rise across the burner would be 1200 degrees while the inlet temperature to the burner would be 500°F for the 1700°F burner exit temperature and 800°F for the 2000°F burner exit temperature.

This criterion was based on the results of the previous combustion tests with JP-4 and emulsified JP-4. This condition represented the maximum capability of the burner, and the performance of JP-4 and emulsified fuels was nearly identical at these conditions.

In addition to the fact that these tests would simulate running conditions of a low and high compression ratio gas turbine cycle, it is to be noted that there would be local hot spots associated with the 2000°F burner exit temperature that would provide accelerated deterioration of some of the material specimens. The conditions at which corrosion tests were conducted are as follows:

Burner exit temperature	1700°F	2000°F
Burner inlet Mach number	0.25	0.27
Burner inlet pressure	70 in. HgA	70 in. HgA
Burner inlet temperature	500°F	800°F
Burner airflow	6500 pph	6200 pph
Nozzle fuel pressure	280-320 psig	280-320 psig

Pre-Test Performance Calibrations

Combustion tests with the temperature and pressure rake installed at the exit of the burner were conducted at the above test conditions with JP-4 fuel in order to provide a baseline calibration. The calibration established the pressure loss, combustion efficiency, and temperature pattern at the burner exit to be encountered during the corrosion testing.

Pre-Test Choke Plane Calibration

Following the performance calibration, the burner exit instrumentation was removed, and the test specimen holding fixture was installed at the burner exit. Dummy vanes, which were temperature and pressure instrumented, were installed in the vane pack in order to verify choking conditions across all the vanes as well as to correlate vane metal temperature with burner exit gas temperature. Figure 13 shows the typical installation of the thermocouple in the leading edges of seven of the 12 instrumented vanes. Figure 14 shows the static pressure taps as installed along the chord at midspan of the remaining five vanes. The location of the pressure-instrumented vanes was such that the measurements were made in the passageways along the end walls as well as in the center area of the burner exit flow path. Both cold and hot flow tests were performed with the instrumented vanes in order to establish choke plane position along the chord of the test vanes.

Corrosion Tests

It had been established on the basis of the combustion experiments previously conducted that all three emulsified fuels would be evaluated against JP-4 in the corrosion tests, because the combustion performance of all three emulsified fuels with the pressure atomizing fuel nozzle showed only slight differences when compared to JP-4 fuel. On the basis of 600 hours of total endurance testing, each vane pack of 12 test material specimens was run for 75 hours at each burner exit temperature level with each fuel. Each vane pack consisted of 2 specimens each of 6 different materials. The specimens were arranged in the holding fixture in pairs of the same material. Since there were six materials, a rotation of the pairs was established at the end of every 12.5 hours of corrosion testing in order to insure that each material was exposed to the same burner exit temperature pattern variation for the same length of time. Prior to testing, each vane specimen was marked for identification, visually inspected, and weighed. The fuels were tested at both temperature levels in the following order: JP-4 followed by emulsified fuel C, emulsified fuel A, and finally emulsified fuel B.

The light off procedure used for all fuels was to first set the burner inlet conditions required, followed by the application of ignition energy and fuel. Combustion was always easily initiated, and very little adjustment of burner parameters or fuel flow was required in order to quickly establish the required steady-state conditions. Shutdown was accomplished by cutting off the burner fuel supply and purging the burner fuel nozzle with nitrogen to expel any residual fuel in the fuel nozzle passages. Burner inlet air pressures, temperatures, and airflow as well as fuel flow rate and pressures were recorded every half hour during the corrosion tests.

Following the completion of the corrosion test on each emulsified fuel, the fuel system was cleaned by flushing with the appropriate chemical solvent which would break the emulsion. This was followed by flushing with JP-4 prior to testing the next emulsified fuel. Emulsified fuel was transferred from 50-gallon drums to the main storage tank by a hand pump. This enabled the test operator to inspect visually each drum for any loose emulsion, which would, if found, be eliminated from the test. During the corrosion tests, samples of the emulsified fuels supplied were inspected for their physical properties as well as analyzed for metallic content. The amount of breakdown of the emulsions after passing through the fuel pump and nozzle, was determined by collecting the spray and filtering it for residue emulsion.

DISCUSSION OF TEST RESULTS

COLD FLOW PROGRAM

1. When using the pressure atomizing fuel nozzle the pressure-flow characteristics of the three emulsified fuels were found to be identical to those of JP-4 fuel for pressure drops above 50 psi, as shown by Figure 21.

2. When using the air-assist fuel nozzle the pressure-flow characteristics of the three emulsified fuels were found to be lower than those of the JP-4 fuel as shown in Figure 22. This condition existed up to at least a 50 psi pressure drop and may have been caused by the resistance to flow of the emulsions up to the point where considerable emulsion breakdown occurs.

3. Most of the mechanical breakdown of the emulsified fuels occurs during the fuel passage through the gear pump. The degree of breakdown increases with increasing pressure rise and fuel flow, as shown in Figures 23 and 24. The remainder of the breakdown occurs during the passage of the fuel through the fuel nozzle. The amount of breakdown occurring in the nozzle is relatively small compared to that which occurs in the pump.

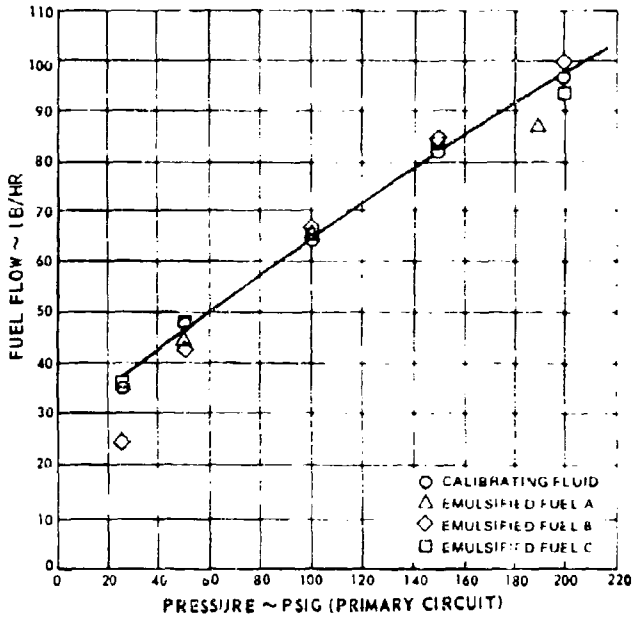

Figure 21. Pressure Versus Fuel Flow Schedule for Three Emulsified Fuels With Pressure Atomizing Nozzle.

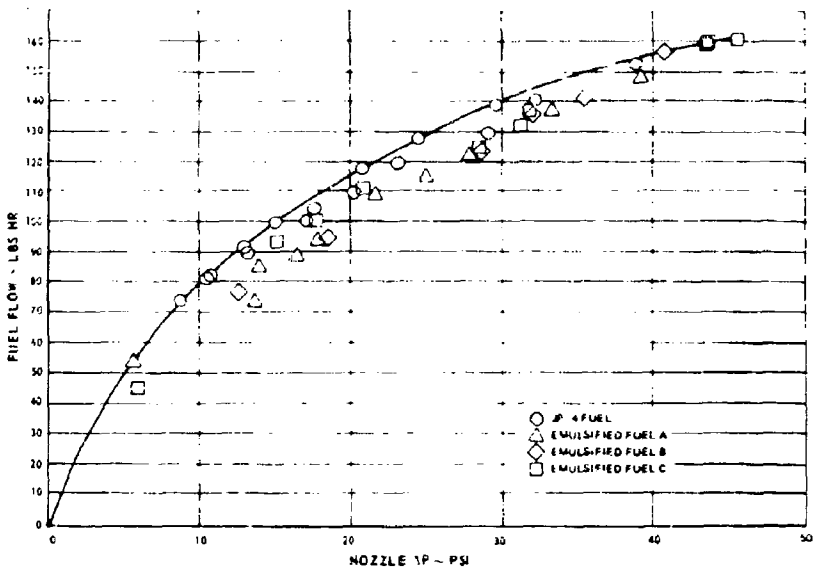

Figure 22. Pressure Versus Fuel Flow Schedule for Three Emulsified Fuels and JP-4 Fuel With Air-Assist Nozzle.

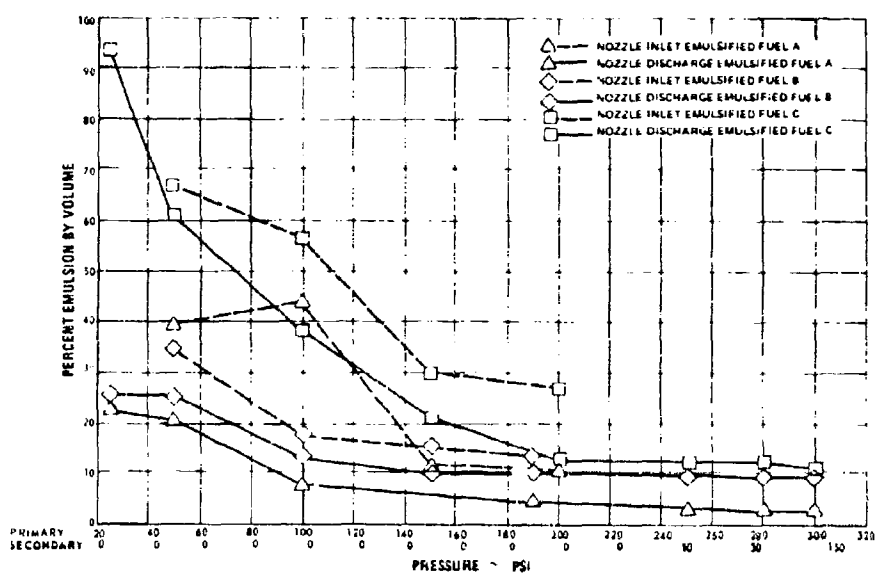

Figure 23. Breakdown of Emulsified Fuel in a Pressure Atomizing System at Room Temperature.

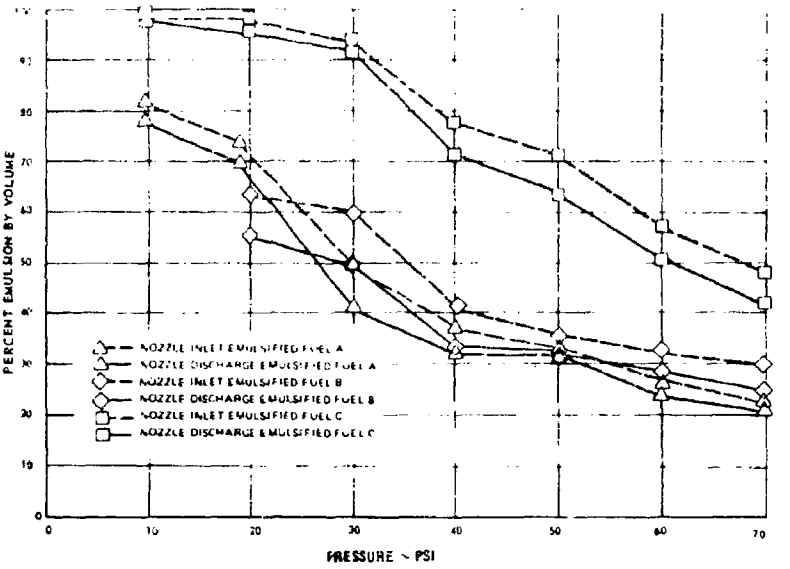

Figure 24. Breakdown of Emulsified Fuel in an Air-Assist System at Room Temperature.

It should be noted that some degree of emulsification persists even after exit of the fuel through the fuel nozzle. This fact was verified by visual observation of the emulsion build-up resulting from the spray impinging on the sides and bottom of the spray booth in addition to the data derived from the samples collected in the collection bottles.

4. Less mechanical breakdown of the emulsion occurs with the air-assist fuel nozzle system than with the pressure atomizing nozzle for the same fuel flow, as indicated by a comparison of Figures 23 and 24. As outlined in 3 above, most of the breakdown occurs because of pump work.

5. Emulsified fuel C exhibits greater resistance to mechanical breakdown than do either emulsified fuel A or B. Fuels A and B displayed similar characteristics with regard to mechanical breakdown, as shown in Figures 23 and 24.

6. The spray cone angle and visual spray patterns obtained with the emulsified fuels are considered to be identical to those obtained with JP-4 fuel. Table I lists measured spray cone angles obtained when flowing emulsified fuels and reference JP-4 fuel through the air-assist and pressure atomizing nozzles at 20 psi, 50 psi, 70 psi, and 300 psi pressure. The only exception was emulsified fuel B, which exhibits a wide angle at the starting flow pressure.

TABLE I. COMPARISON OF SPRAY CONE ANGLES OF EMULSIFIED FUELS AND JP-4

Fuel	Air-Assist Fuel Nozzle (7.2-PSI Air Supply)		Pressure Atomizing Fuel Nozzle	
	Spray Angle at 20 PSI (degrees)	Spray Angle at 70 PSI (degrees)	Spray Angle at 50 PSI (degrees)	Spray Angle at 300 PSI (degrees)
JP-4 Fuel	78	78	85	85
Emulsified Fuel A	75	80	85	85
Emulsified Fuel B	115	75	85	85
Emulsified Fuel C	78	78	85	85

The series of photographs included in Figures 25 through 36 present a comparison of spray cone patterns obtained with both the air-assist and the pressure atomizing fuel nozzles flowing all three emulsified fuels and the reference JP-4 fuel. Figures 25 through 30 show the spray patterns obtained with the emulsified fuels and the pressure atomizing nozzle. Figures 31 through 33 show the patterns obtained with the air-assist nozzle and emulsified fuels, and Figures 34 through 36 show the patterns obtained with the JP-4 reference fuel. The photographs and simultaneous visual observations showed the spray cone to be fully developed, with no major differences between the three fuels and the baseline JP-4 fuel. It is to be noted that because of the use of a different photographic range, Figures 29 and 30 show an erroneous difference for the spray qualities of emulsified fuel C and the other fuels. The flow range covered included operation on the primary circuit alone as well as on both the primary and the secondary circuits. Neither the spray pattern nor the emulsified fuel breakdown rate appeared to be affected by the inception of secondary fuel flow.

(A) 50 PSI PRIMARY
0 PSI SECONDARY

(B) 75 PSI PRIMARY
0 PSI SECONDARY

(C) 100 PSI PRIMARY
0 PSI SECONDARY

Figure 25. Spray Patterns of Emulsified Fuel A Flowing Through A Pressure Atomizing Nozzle at Indicated Pressures.

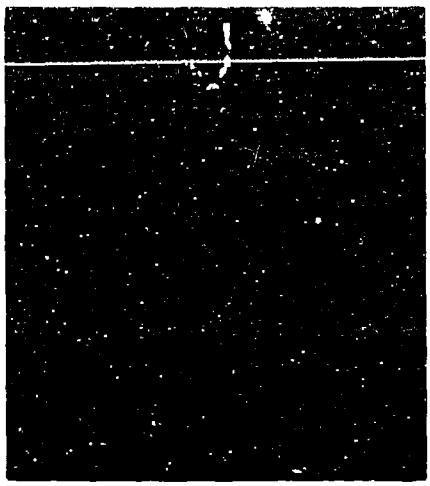

(A) 150 PSI PRIMARY
0 PSI SECONDARY

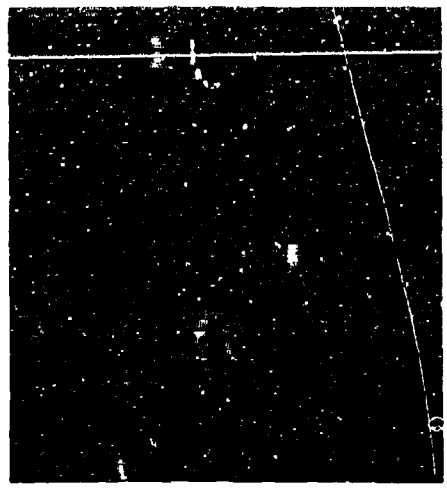

(B) 200 PSI PRIMARY
0 PSI SECONDARY

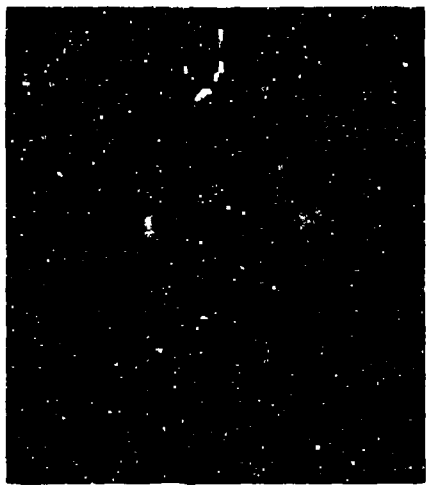

(C) 200 PSI PRIMARY
5 PSI SECONDARY

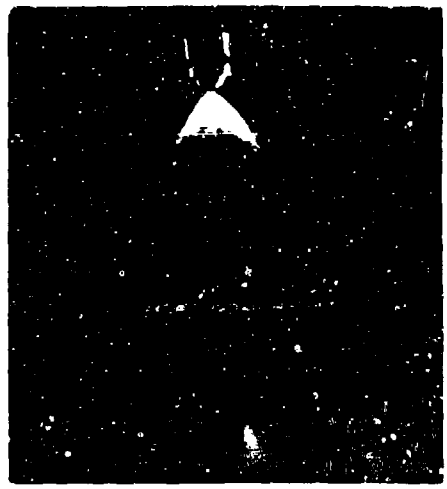

(D) 300 PSI PRIMARY
150 PSI SECONDARY

Figure 26. Spray Patterns of Emulsified Fuel A Flowing Through a Pressure Atomizing Nozzle at Indicated Pressures.

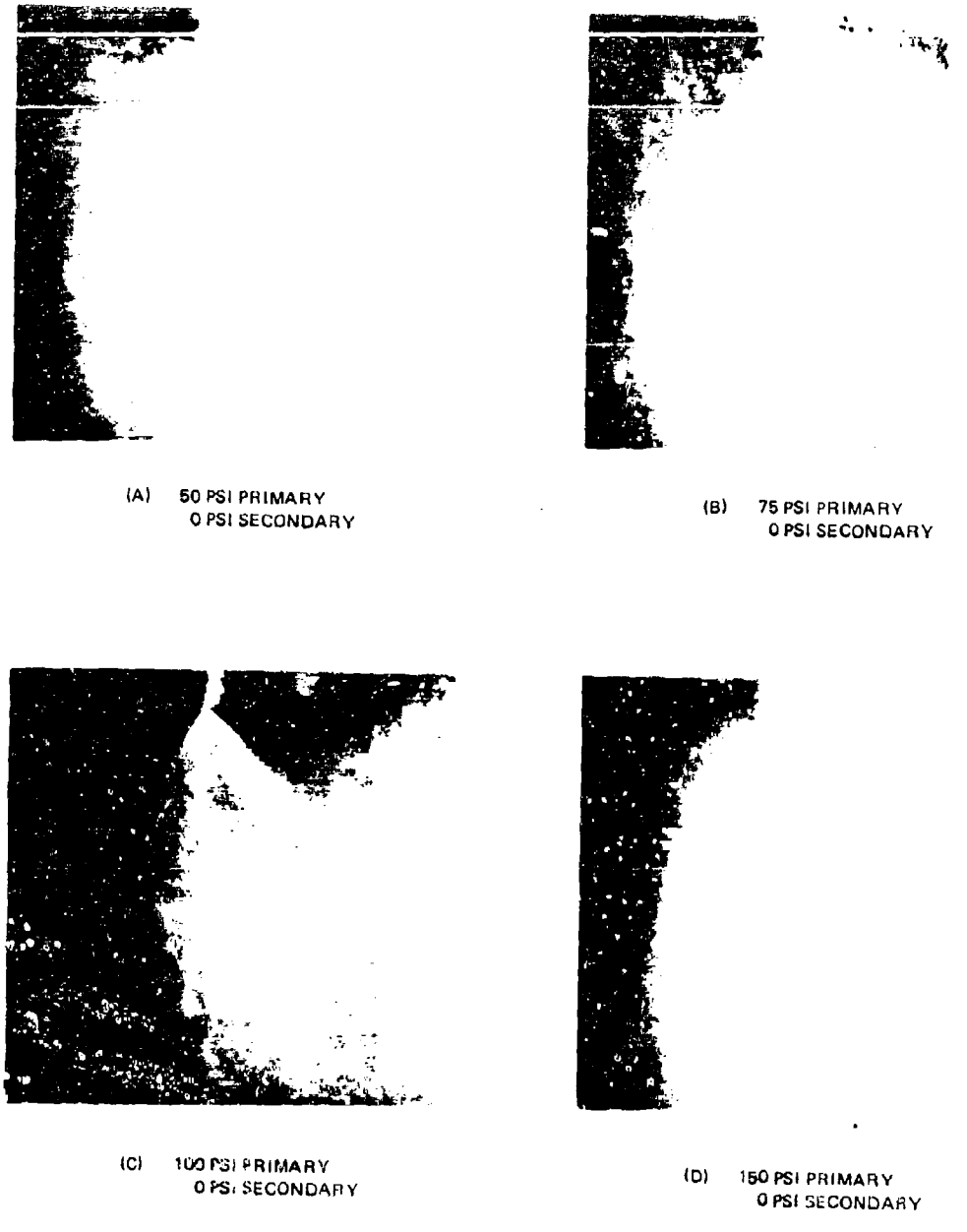

Figure 27. Spray Patterns of Emulsified Fuel B Flowing Through a Pressure Atomizing Nozzle at Indicated Pressures.

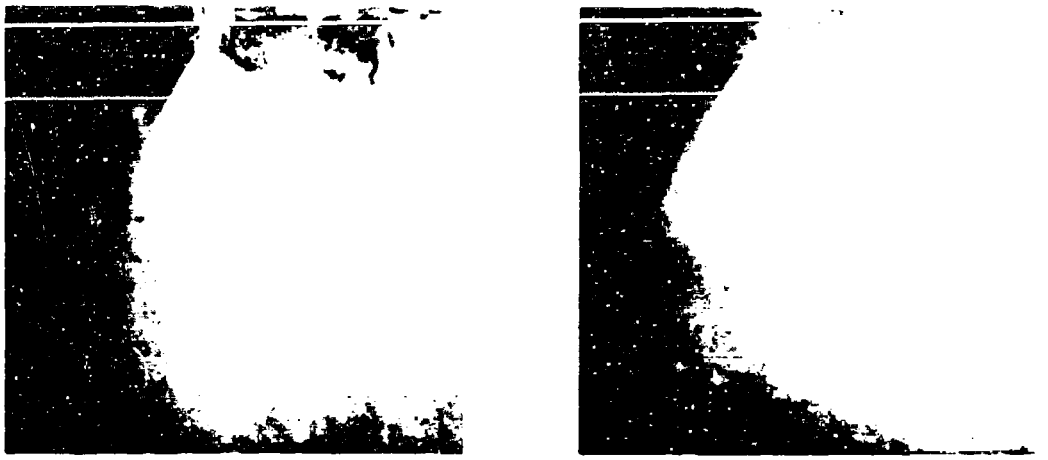

(A) 200 PSI PRIMARY
0 PSI SECONDARY

(B) 200 PSI PRIMARY
5 PSI SECONDARY

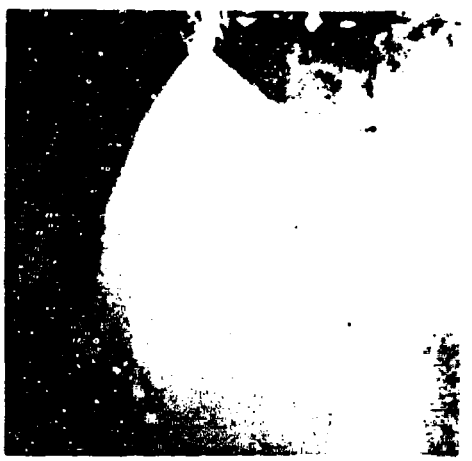

(C) 300 PSI PRIMARY
150 PSI SECONDARY

Figure 28. Spray Patterns of Emulsified Fuel B Flowing Through a Pressure Atomizing Nozzle at Indicated Pressures.

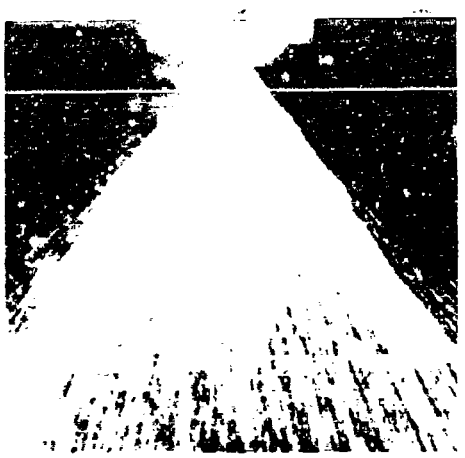

(A) 50 PSI PRIMARY
0 PSI SECONDARY

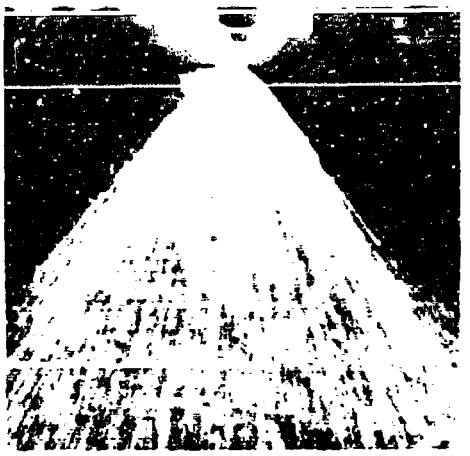

(B) 75 PSI PRIMARY
0 PSI SECONDARY

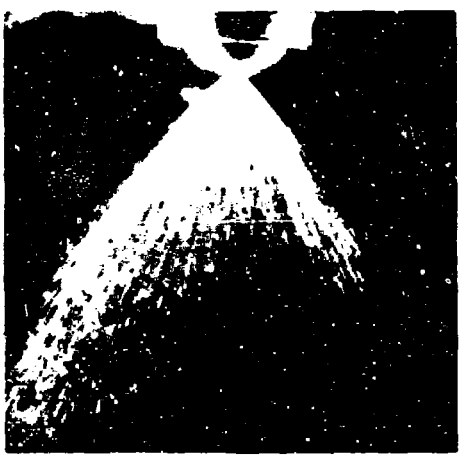

(C) 100 PSI PRIMARY
0 PSI SECONDARY

(D) 150 PSI PRIMARY
0 PSI SECONDARY

Figure 29. Spray Patterns of Emulsified Fuel C Flowing Through a Pressure Atomizing Nozzle at Indicated Pressures.

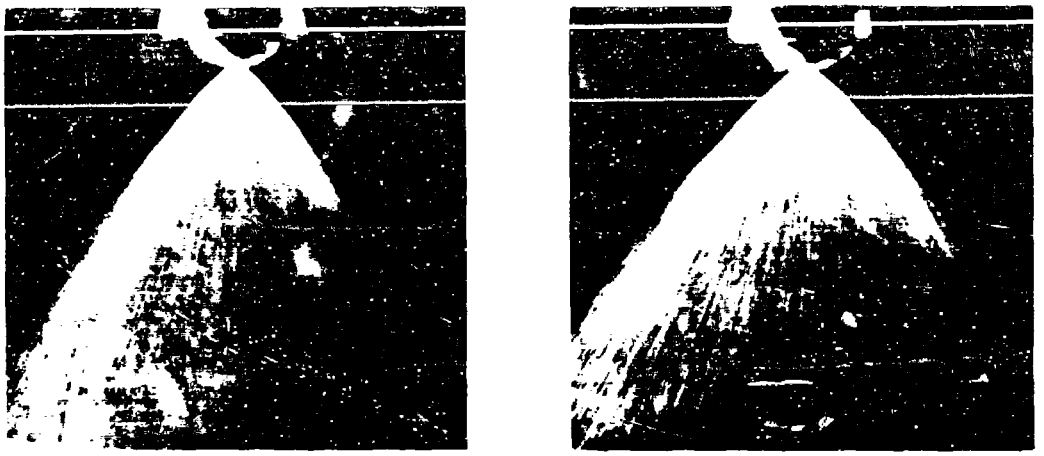

(A) 200 PSI PRIMARY
0 PSI SECONDARY

(B) 200 PSI PRIMARY
6 PSI SECONDARY

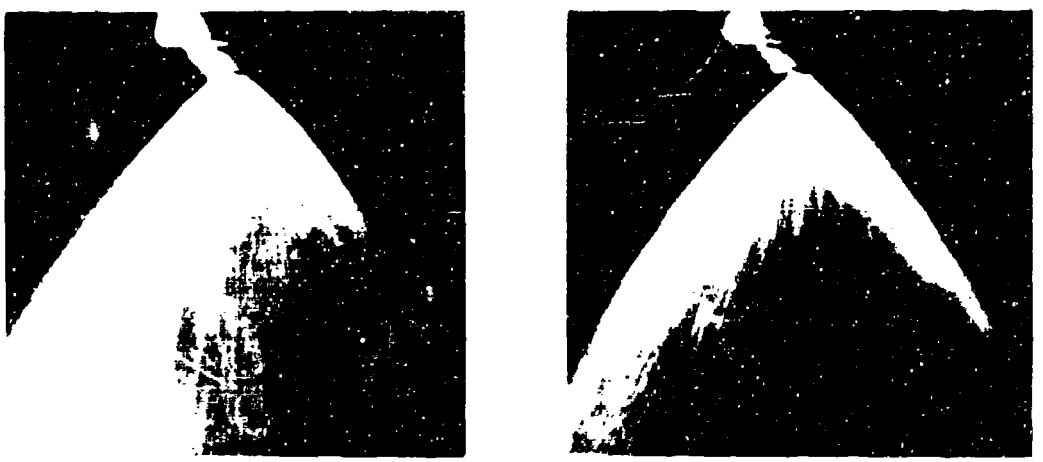

(C) 250 PSI PRIMARY
5 PSI SECONDARY

(D) 300 PSI PRIMARY
150 PSI SECONDARY

Figure 30. Spray Patterns of Emulsified Fuel C Flowing Through a Pressure Atomizing Nozzle at Indicated Pressures.

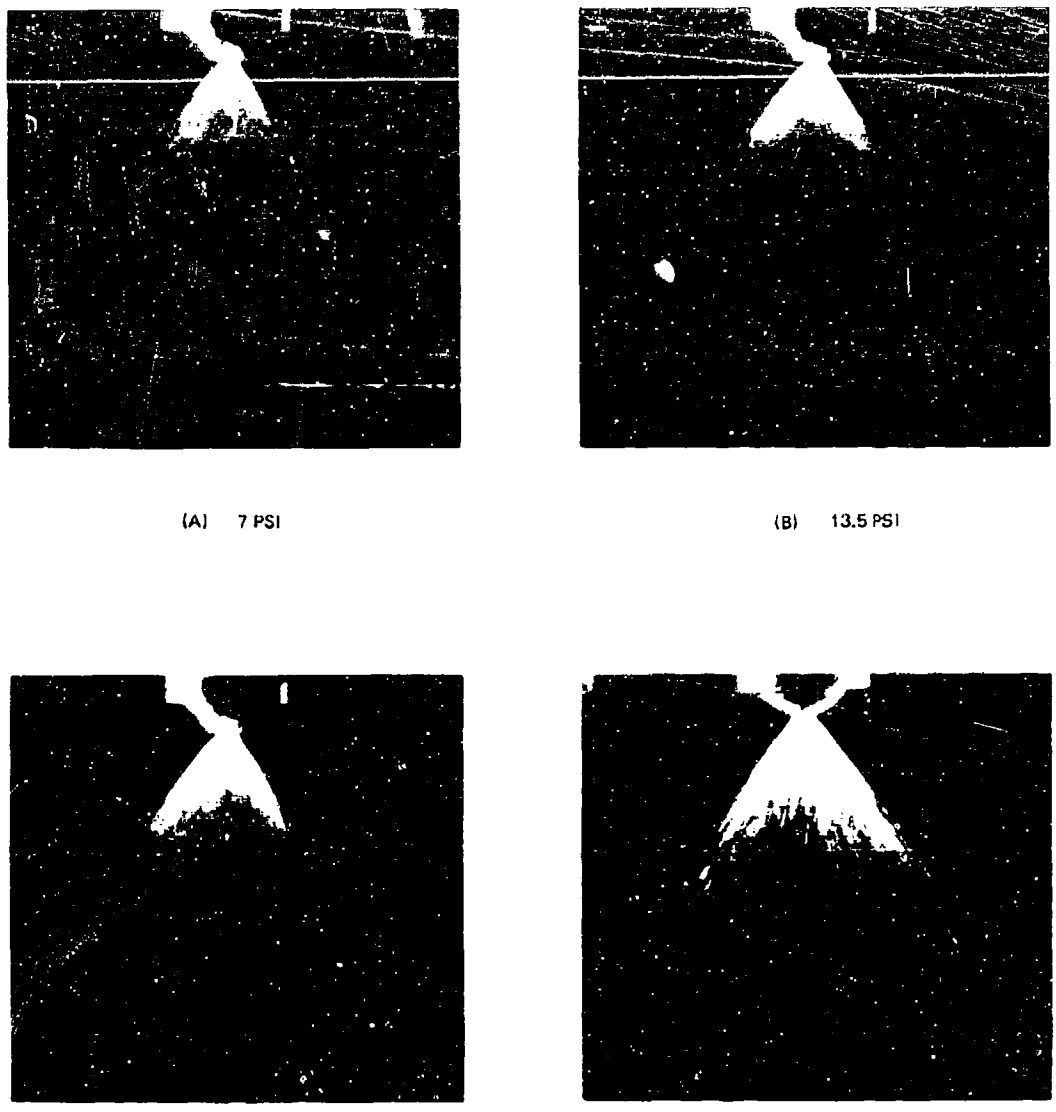

Figure 31. Spray Patterns of Emulsified Fuel A Flowing Through an Air-Assist Nozzle at Indicated Pressures With 2 SCFM Airflow Through the Secondary.

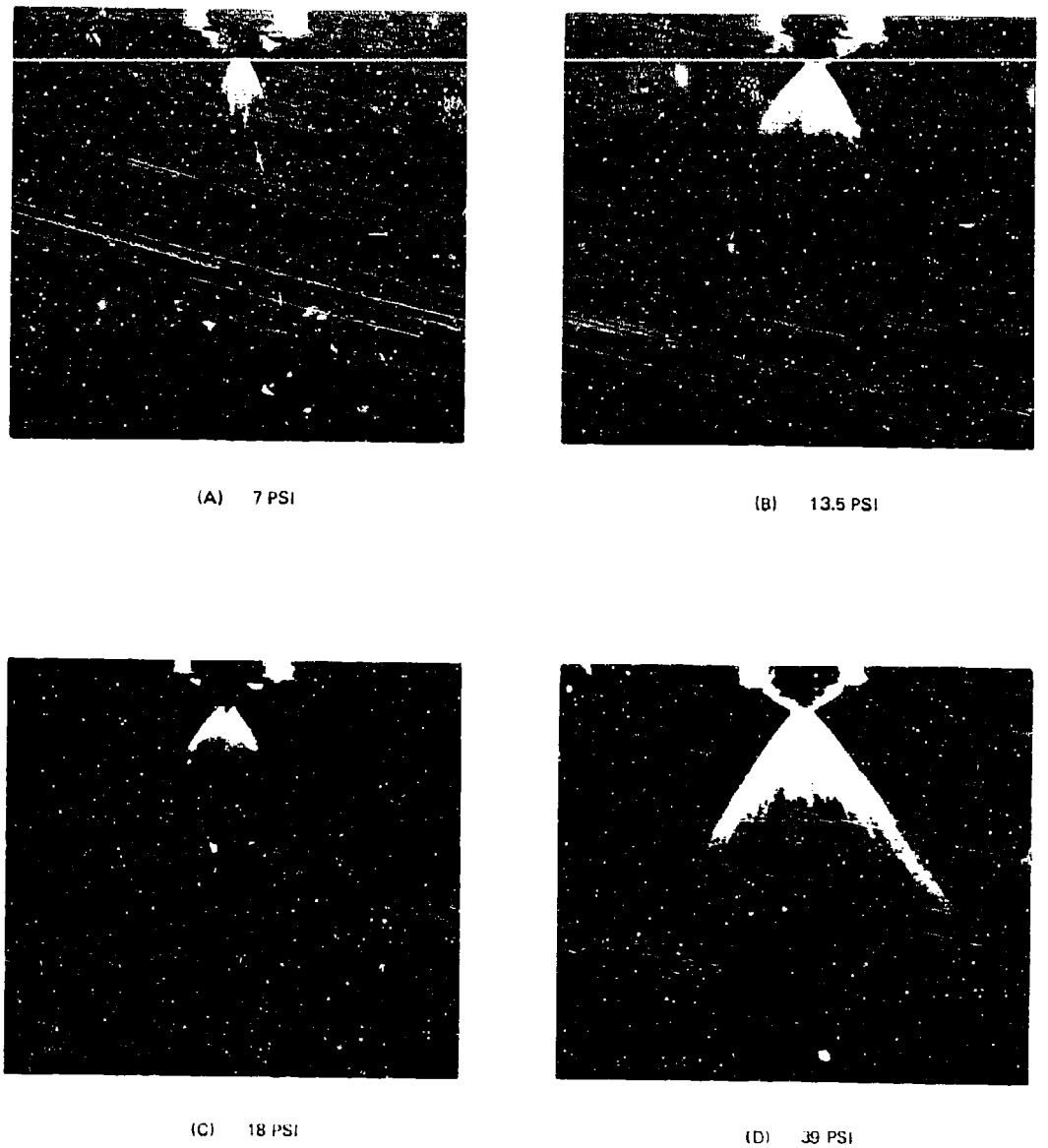

Figure 32. Spray Patterns of Emulsified Fuel B Flowing Through an Air-Assist Nozzle at Indicated Pressures With 2 SCFM Airflow Through the Secondary.

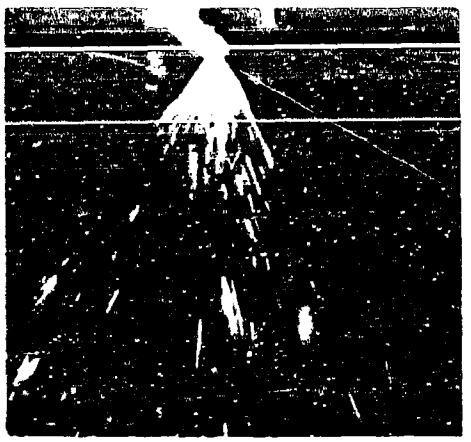

(A) 7 PSI

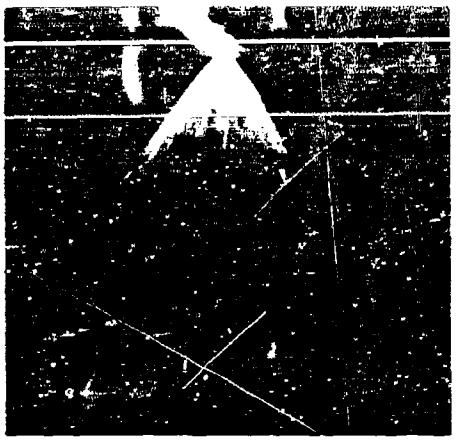

(B) 13.5 PSI

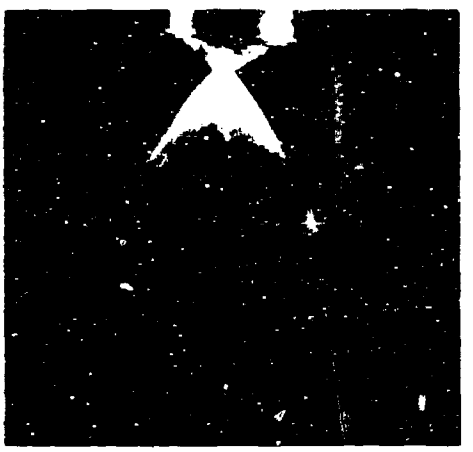

(C) 8 PSI

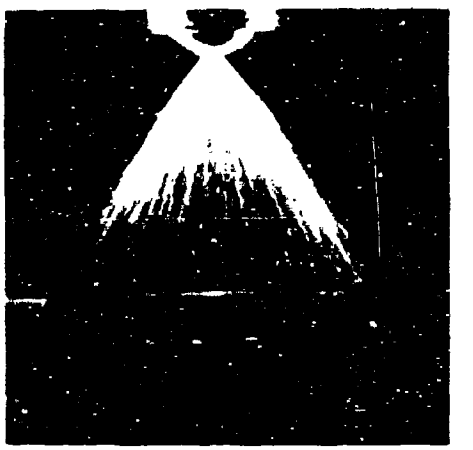

(D) 39 PSI

Figure 33. Spray Patterns of Emulsified Fuel C Flowing Through an Air-Assist Nozzle at Indicated Pressures With 2 SCFM Airflow Through the Secondary.

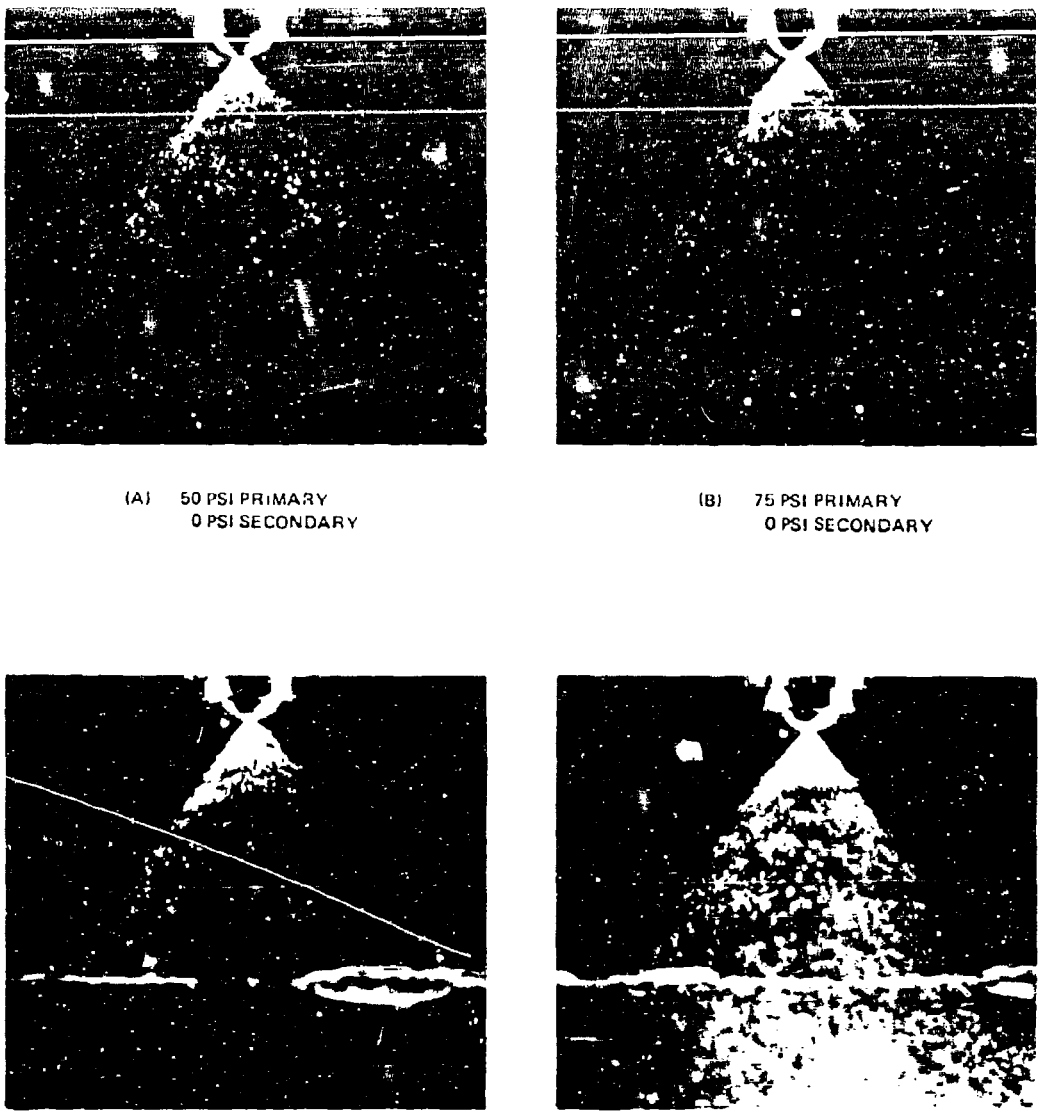

(A) 50 PSI PRIMARY
0 PSI SECONDARY

(B) 75 PSI PRIMARY
0 PSI SECONDARY

(C) 100 PSI PRIMARY
0 PSI SECONDARY

(D) 150 PSI PRIMARY
0 PSI SECONDARY

Figure 34. Spray Patterns of JP-4 Fuel Flowing Through a Pressure Atomizing Nozzle at Indicated Pressures.

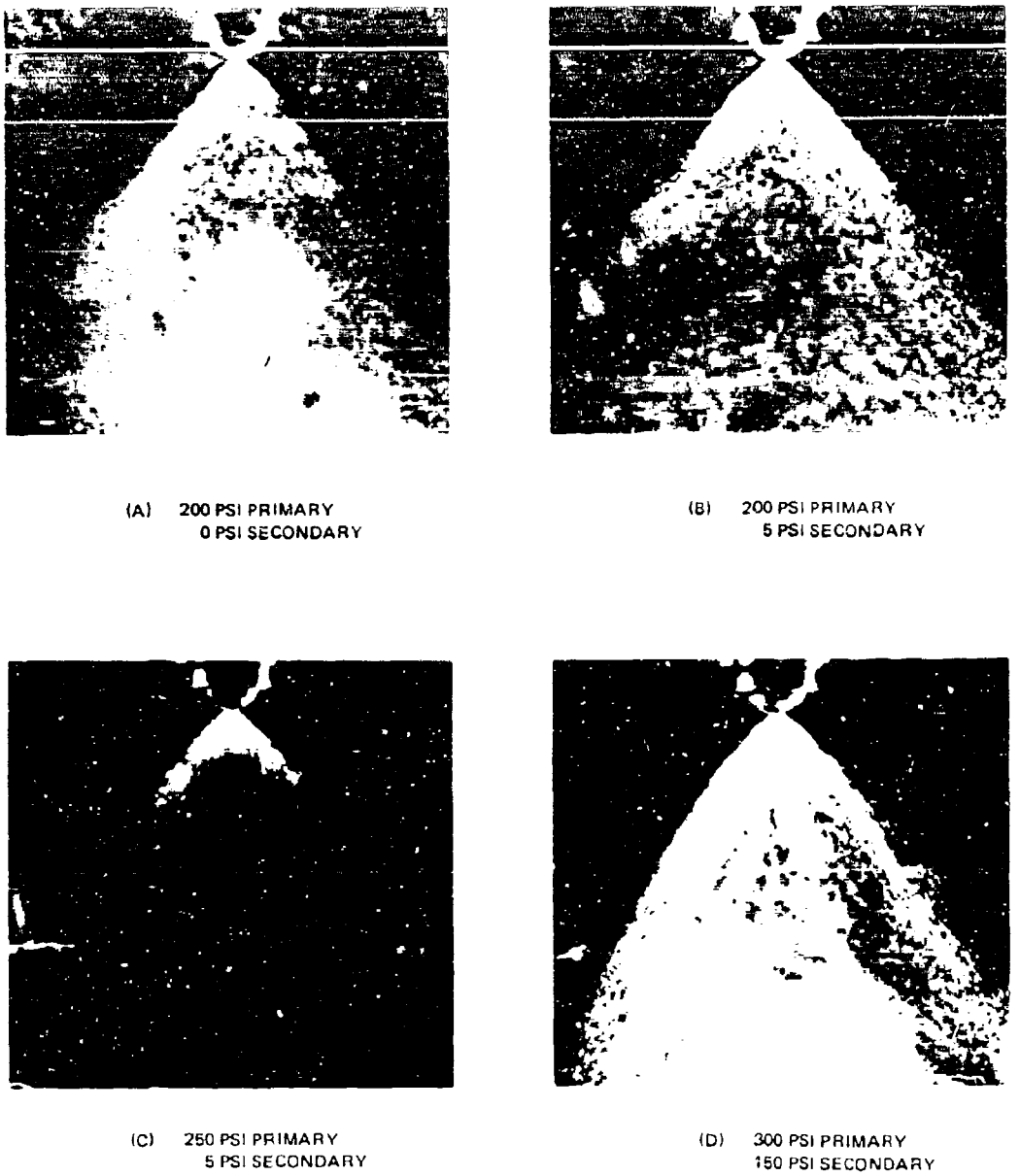

Figure 35. Spray Patterns of JP-4 Fuel Flowing Through a Pressure Atomizing Nozzle at Indicated Pressures.

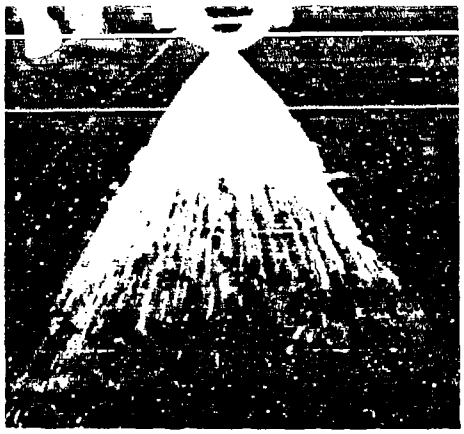

(A) 7 PSI

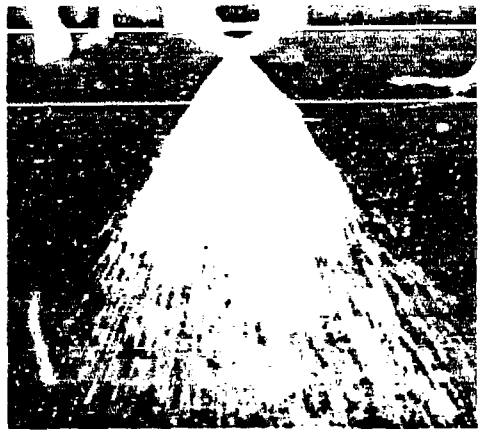

(B) 13.5 PSI

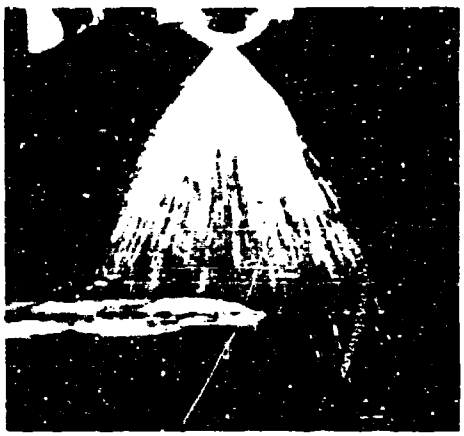

(C) 18 PSI

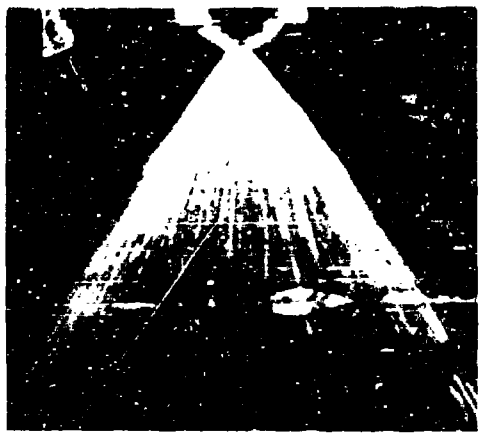

(D) 39 PSI

Figure 36. Spray Patterns of JP-4 Fuel Flowing Through an Air-Assist Nozzle at Indicated Pressures with 2 SCFM Airflow Through the Secondary.

The evaluation of the photographs taken with the air-assist nozzle shows a fairly well developed spray cone at low flows (50 pph) and 2.0 SCFM air-assist (7.2 psi air supply). Some streakiness, however, was apparent with all fuels tested with the air assist fuel nozzle. At higher flow rates, all spray cone patterns were uniform.

7. On the basis of the spray droplet analysis, it was concluded that the atomization characteristics of the emulsified fuels would be entirely satisfactory for combustor testing when using the JT12 pressure atomizing nozzles and marginally satisfactory when using the air-assist fuel nozzles.

Figures 37 and 38 show the droplet size distribution determined for all three emulsified fuels and the reference JP-4 fuel when using the air-assist nozzle at a fuel pressure of 30 and 70 psi with air pressures of 7.2 psi in both cases. Figure 39 presents the droplet size distribution with the pressure atomizing nozzle at 50-55 psi. The largest measured droplet diameter for each fuel for both nozzle types is shown in Table II.

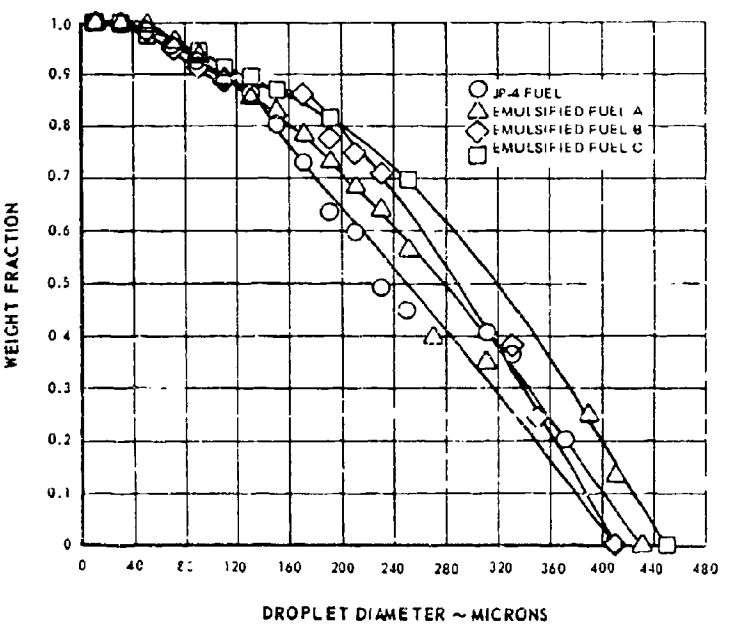

Figure 37. Droplet Size Distribution Measured With Emulsified Fuels A, B, and C and JP-4 Reference Fuel Using Air-Assist Fuel Nozzle Operating at 30-PSI Fuel Pressure and 7.2-PSI Air Pressure.

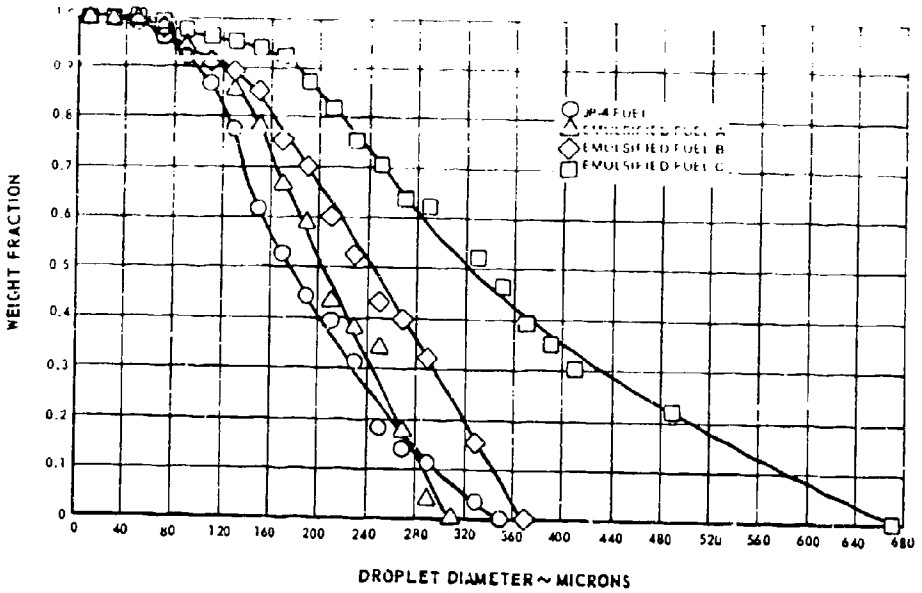

Figure 38. Droplet Size Distribution Measured With Emulsified Fuels A, B, and C and JP-4 Reference Fuel Using Air-Assist Fuel Nozzle Operating at 70-PSI Fuel Pressure and 7.2-PSI Air Pressure.

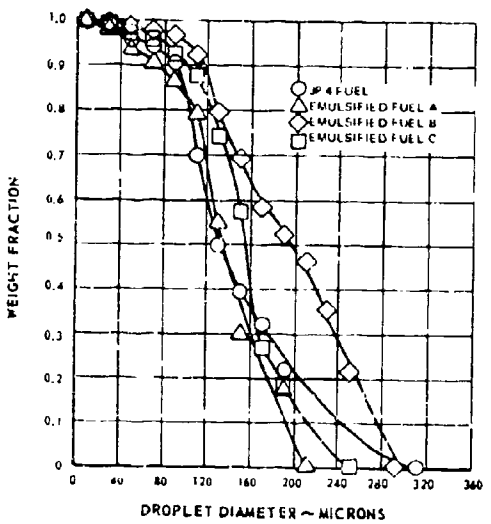

Figure 39. Droplet Size Distribution Measured With Emulsified Fuels A, B, and C and JP-4 Reference Fuel Using Pressure Atomizing Fuel Nozzle Operating at 50-55 PSI Fuel Pressure.

TABLE II. DIAMETERS OF TARGET SUMMARIZED DROPLETS

Fuel Type	Air-Assist Nozzle Light-off Flow (microns)	Air-Assist Nozzle Maximum ΔP Flow (microns)	Pressure Atomizing Nozzle Light-off Flow (microns)
JP-4 Fuel	410	350	310
Emulsified Fuel A	430	310	210
Emulsified Fuel B	410	370	290
Emulsified Fuel C	450	670	250

The atomization characteristics are summarized in Figure 40. This bar chart shows the Sauter Mean Diameter (SMD) for the sprays at the conditions listed in Figures 37, 38, and 39. It would appear that in the case of the air-assist fuel nozzle the atomization capability of this design is strongly influenced by the breakdown characteristics of the emulsified fuel. In this case emulsified fuel C, which exhibits the greatest resistance to breakdown, also produced the coarsest atomization. It appears that the pressure atomizing nozzle design is not greatly influenced by either emulsion breakdown or initial yield value above 50 psi fuel nozzle pressure drop.

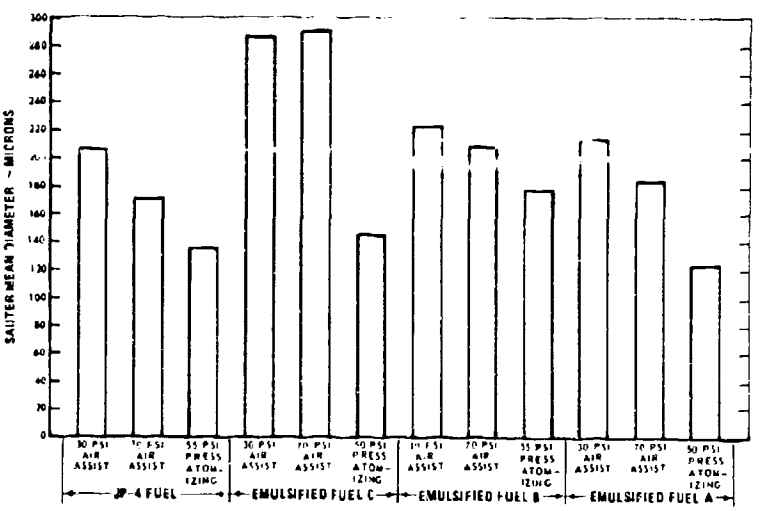

Figure 40. Summary of Atomization Characteristics of Three Emulsified Fuels and JP-4 Reference Fuel Showing Sauter Mean Diameter of Spray Cone Fuel Droplets Measured in Tests With Air-Assist and Pressure Atomizing Fuel Nozzles.

With the present apparatus, it was not possible to get clear photomicrographs of any of the fuels with the pressure atomizing nozzle at 300 psi, therefore, no individual droplet size distribution was attained. However, by using an optical apparatus utilizing a light scattering technique to define spray quality, it was determined that the SMD of the emulsified fuels decreases at the same rate as for JP-4 fuel with increasing pressure drop across the nozzle.

LABORATORY INSPECTION PROGRAM

The results of laboratory testing are summarized in Table III. All values quoted in the table represent an average of at least two determinations for each property and in most cases three determinations were made.

The yield value of the three fuels remained consistent and at a level anticipated for each formulation. Emulsified fuel C increased in yield value by 40 percent between F-1969-A and F-1969-B. This variance could be due to batch-to-batch differences or storage environment. All fuel drums supplied for this program were stored horizontally in drum racks. Some of the fuel, then, was exposed to the weather for a period extending from the Fall through the Winter and well into the Spring.

TABLE III. LABORATORY INSPECTION RESULTS

		Yield Value ($dynes/cm^2$)	Net Heat of Combustion (Btu/lb.)	Water Content (% by wt.)	Specific Gravity
Emulsified Fuel A	F-1957	946	18,400	1.5	0.763
	F-1971-A	1148	18,388	1.5	0.761
	F-1971-B	1150	18,382	1.5	0.758
	F-1971-D	1119	18,310	1.47	0.764
Emulsified Fuel B	F-1958	1906	18,325	0.83	0.778
	F-1972-A	2075	18,275	0.79	0.779
	F-1972-B	1982	18,263	0.90	0.778
	F-1972-D	2190	18,205	1.12	0.775
Emulsified Fuel C	F-1969	946	18,160	1.51	0.775
	F-1969-A	996	18,134	2.70	0.769
	F-1969-B	1380	18,316	2.60	0.775
	F-1969-D	857	18,230	1.87	0.774

The net heat of combustion of the emulsified fuels consistently fell short of the JP-4 specification value of 18,400 Btu/lb net. This reduction in heating value was anticipated due to the presence of water in the emulsions. There is no question that with the loss of heating value there will be a corresponding increase in thrust specific fuel consumption.

The specific gravity of the emulsions was at a level equal to that of JP-4.

The water content of emulsified fuels A and C were found to be at the same levels reported by the fuel suppliers. Emulsified fuel B water content, however, exceeded the anticipated level.

COMBUSTION PROGRAM

1. Results of the combustor performance tests with JP-4 and the pressure atomizing nozzle at the 500°F baseline condition are shown in Figures 41 thru 43. A "best fit" curve has been drawn through the data points and is used as a reference line for the performance comparison with the emulsified fuel data for similar nozzles and inlet conditions. Similar baseline curves have been generated for the other operational combination of inlet temperature and fuel nozzle with JP-4 fuel. These are shown, as required, in the appropriate figures.

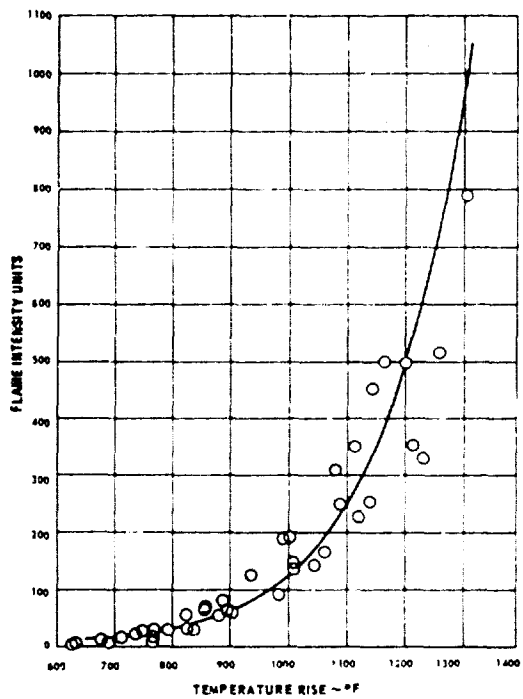

Figure 41. Flame Intensity Measured 8.1 Inches Upstream of the Burner Exit Versus Temperature Rise for JP-4 Fuel With Pressure Atomizing Nozzle at 500°F Inlet Temperature.

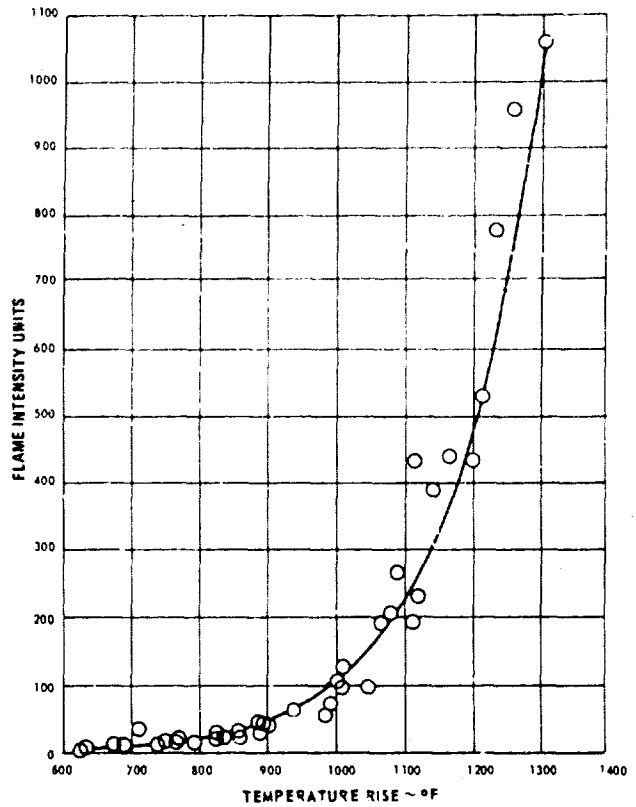

Figure 42. Flame Intensity Measured at Burner Exit Versus Temperature Rise for JP-4 Fuel With Pressure Atomizing Nozzle at 500°F Inlet Temperature.

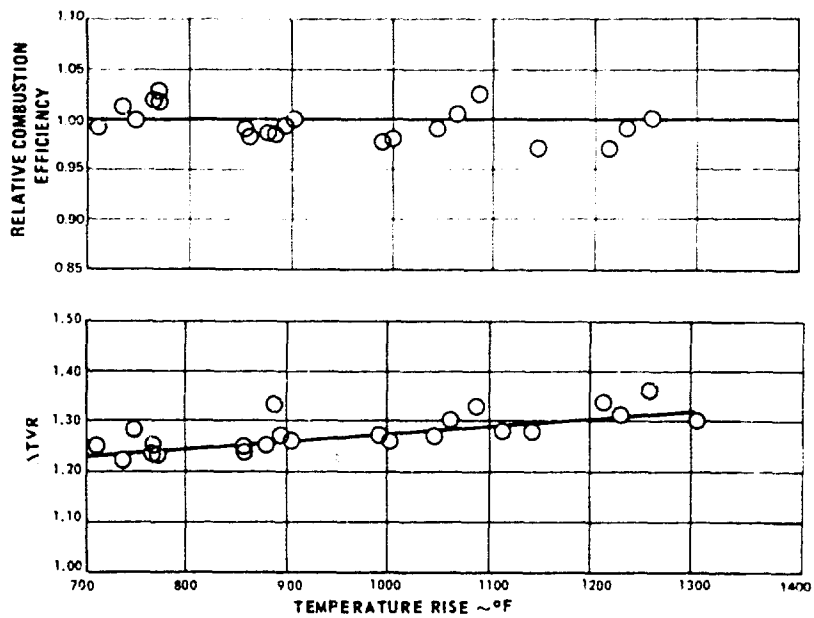

Figure 43. Relative Combustion Efficiency and ΔTVR Versus Temperature Rise of JP-4 Fuel With Pressure Atomizing Nozzle at 500°F Inlet Temperature.

2. The flame intensity measured 8.1 inches upstream of the burner exit was found to be higher than the JP-4 500°F baseline for all the emulsified fuels. As shown in Figures 44 and 45, combustion activity with the emulsified fuels and the pressure atomizing and air-assist nozzle is higher than with the JP-4 fuel and the pressure atomizing nozzle for the 500°F burner inlet baseline.

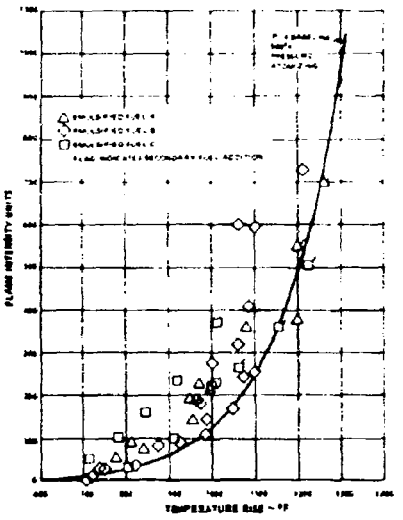

Figure 44. Flame Intensity Measured 8.1 Inches Unpstream of the Burner Exit Plane Versus Temperature Rise With Pressure Atomizing Nozzle at 500°F Inlet Temperature.

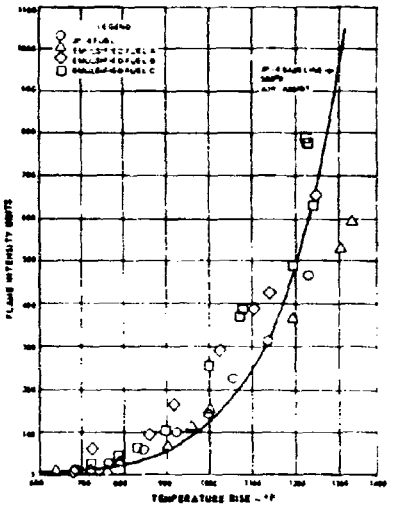

Figure 45. Flame Intensity Measured 8.1 Inches Upstream of the Burner Exit Plane Versus Temperature Rise With Air-Assist Nozzle at 500°F Inlet Temperature.

3 The flame intensity measured 8.1 inches upstream of the burner exit was found to be the same as the JP-4 800°F baselines for all emulsified fuels. As shown in Figures 46 and 47, combustion activity with the emulsified fuels is very similar to that of the JP-4 fuel with pressure atomizing or air-assist nozzles and 800°F burner inlet baseline.

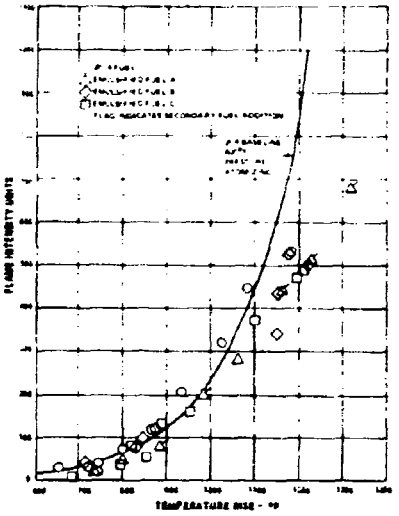

Figure 46. Flame Intensity Measured 8.1 Inches Upstream of the Burner Exit Plane Versus Temperature Rise With Pressure Atomizing Nozzle at 800°F Inlet Temperature.

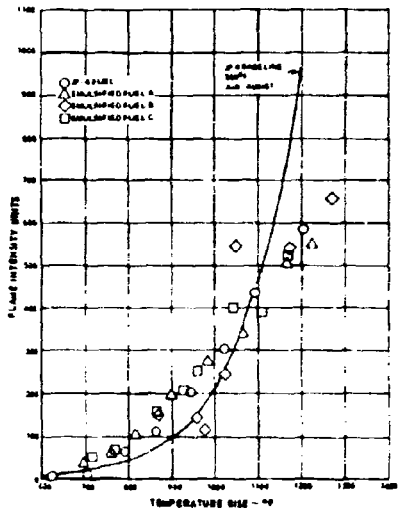

Figure 47. Flame Intensity Measured 8.1 Inches Upstream of the Burner Exit Plane Versus Temperature Rise With Air-Assist Nozzle at 800°F Inlet Temperature.

It appears that when using emulsified fuels that flame intensity measured 8.1 inches upstream of the burner exit was found to be a function of inlet conditions. As such, shorter (high intensity) burners with moderate compressor discharge temperatures (below 800°F) would be expected to encounter problems with emulsified fuels.

4. The flame intensity at the burner exit was found to be the same for the emulsified fuels and the JP-4 baseline when using the pressure atomizing injection system. As shown in Figures 48 and 49, there was no significant difference in combustion activity at the burner exit between all the emulsified fuels and the JP-4 baseline fuel at either the 500°F or the 800°F burner inlet temperature condition.

5. At 500°F inlet temperature, the flame intensity at the burner exit was found to be slightly higher for the air-assist nozzle and emulsified fuels B and C, as shown in Figure 50. However, very little difference was noted between the emulsified fuels and JP-4 at the 800°F inlet condition, as shown in Figure 51.

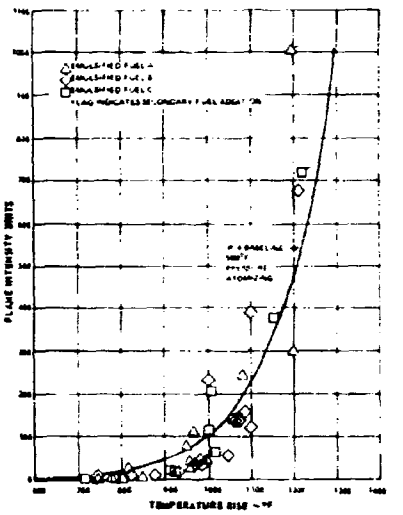

Figure 48. Flame Intensity Measured at the Burner Exit Plane Versus Temperature Rise With Pressure Atomizing Nozzle at 500°F Inlet Temperature.

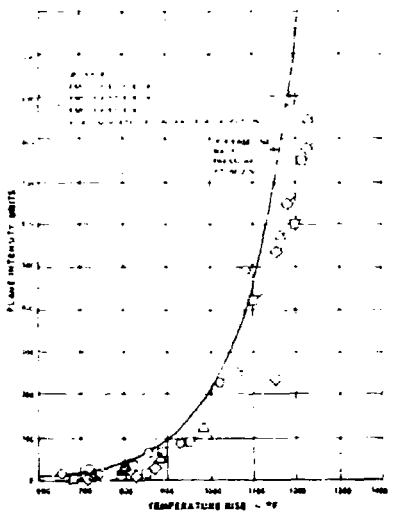

Figure 49. Flame Intensity Measured at the Burner Exit Plane Versus Temperature Rise With Pressure Atomizing Nozzle at 800°F Inlet Temperature.

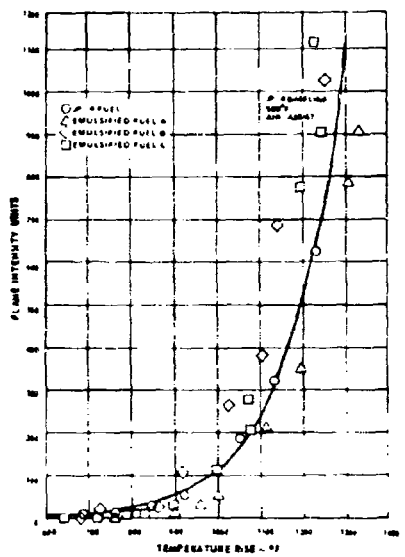

Figure 50. Flame Intensity Measured at the Burner Exit Plane Versus Temperature Rise With Air-Assist Nozzle at 500°F Inlet Temperature.

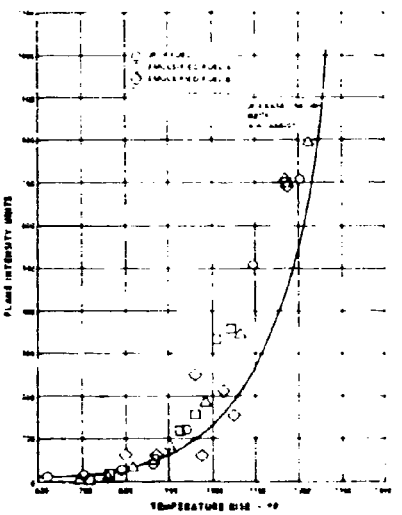

Figure 51. Flame Intensity Measured at the Burner Exit Plane Versus Temperature Rise With Air-Assist Nozzle at 800°F Inlet Temperature.

6. No loss in combustion efficiency could be attributed to running on the emulsified fuels compared at similar inlet conditions and configurations with JP-4 fuel. The relative combustion efficiencies for the emulsified fuels are compared to that of JP-4 in Figures 52 through 55. All efficiency values were calculated on the following net heating values: JP-4 (18,500 Btu/lb), emulsified fuel A (18,390 Btu/lb), emulsified fuel B (18,288 Btu/lb), and emulsified fuel C (18,200 Btu/lb). The net heating values for emulsified fuels were based on the averages of the laboratory-measured heating values, as shown in Table III. The combustion products for the emulsified fuels and JP-4 are given in Table IV.

7. Except for CO content when running emulsified fuel B with the air-assist nozzle, there was no significant difference between exhaust gas components for the four fuels. (See Table IV.) Although the sulfur dioxide content of the emulsified fuel is shown higher than JP-4, the absolute quantity measured is still very low. On this basis it was judged that the sulfur content of the emulsified fuels was comparable to that of JP-4 fuel. Attempts were made to determine the amount of particulates in the exhaust; but because of the accumulation of water in the filter holder, no meaningful data were obtained. Extensive modification of the holder or greater heating of the gas sampling line would have been required to correct the situation.

8. Burner exit temperature pattern factor (ΔTVR) was nearly identical with the emulsified fuels and JP-4 at design temperature rise of 1200°F for the pressure atomizing nozzle, as shown in Figures 52 and 53. There appears, however, to be a slight increase in temperature factor for emulsified fuels, especially emulsified fuel C, at the burner lower temperature rise for the 500°F inlet condition.

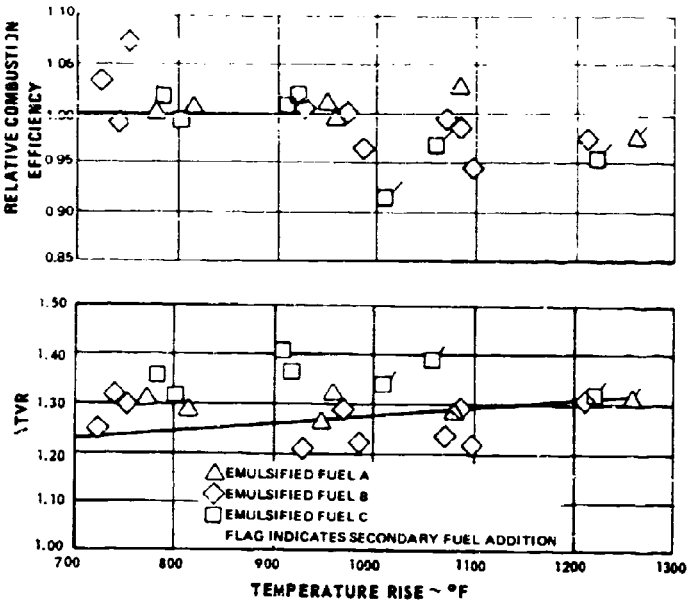

Figure 52. Relative Combustion Efficiency and ΔTVR Versus Temperature Rise With Pressure Atomizing Nozzle at 500°F Inlet Temperature.

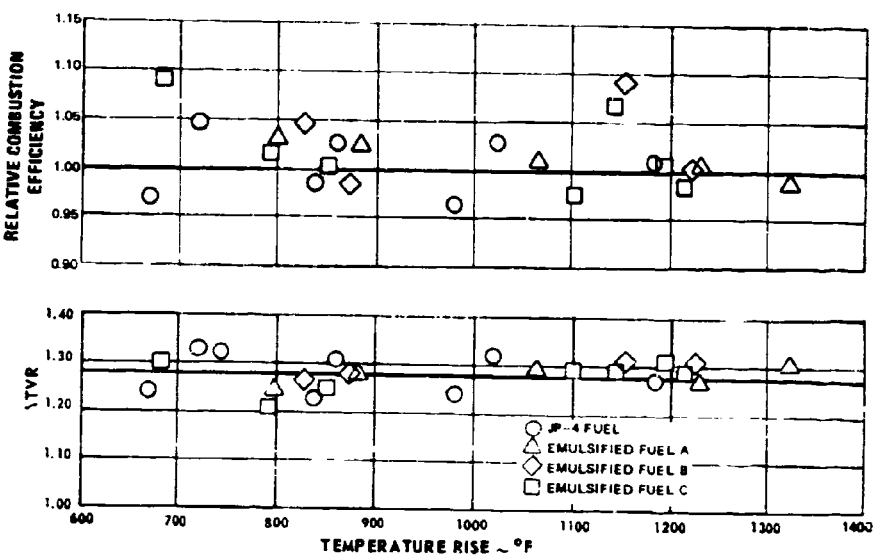

Figure 53. Relative Combustion Efficiency and ΔTVR Versus Temperature Rise With Pressure Atomizing Nozzle at 800°F Inlet Temperature.

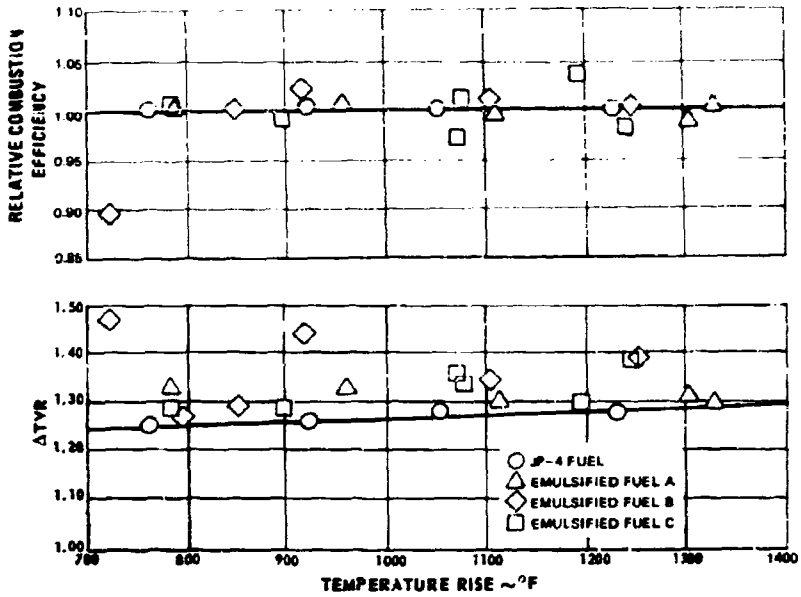

Figure 54. Relative Combustion Efficiency and ΔTVR Versus Temperature Rise With Air-Assist Nozzle at 500°F Inlet Temperature.

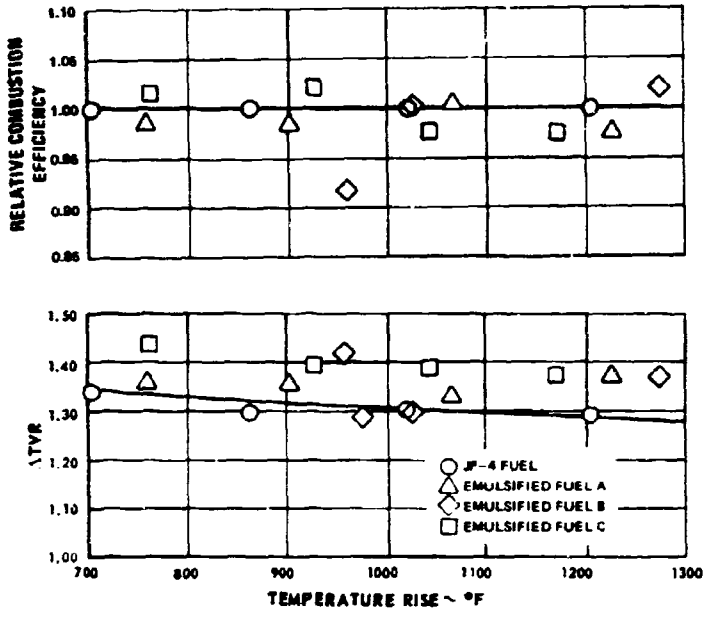

Figure 55. Relative Combustion Efficiency and ΔTVR Versus Temperature Rise With Air-Assist Nozzle at 800°F Inlet Temperature.

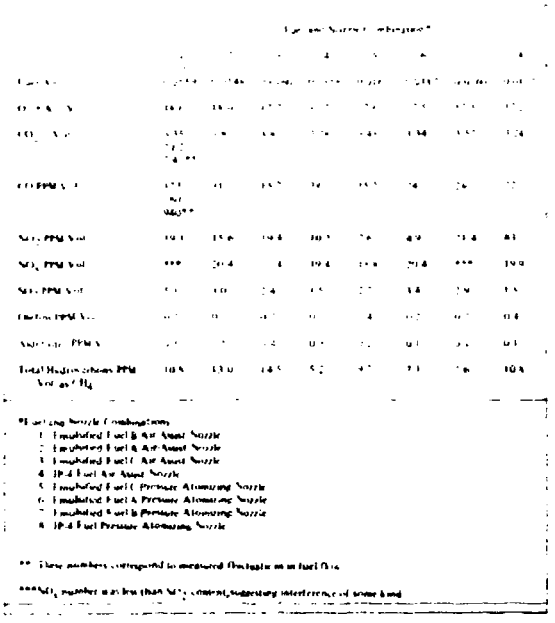

9. Burner exit temperature pattern factor (ΔTVR) appears to be somewhat higher with the emulsified fuels and JP-4 for the air-assist nozzle, as shown in Figures 54 and 55. This difference increases at the lower temperature rise conditions.

10. Smoke emission with emulsified fuels A and C was found to be consistently less, whereas emulsified fuel B smoke emission was equal to or greater than that measured with JP-4 fuel under the same conditions, as shown by Figures 56 through 59. An increase in smoke emission was noted for all fuels with the air-assist nozzle at 500°F inlet temperature (Figure 58). At 800°F inlet temperature, there was no significant difference in smoke emission between the pressure atomizing and air-assist nozzle for JP-4 fuels (Figures 57 and 59).

11. No significant change in burner exit radial average profiles was measured with emulsified fuels compared to the baseline tests. Typical radial average burner exit temperature profiles are shown in Figures 60 through 63. Although some variations in profile were observed in the various baseline and emulsified fuel tests, it was concluded that no significant shift of the location of the average maximum peak temperature could be attributed to the use of emulsified fuels. A shift of the average maximum peak temperature toward the I.D. would have deleterious effect on the durability of the first stage turbine blade.

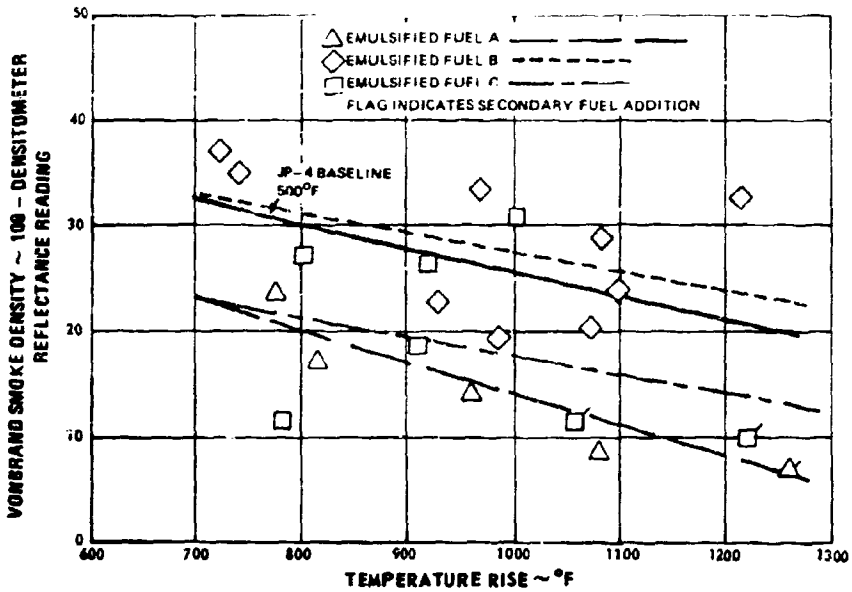

Figure 56. Smoke Density Versus Temperature Rise With Pressure Atomizing Nozzle at 500°F Inlet Temperature.

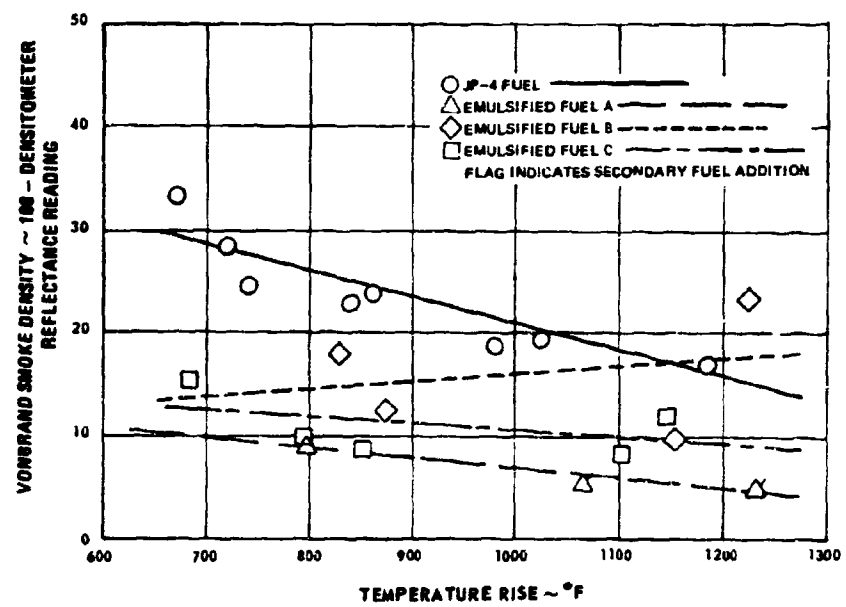

Figure 57. Smoke Density Versus Temperature Rise With Pressure Atomizing Nozzle at 800°F Inlet Temperature.

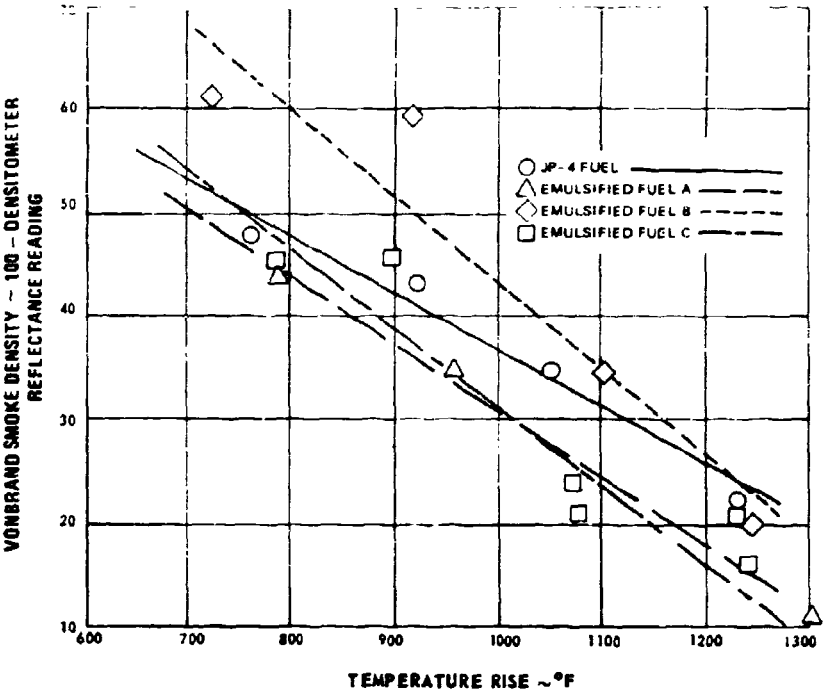

Figure 58. Smoke Density Versus Temperature Rise With Air-Assist Nozzle at 500°F Inlet Temperature.

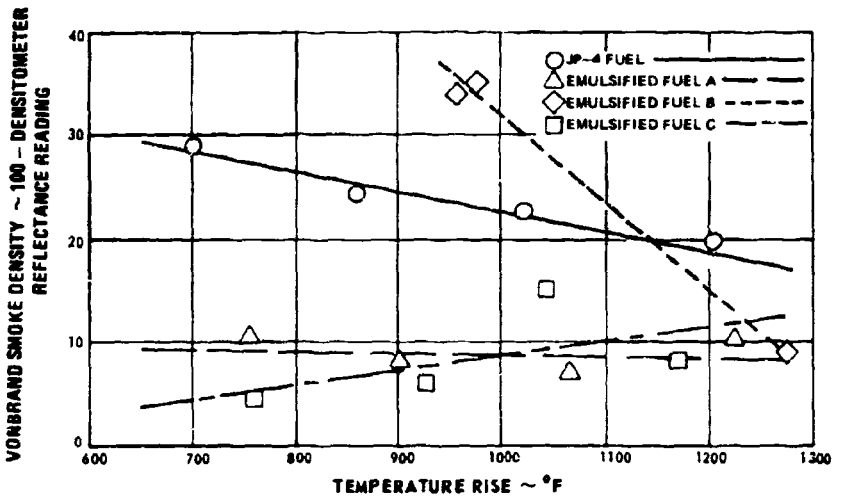

Figure 59. Smoke Density Versus Temperature Rise With Air-Assist Nozzle at 800°F Inlet Temperature.

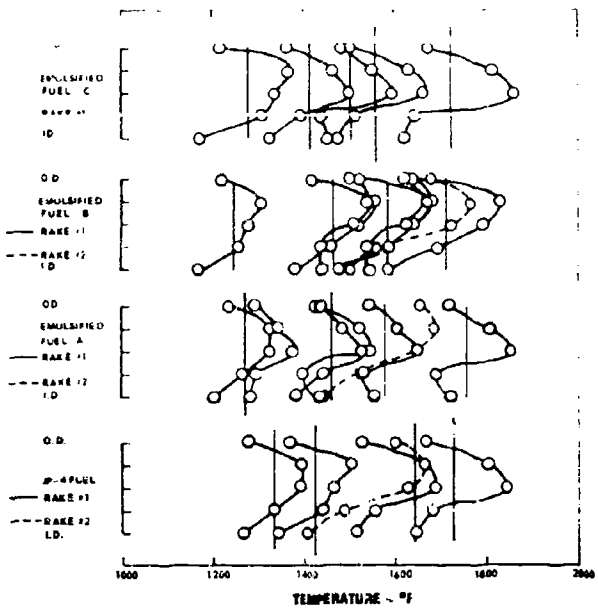

Figure 60. Average Radial Burner Exit Temperature Profiles When Running With Pressure Atomizing Nozzle at 500°F Inlet Temperature.

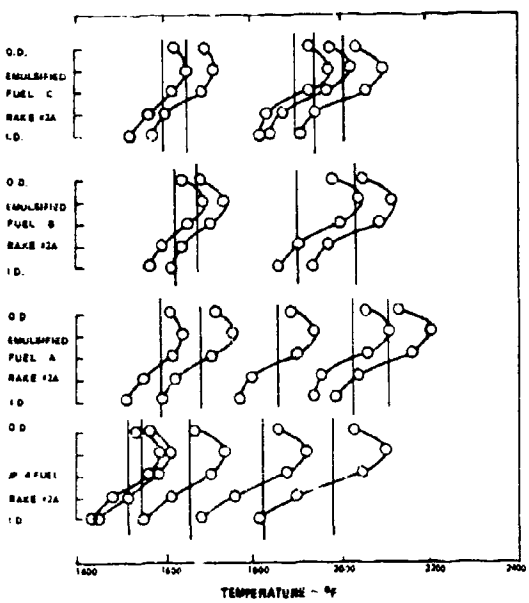

Figure 61. Averag Radial Burner Exit Temperature Profiles When Running With Pressure Atomizing Nozzle at 860°F Inlet Temperature.

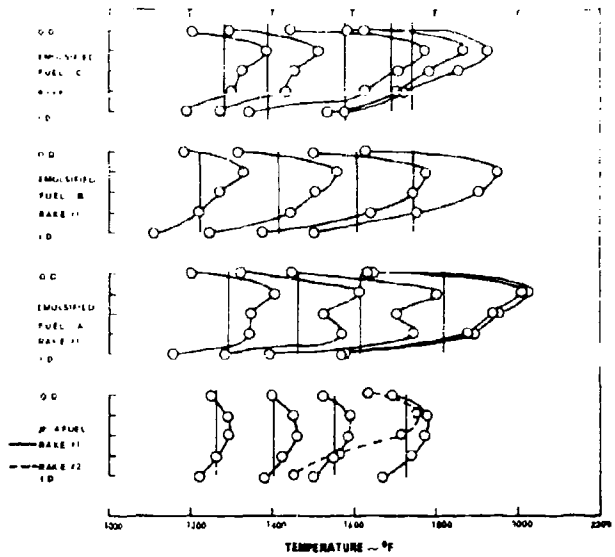

Figure 62. Average Radial Burner Exit Temperature Profiles When Running With Air-Assist Nozzle at 500°F Inlet Temperature.

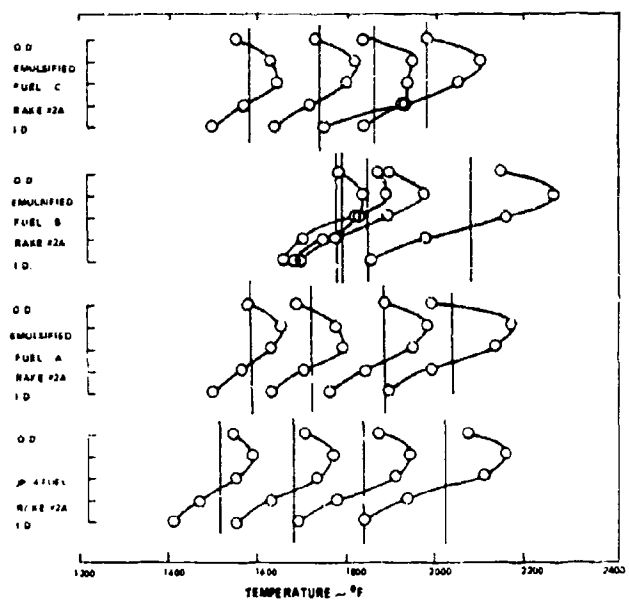

Figure 63. Average Radial Burner Exit Temperature Profiles When Running With Air-Assist Nozzle at 800°F Inlet Temperature.

12. Burner skin durability did not appear to be affected by the fuel injection system. Skin temperature patterns obtained when operating at 500°F burner inlet temperature with JP-4 fuel and the pressure atomizing or air-assist nozzle were almost identical.

13. Burner skin durability did not appear to be affected by the use of any of the emulsified fuels. Skin temperature patterns obtained when operating at 500°F burner inlet temperature with the three emulsified fuels and the pressure atomizing and air-assist nozzles were very similar, and in some cases essentially identical temperature patterns were noted for the different emulsions and JP-4 fuel. Skin temperatures as measured by stitch thermocouples placed in the burner liner, as shown in Figure 64, for the three emulsified fuels and two fuel injection schemes are presented in Table V.

Figure 64. Burner Liner for Combustion Tests Showing Installation of Skin Thermocouples.

TABLE V. COMPARISON OF BURNER SKIN TEMPERATURES

Fuel	Nozzle Type	Fuel Flow (lb/hr)	Burner Inlet Temp (°F)	Temp Rise (°F)	Temp* Louver No. 1 (°F)	Temp* Louver No. 2 (°F)	Temp* Louver No. 3 (°F)	Temp* Louver No. 4 (°F)	Temp* Louver No. 5 (°F)
JP-4 Fuel	Pressure Atomizing	145.0	500	1125	1260/1265	1140/1165	1150/1145	1025/1110	1025/1010
Emulsified Fuel A	Pressure Atomizing	137.0	500	1125	1225/1170	1110/1125	1125/1115	1000/1080	990/ 970
Emulsified Fuel B	Pressure Atomizing	140.7	500	1125	1280/1230	1150/1170	1180/1160	1040/1125	1035/1015
Emulsified Fuel A	Pressure Atomizing	145.0	500	1125	1245/1225	1145/1160	1170/1150	1035/1120	1040/1010
JP-4 Fuel	Air-Assist	145.0	500	1125	-	1305/1378	1275/1280	1060/1185	1070/1030
Emulsified Fuel A	Air-Assist	151.0	500	1125	-	1295/1370	1225/ -	1170/1200	1185/1060
Emulsified Fuel B	Air-Assist	144.0	500	1125	-	1290/1365	1270/1295	1065/1180	1070/1045
Emulsified Fuel C	Air-Assist	147.0	500	1125	-	1270/1345	1230/ -	1020/1150	1025/1000

*Temperature read at 2 thermocouples on each louver

14. No significant difference in snap acceleration characteristics was recorded between the emulsified fuels and JP-4 at baseline conditions for either the pressure atomizing fuel nozzle or the air-assist nozzle, as shown in Figures 65 and 66. Steady-state conditions were attained within 3 to 4 seconds after snap acceleration (reference Appendix I). It is interesting to note in Figure 66 that the rate of nozzle pressure increase is higher for emulsified fuels than for JP-4, probably, in part, due to the lower flow-pressure characteristics of the emulsified fuels, as shown by Figure 22

15. Light-off test recordings at sea level conditions indicated no unsatisfactory characteristics for any emulsified fuel as compared to JP-4 for either the pressure atomizing fuel nozzle or the air-assist nozzle, as shown in Figures 67 and 68. Average light-off times at sea level conditions are listed in Table VI. Although the light-off times with the air-assist nozzle and emulsified fuels lag consistently behind the JP-4 fuel, this is not considered detrimental since under the same conditions the times compare favorably with the times established with the pressure atomizing nozzle.

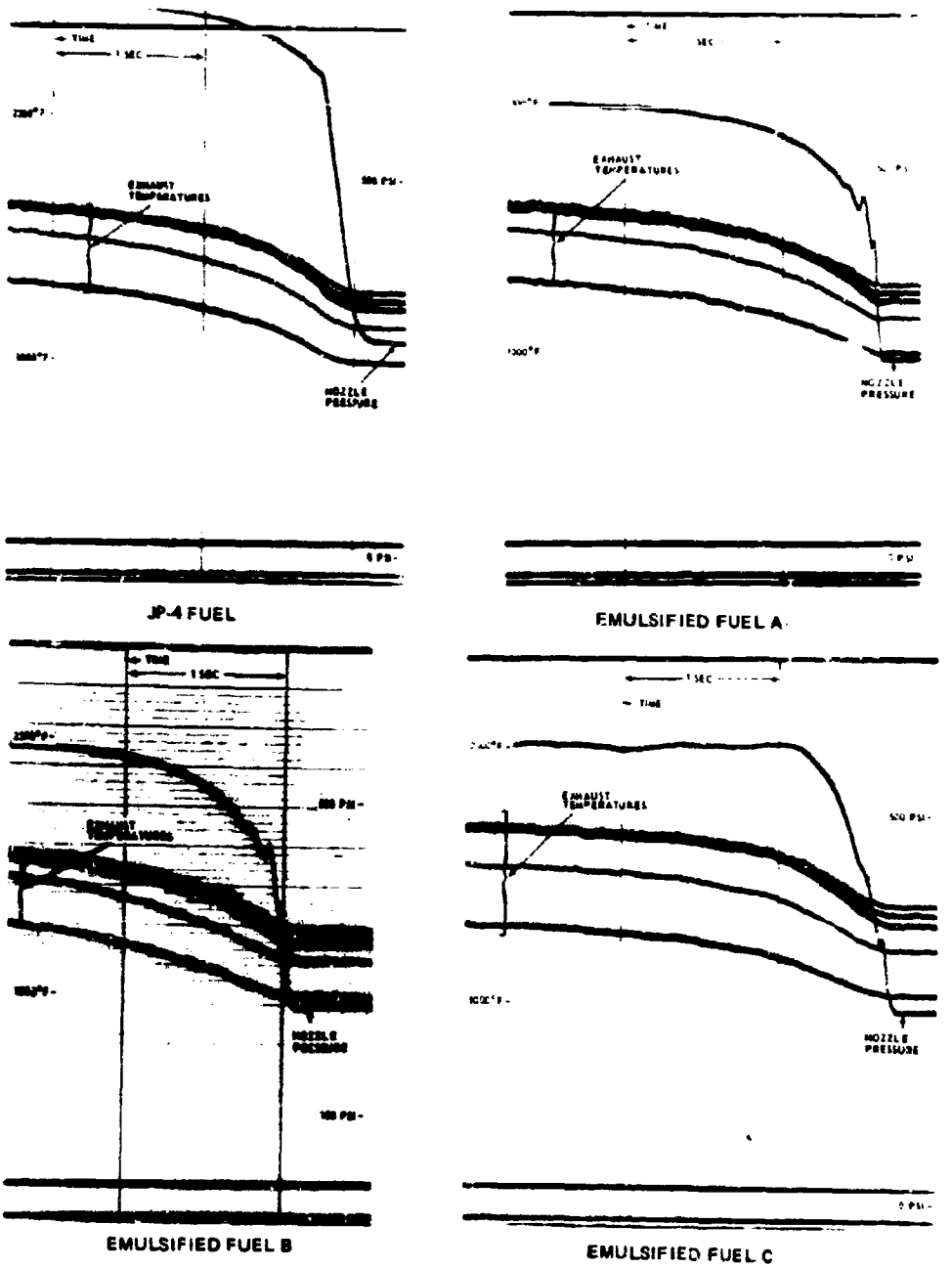

Figure 65. Transient Test Recorder Traces Showing Fuel Pressure and Exhaust Temperature Fluctuation When Varying Fuel Flow From Point 2 to Point 7 Test Conditions Using a Pressure Atomizing Nozzle with JP-4 and Emulsified Fuels.

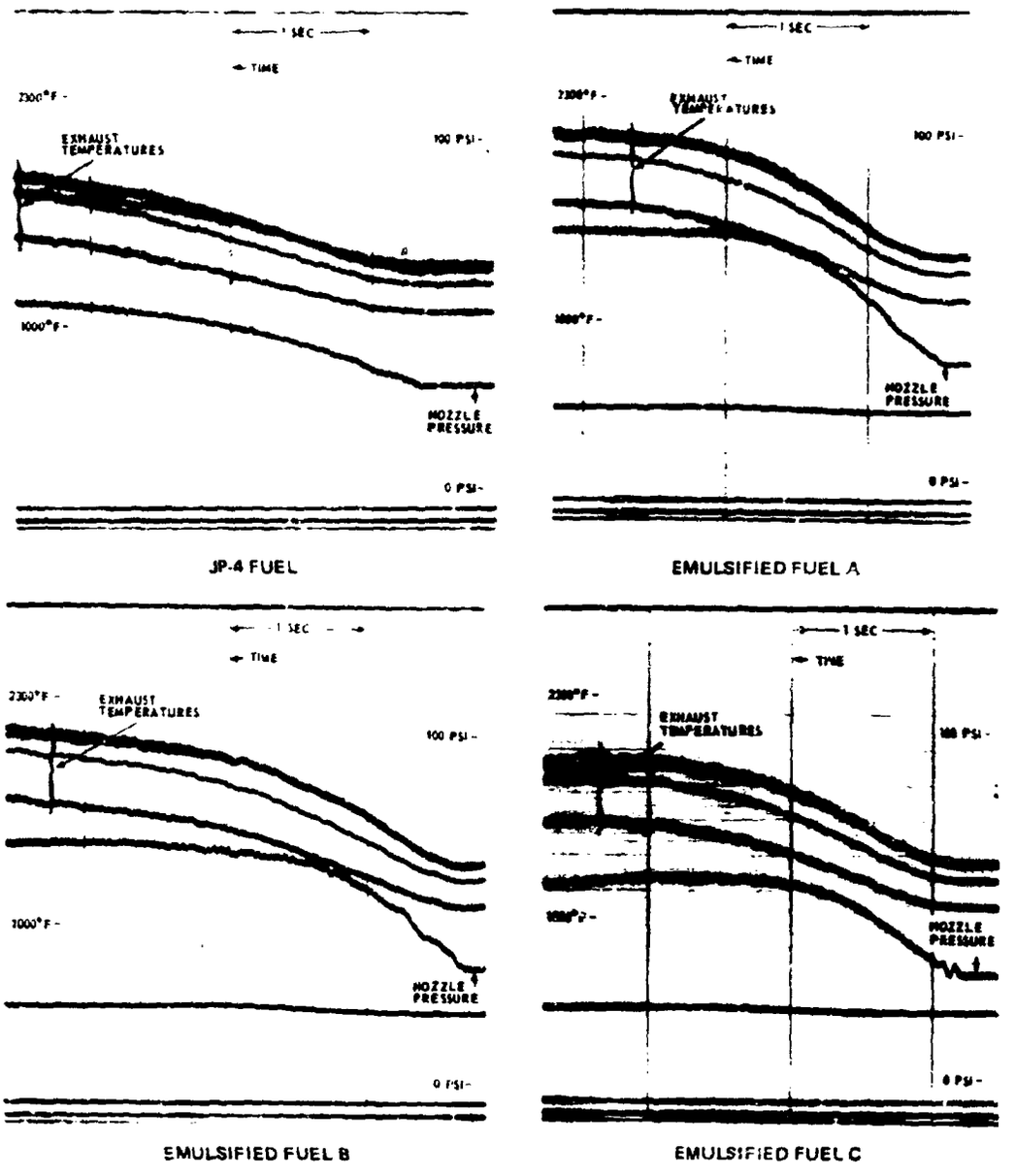

Figure 66. Transient Test Recorder Traces Showing Fuel Pressure and Exhaust Temperature Fluctuation When Varying Fuel Flow From Point 2 to Point 7 Test Conditions Using an Air-Assist Nozzle with JP-4 and Emulsified Fuels.

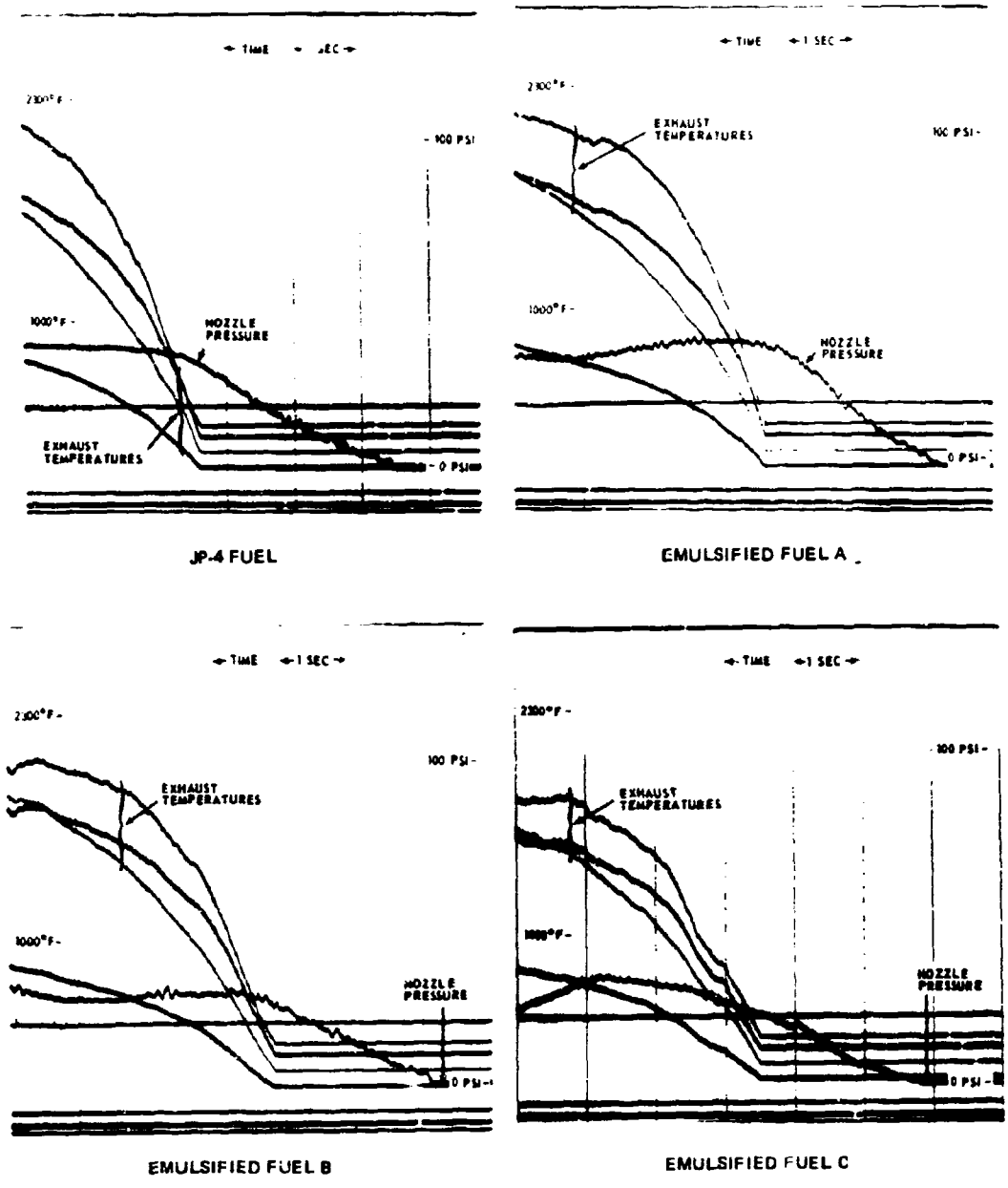

Figure 67. Light-off Test Recorder Traces Showing Elapsed Time Between Nozzle Pressure Buildup and Ignition When Using a Pressure Atomizing Nozzle With JP-4 and Emulsified Fuels.

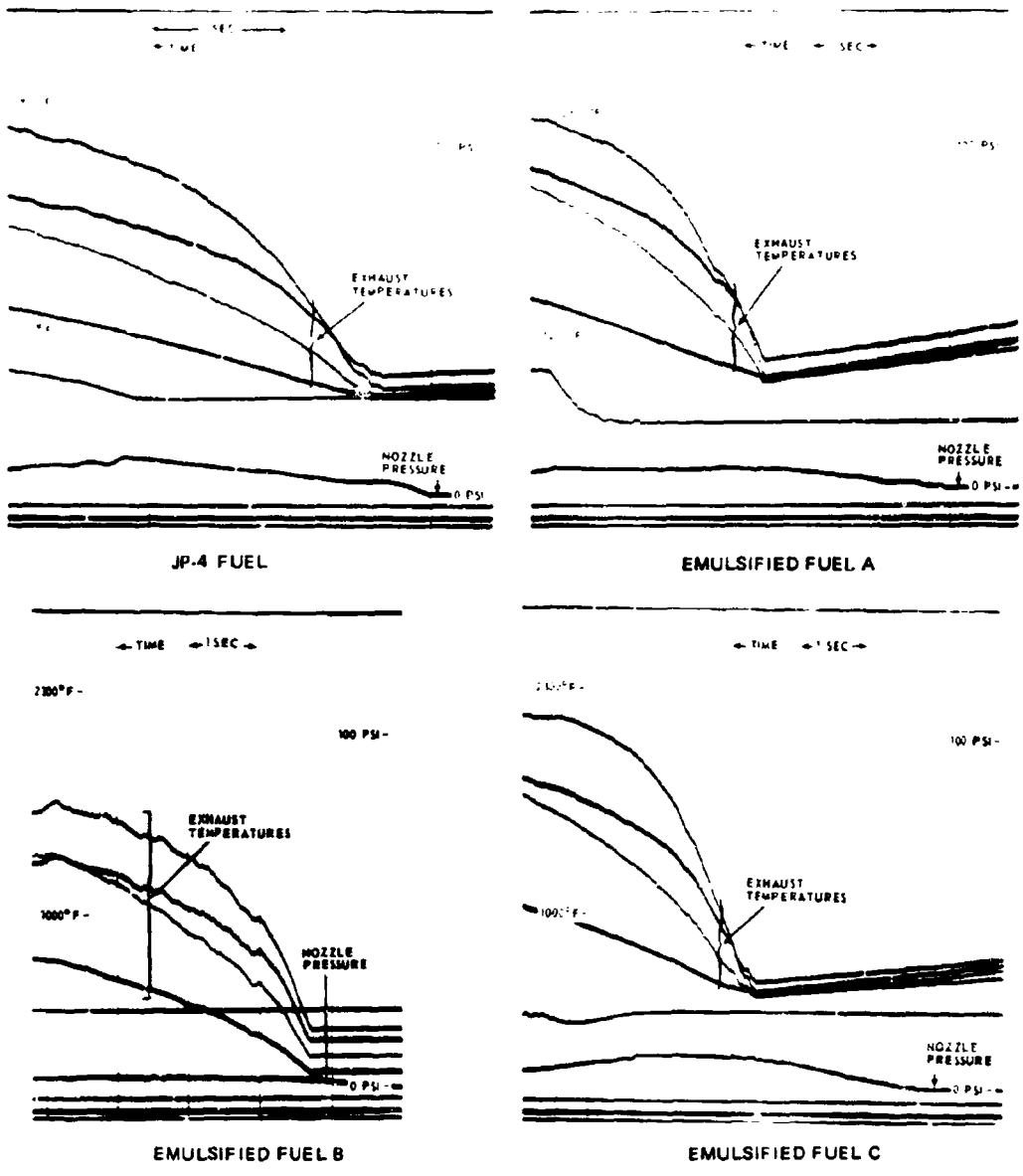

Figure 68. Light-off Test Recorder Traces Showing Elapsed Time Between Nozzle Pressure Buildup and Ignition When Using an Air-Assist Nozzle With JP-4 and Emulsified Fuels.

TABLE VI. AVERAGE LIGHT-OFF TIMES AT SEA LEVEL

Fuel	Pressure Atomization Nozzle (seconds)	Air-Assist Nozzle (seconds)
JP-4 Fuel	2.51	0.33
Emulsified Fuel A	2.07	2.86
Emulsified Fuel B	1.83	1.13
Emulsified Fuel C	1.87	1.54

Static Conditions – Fuel Flow – 55 lb/hr
Air flow – 585 lb/hr
Air temperature – 100°F
Ignition – 4 joules
Fuel temperature – ambient

16. Numerous instances of plugging the fuel nozzle primary screen (0.009 in. diameter perforations) were experienced when running with emulsified fuels. A typical laboratory examination of the material plugging the primary screen was performed as follows: Micro-examination of deposits removed from the nozzle screen showed carbonaceous fibers and brown metallic materials present. Spectro-analysis showed the metallic material to be predominately iron, with smaller amounts of nickel, aluminum, silicon, copper, silver, and zinc. Infrared and chromatographic analysis of chloroform extract of a small amount of the deposit indicated a material similar to oil.

    No particular correlation between plugging and operation with any given emulsified fuel was established. The frequency of plugging did not seem to be related to either the fuel used or the running conditions.

17. No excessive deposits on the burner liner interior or buildup around the fuel nozzle face was encountered during the combustion tests. The one exception was that discovered after running emulsified fuel B at 500°F burner inlet temperature with the pressure atomizing nozzle, as shown by Figure 69. A semihard carbon deposit had formed on the swirler vanes, partially closing the swirler passages.

18. Test results, as shown by Figure 70, indicate some loss in relight capability at the low airflow range (i.e., low forward speed and therefore lower compressor windmill rotation). This loss could account for approximately 5,000 feet in altitude in this range for a typical aircraft installation. There appears to be no loss in relight capability with the emulsified fuels relative to JP-4 at the higher flight speeds.

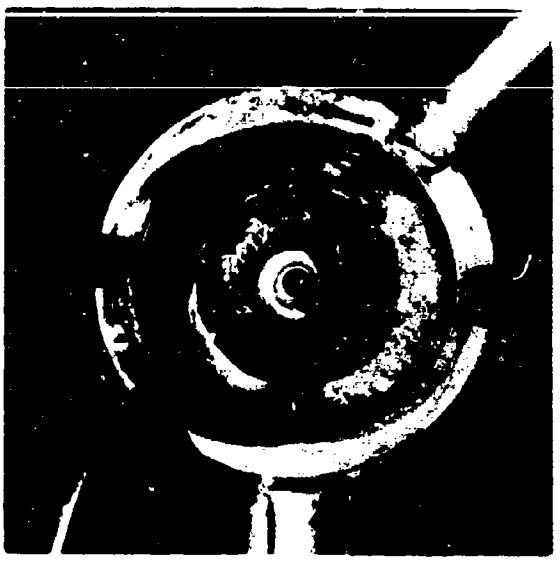

Figure 69. Nozzle Nut Assembly of Pressure Atomizing Nozzle After Test With Emulsified Fuel B at 500°F Inlet Temperature. (View Looking Upstream Shows Carbon Deposits in the Air Swirl Passages of the Nozzle Nut.)

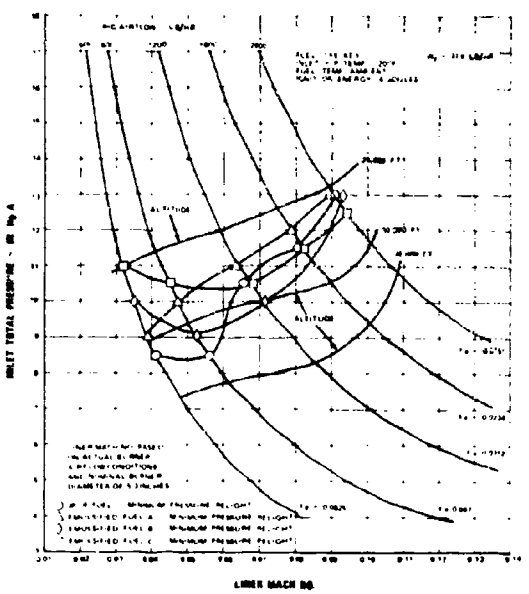

Figure 70. Comparison of Minimum Pressures and Mach Numbers Required by JP-4 and Emulsified Fuels for Burner Relight.

19. Lean blowout tests at sea level conditions indicate no deterioration in lean stability for any emulsified fuel compared to JP-4. Table VII lists lean stability data for JP-4 and the emulsified fuels. Fuel air ratios shown for JP-4 were based on instantaneous fuel-flow rate readings at blowout. Fuel air ratios for the emulsified fuels were based on fuel-flow rates measured during a continuous burning condition at which blowout appeared imminent, due to the lack of reliable instantaneous flow measuring device. The above conclusion was based upon these data together with numerous unrecorded observations made during the corrosion testing.

TABLE VII. LEAN STABILITY LIMITS

Fuel	Fuel Nozzle Type	Inlet Air Temp. (°F)	Lean Limit Fuel-Air Ratio*
JP-4	Air-Assist	500	0.0026
JP-4	Air-Assist	800	0.0026
JP-4	Pressure Atomizing	500	0.0030
Emulsified Fuel A	Air-Assist	500	0.0067
Emulsified Fuel A	Air-Assist	800	0.0064
Emulsified Fuel A	Pressure Atomizing	500	0.0061
Emulsified Fuel A	Pressure Atomizing	800	0.0056
Emulsified Fuel B	Air-Assist	500	0.0039
Emulsified Fuel B	Pressure Atomizing	800	0.0057
Emulsified Fuel C	Air-Assist	500	0.0060
Emulsified Fuel C	Pressure Atomizing	800	0.0062

*Fuel air ratio based on instantaneous fuel flow rate at blowout for JP-4 fuel air ratio based on fuel flow rate for continuous burning, blowout imminent for all emulsified fuels.

CORROSION PROGRAM

Pre-Test Performance and Choke Plane Calibration

Results from the pre-test calibration in terms of temperature pattern and combustion efficiency showed JP-4 to be within satisfactory limits when compared to previous combustion data generated in another test stand with JP-4 fuel. The temperature pattern generated for the 1700° and 2000°F corrosion test points is shown in Figures 71 and 72. The same figures show the vane leading edge metal skin temperatures with JP-4 fuel measured by the imbedded thermocouple described earlier. A comparison of the exhaust gas and vane temperatures indicates that the maximum vane surface temperature is approximately 200°F cooler than the local surrounding gas temperature while operating at an overall average exit temperature of 2000°F. Pyrometer readings taken while sighting at the hottest portions of the vane leading edge has confirmed this thermocouple measurement. This local hot spot (approximately 2100°F) imposed a severe local hardship on the metal since this is near the incipient melting point.

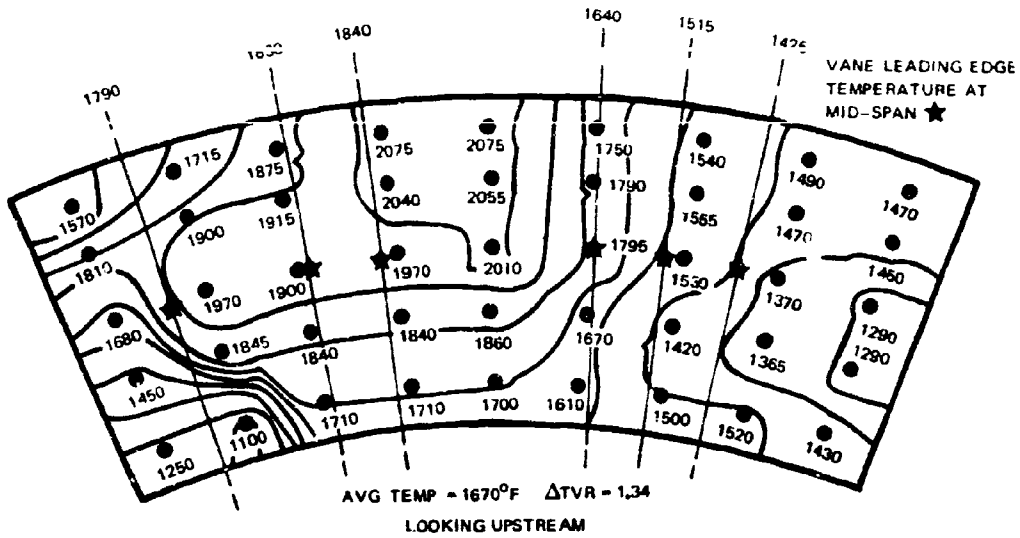

Figure 71. Typical Gas Temperature Profile at Vane Pack Location Showing Isotherm Pattern at 100°F Intervals and Temperature at Data Points.

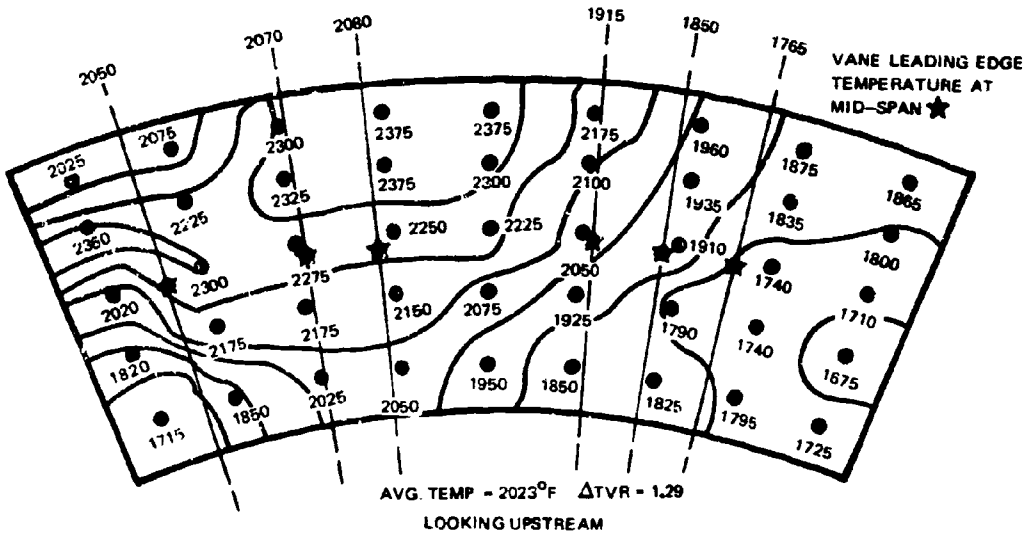

Figure 72. Typical Gas Temperature Profile at Vane Pack Location Showing Isotherm Pattern at 100°F Intervals and Temperature at Data Points.

Vane surface temperatures were found to be approximately 100°F lower than the local surrounding gas temperature while operating at 1700°F overall average burner exit gas temperature. The maximum surface temperature of the vanes was therefore estimated at approximately 1950°F.

The cold and hot choke plane calibrations as indicated by the pressure instrumented vane pack show that completely choked flow across all vanes would be attainable at the corrosion test conditions. Figure 73 shows the variation in turbine inlet flow parameter with pressure ratio across the throat of the vane pack for various gas temperatures. It can be seen that choking conditions are established at and above pressure ratios of 1.84. The stagnation pressure in this instance is derived from total pressure loss data measured from the pre-test calibrations as well as previous combustion performance data. The conditions at which the combustor was run for the corrosion tests are indicated in the same figure for reference. This indicates that the tests were run under hard choke conditions. The location of the choke plane is indicated by Figure 74. This figure also shows the variation in static pressure along the chord of the vane for several flow conditions. Indications are that the throat, and therefore a sonic condition, occurs at the 65 percent station. A supersonic flow regime exists to the 72 percent chord station when operating under hot conditions. It was demonstrated that a shock condition could be induced at the 72 percent station by a slight increase in the downstream pressure after the vane pack. Based on this, it is estimated that the shock condition exists between 75 to 85 percent of the chord during corrosion tests. A comparison of the static pressure variations along the vanes next to the end walls of the vane holding fixture indicated that sonic conditions are maintained there as well as in the center stream of the burner exit.

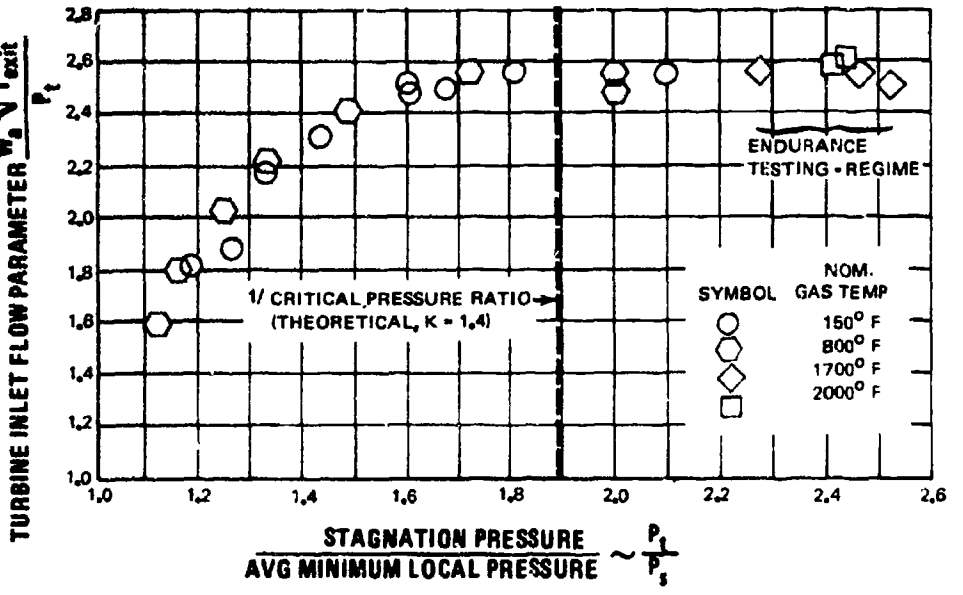

Figure 73. Vane Pack Choke Characteristics.

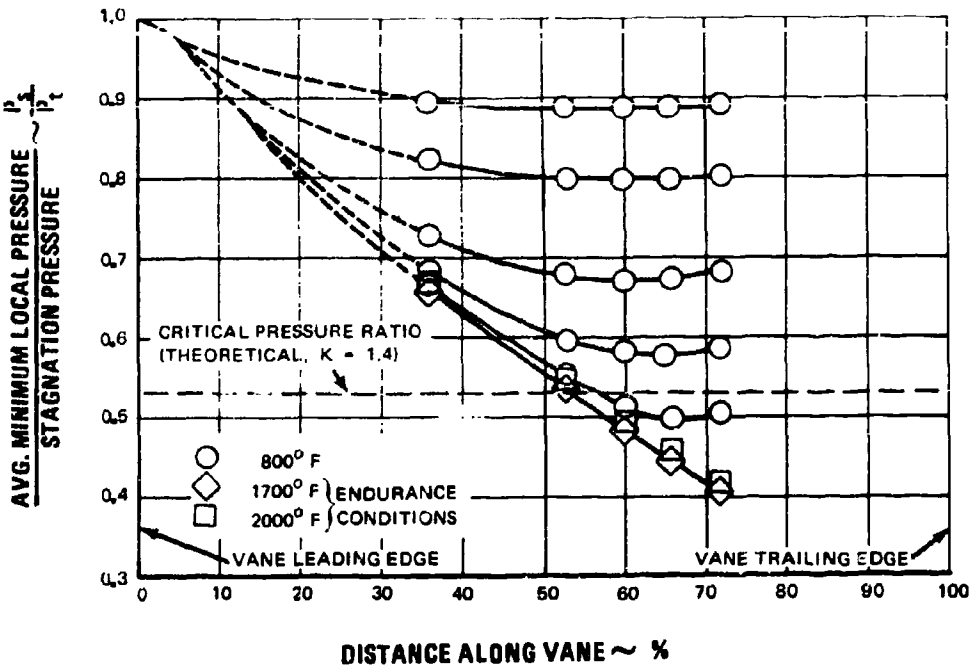

Figure 74. Location of Choking Plane.

Operating Experience With JP-4 and Emulsified Fuels

JP-4 Fuel

No operational difficulties were encountered while testing with JP-4 fuel for 75 hours at 1700°F burner exit temperature, however, excessive hard carbon buildup was experienced at local areas in the dome of the burner when operating at 2000°F burner exit temperature. Most of the carbon formed downstream of the cross-over tubes which themselves provide recirculatarity zones and therefore, favorable conditions for carbon accumulation. This excessive buildup of carbon in the burner can was attributed to operation at off-design conditions in order to attain the 2000°F temperature. The carbon formation at 2000°F exit temperature was discovered upon inspection of the test vane specimens after the third 12.5 hour cycle of the 75 hour endurance run. A pair of Chromalloy coated W.I. 52 material vane specimens showed excessive leading edge corrosion, which was analyzed as having been caused by carbon impingement during the preceding 12.5 hour endurance cycle. No other difficulties were encountered during the 75 hours at 2000°F.

Emulsified Fuel C

Relatively few difficulties were experienced with emulsified fuel C during the 150-hour test. Flow resistance for 45 feet of 5/8 in. I.D. flexible supply line was measured to be 20 psi at first but dropped to 8-10 psi for the majority of the tests. Hard carbon accumulations in the dome of the burner continued to be encountered at an equal or slightly lower rate than that obtained with JP-4 fuel at 2000°F burner exit temperature. It was observed that a brownish colored scale was accumulating on the vane material specimens while using emulsified fuel C at 1700°F burner exit conditions. For the next run, a dummy set of new vanes was substituted and the fuel was changed back to JP-4. After 12.5 hours of running with the JP-4, it was observed that no scale was being formed; however, scale formation was again noticeable on the same vanes after switching back to emulsified fuel C. Thus, it appears that emulsified fuel C was the cause of the scale formation. The major difficulty encountered was that the 40-micron fuel filters plugged after 10 hours and then again at 120 hours of operation (a plugging condition was assumed to occur when the pressure drop across the filter exceeded 5 psi; the normal pressure drop was approximately 1 psi with emulsified fuel C). Visual examination of the contamination plugging the filter showed it to consist of metal chips and such other materials as paint chips, crystalline and fibrous material.

Emulsified Fuel A

Relatively few difficulties were experienced with emulsified fuel A during the 150-hour test. Carbon buildup and flow resistance were the same as experienced with emulsified fuel C and JP-4 fuel. However, some fuel nozzle primary screen plugging was encountered during the 2000°F burner exit operation which necessitated the subsequent removal of two fuel nozzles. Also, minor flow control fluctuations (unrelated to the above plugging) were experienced throughout the 150 hours of operation.

Emulsified Fuel B

Severe difficulties in the following areas were encountered with emulsified fuel B during the 150-hour corrosion test rig. High resistance to flow through the 40-micron filters occurred at least six times during the test, requiring shutdown to investigate each incident. Inspection and cleaning of the filters revealed only traces of silt-type dirt and very thick emulsion. Severe fuel flow control fluctuations were experienced from the start of the tests, thereby necessitating the use of a variable-speed drive for the main fuel pump in place of the constant-speed drive with flow bypass as used with emulsified fuels A and C.

Severe fuel nozzle primary screen plugging was encountered when operating at both 2000°F and 1700°F burner exit temperatures. This plugging occurred a substantial number of times, necessitating shutdown and replacement of the screen and/or nozzle. Figure 75 shows the typical accumulation found on the primary screen of the fuel nozzle. Microscopic examination showed predominately metal chips, paint chips,

fibers, crystals, and carbon. Chemical analysis showed that inorganics and metallics made up 75 percent of the material, while the remainder was classified as carbonaceous and volatile. Spectroanalysis indicated zinc, copper, lead, silver, tin, cadmium, iron, magnesium, and silicon.

Soft carbon accumulation of the nozzle face and swirl vanes as shown by Figure 69 was encountered several times. This condition may have been caused by the emulsified fuel oozing from the fuel nozzle during shutdown.

Figure 75. JT12 Fuel Nozzle After 27.75 Hours Running at 800°F Inlet Temperature Using Emulsified Fuel B.

Emulsion Breakdown

Emulsion breakdown results with the fuel systems used for the corrosion testing are shown in Figure 76. Emulsified fuels A and B demonstrated breakdown characteristics similar to those obtained during the combustion test program. Emulsified fuel C continued to be the most resistant to breakdown, showing substantially higher emulsion percentage than those obtained on previous tests. No explanation is offered other than the comment that emulsified fuel C had been in outside storage since mid-January, a period of 4 months prior to its use. It was noted that the yield value of the emulsion used during the corrosion tests was approximately 100 dynes/cm^2 less than had been previously measured for this fuel. No significant differences in emulsion breakdown could be established between the bypass system and the variable-speed pump system using emulsified fuel B. A typical value of fuel pump pressure rise encountered during the corrosion tests was 275 psi.

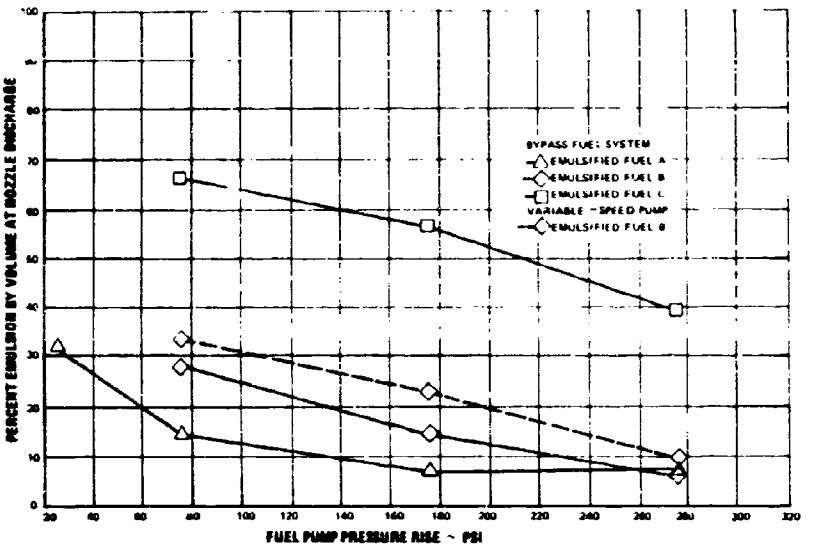

Figure 76. Breakdown of Emulsified Fuels in a Pressure Atomizing System at Room Temperature.

Details of Examination

Visual examination of experimental vanes after 75 hours exposure time (Figures 77 through 84) showed that vanes operated with emulsified fuel C exhibited a brownish colored scale, which appeared more predominant on the 1700°F vanes than those exposed at 2000°F. This scale was identified by X-ray diffraction (XRD) and X-ray fluorescence (XRF) techniques as primarily Fe_3O_4 and $CaSO_4$ in that order of predominance (Table VIII). Vanes operated with JP-4 and emulsified fuels A and C appeared to have no surface deterioration at 1700°F; however, emulsified fuel B produced severe attack on both the airfoil hot sections and vane platforms. The extensive base metal attack on the vane platform of several alloys was believed to be indicative of the corrosive nature of emulsified fuel B, and it was unique to the test vanes operated at 1700°F. At 2000°F, all vanes showed at least partial deterioration in the uncoated condition, with U-500 vanes appearing most severely attacked, regardless of fuel type. Emulsified fuel B appeared to cause more severe surface corrosion on the uncoated alloys.

After 75 hours' exposure with each fuel type at 1700°F, relative weight changes for each vane were calculated. Relative weight changes are tabulated in Table IX.

Slight weight gains were observed for vanes operated with JP-4 fuel at 1700°F, except wrought U-700 and wrought U-500, which exhibited weight losses of -0.01 and -0.03 gram respectively. All vanes tested with emulsified fuels A and C at 1700°F showed weight gains of about +0.01 and +0.05 gram respectively.

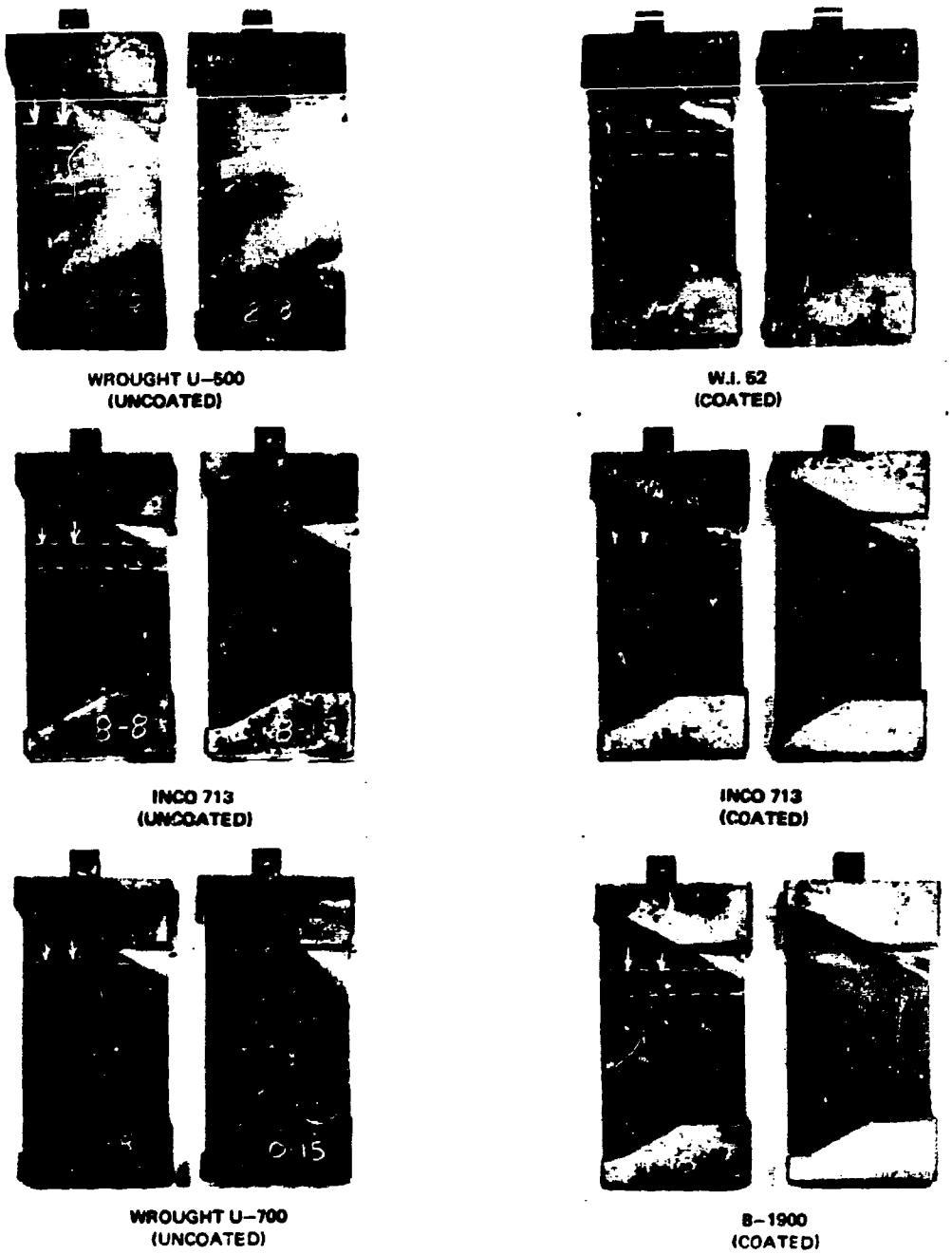

Figure 77. Test Vanes After Exposure for 75 Hours at 1700°F to JP-4 Fuel. (Dashed Lines and Arrows on Vanes Denote Location of Sectioning for Metallographic Examination.)

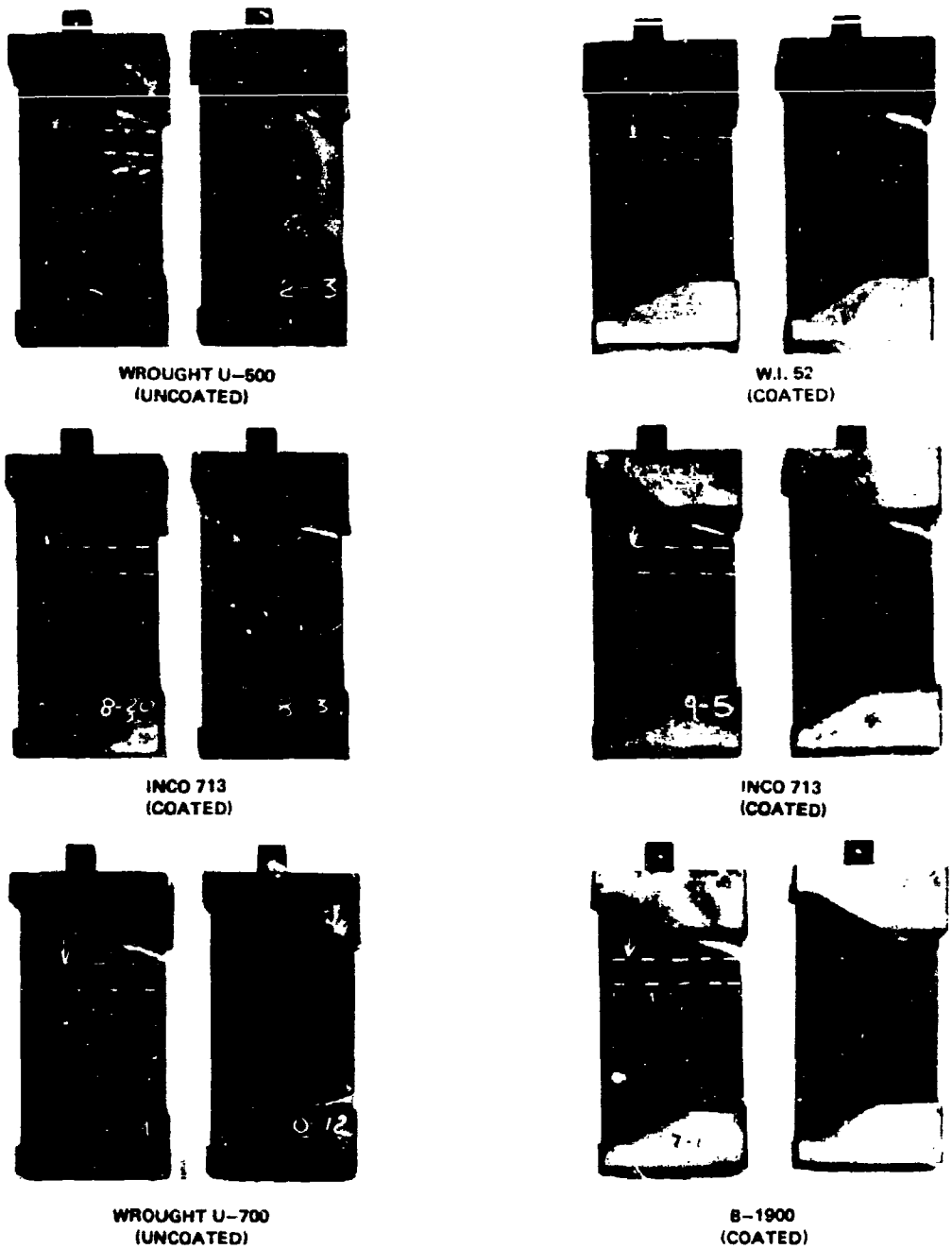

Figure 78. Test Vanes After Exposure for 75 Hours at 1700°F to Emulsified Fuel A. (Dashed Lines and Arrows on Vanes Denote Location of Sectioning for Metallographic Examination.)

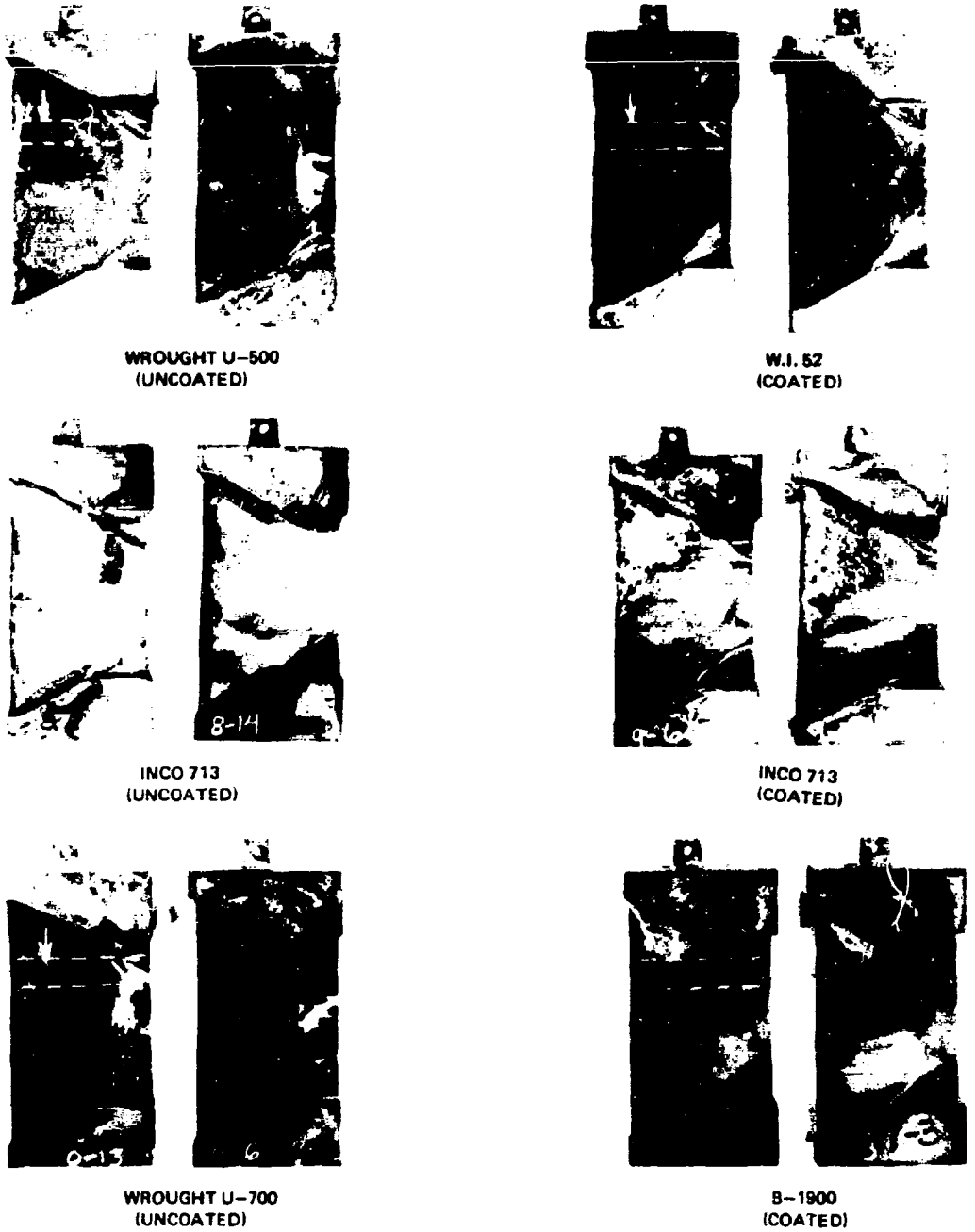

Figure 79. Test Vanes After Exposure for 75 Hours at 1700°F to Emulsified Fuel B. (Dashed Lines and Arrows on Vanes Denote Location of Sectioning for Metallographic Examination.)

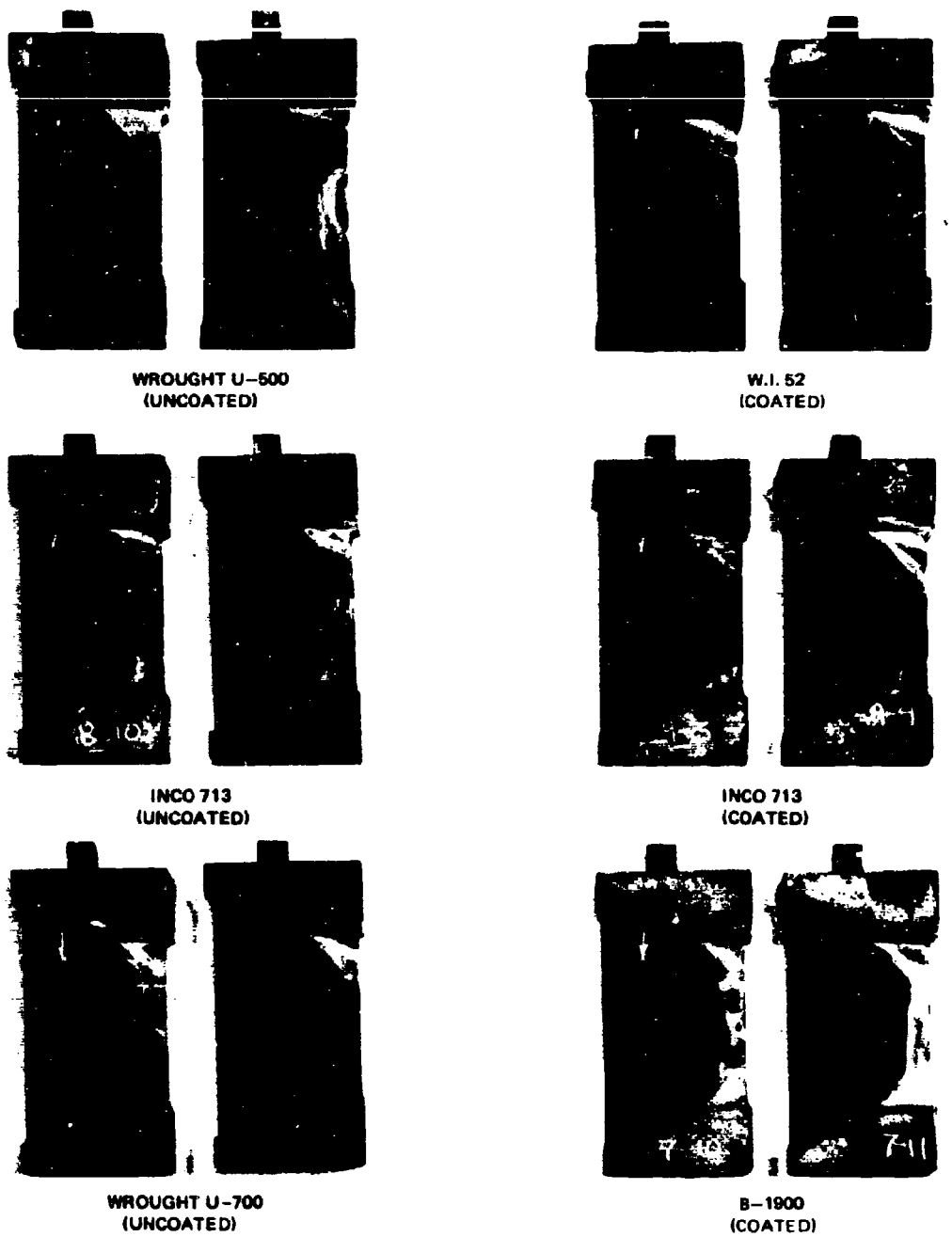

Figure 80. Test Vanes After Exposure for 75 Hours at 1700°F to Emulsified Fuel C. (Dashed Lines and Arrows on Vanes Denote Location of Sectioning for Metallographic Examination.)

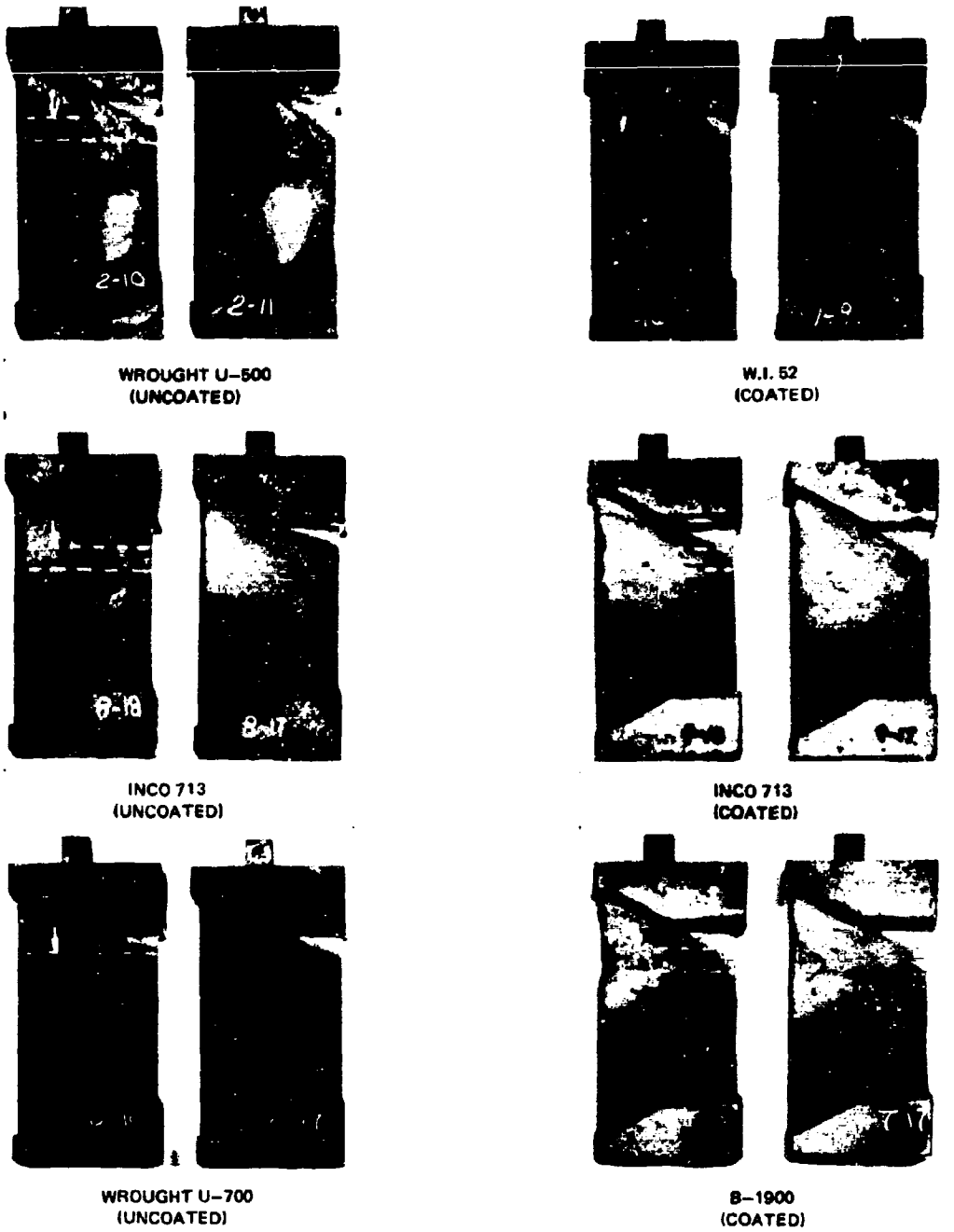

Figure 81. Test Vanes After Exposure for 75 Hours at 2000°F to JP-4 Fuel. (Dashed Lines and Arrows on Vanes Denote Location of Sectioning for Metallographic Examination.)

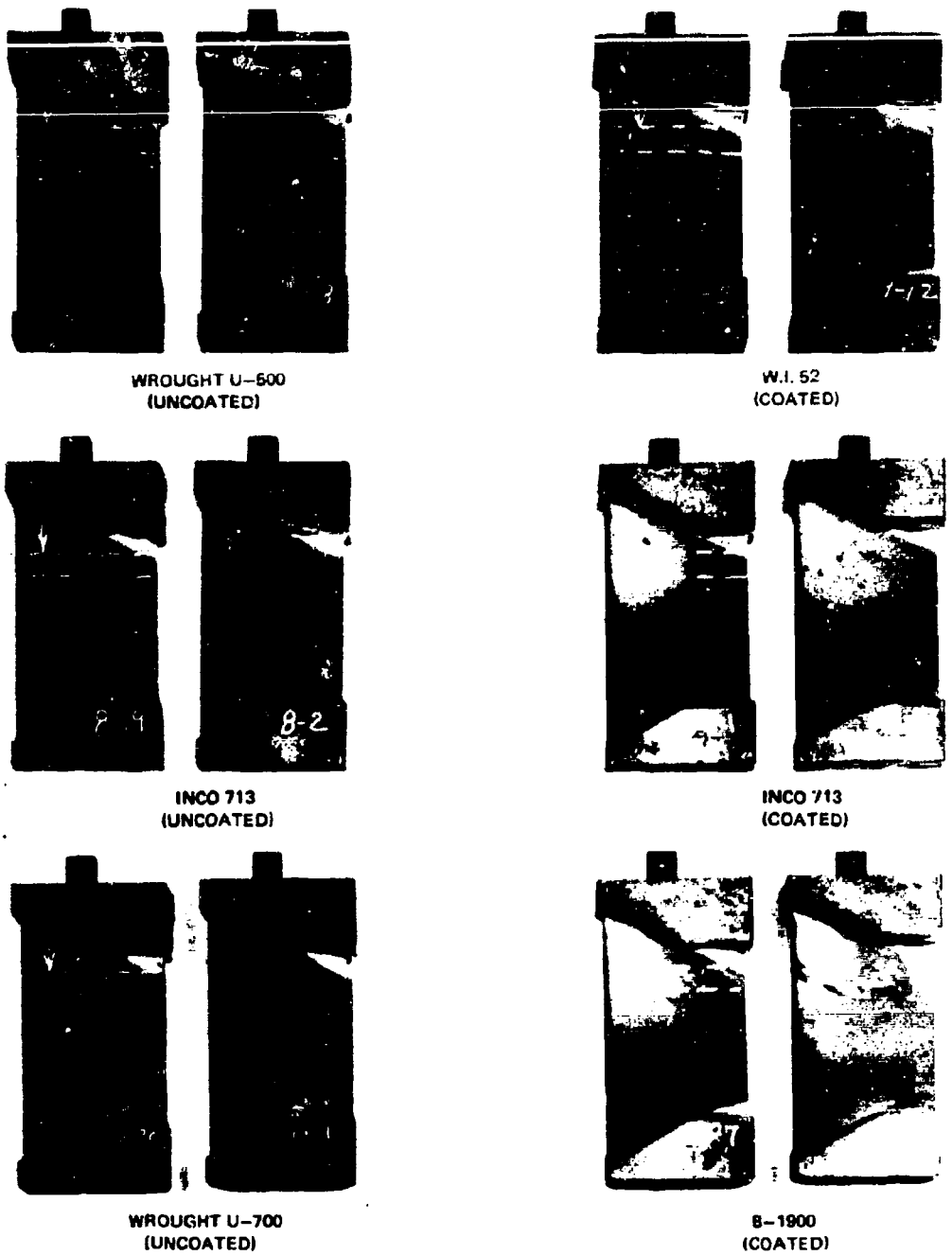

Figure 82. Test Vanes After Exposure for 75 Hours at 2000°F to Emulsified Fuel A. (Dashed Lines and Arrows on Vanes Denote Location of Sectioning for Metallographic Examination.)

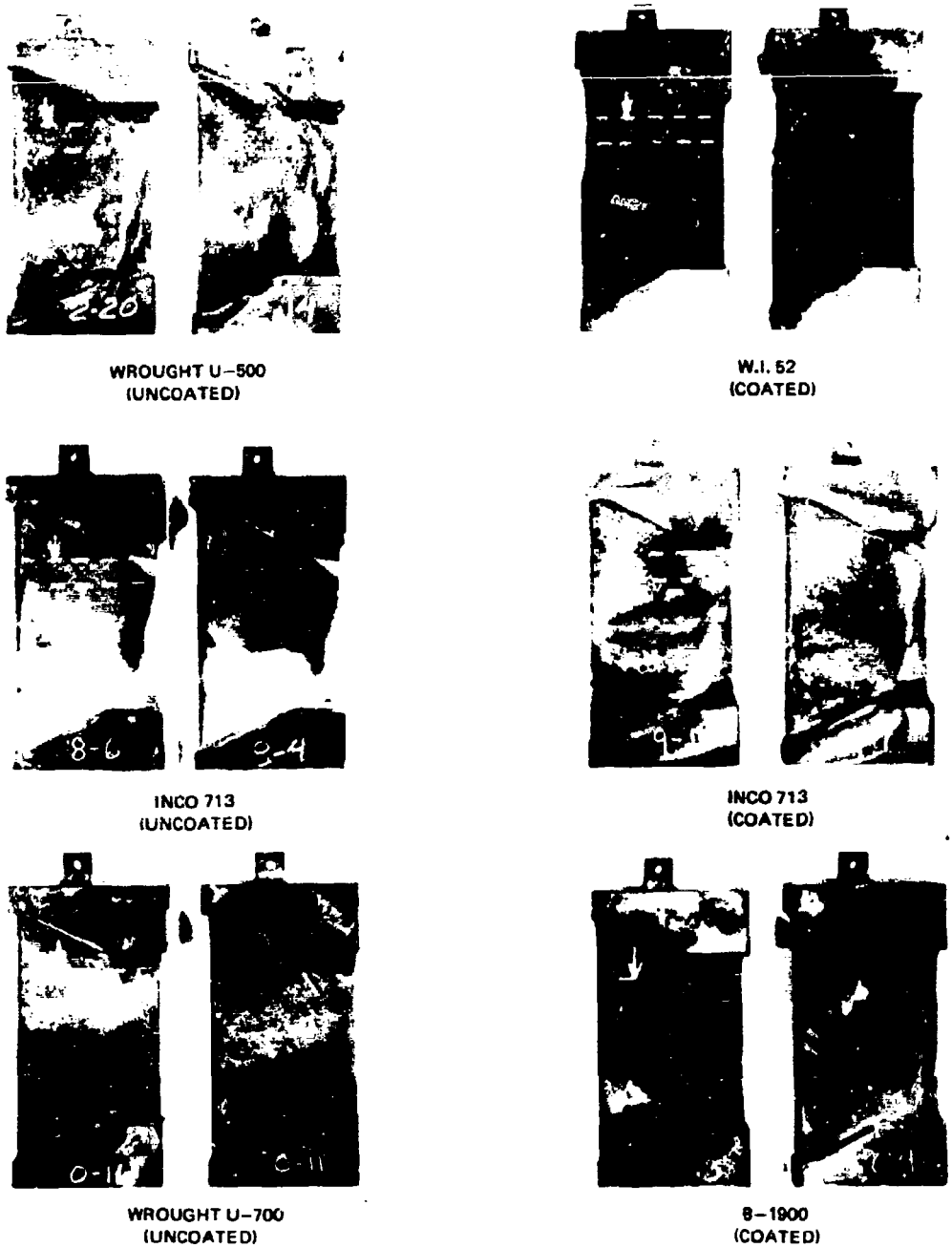

Figure 83. Test Vanes After Exposure for 75 Hours at 2000°F to Emulsified Fuel B. (Dashed Lines and Arrows on Vanes Denote Location of Sectioning for Metallographic Examination.)

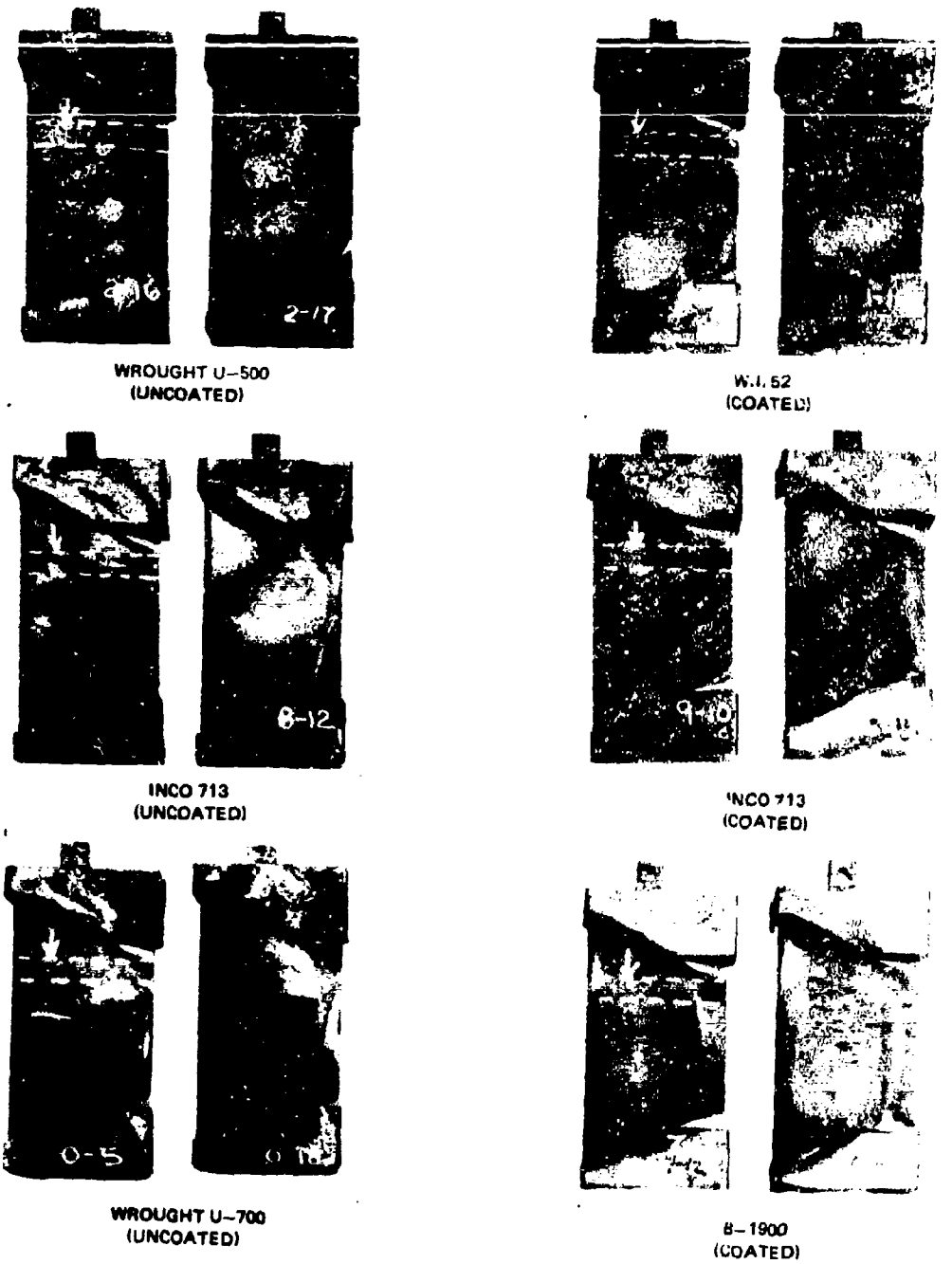

Figure 84. Test Vanes After Exposure for 75 Hours at 2000°F to Emulsified Fuel C. (Dashed Lines and Arrows on Vanes Denote Location of Sectioning for Metallographic Examination.)

TABLE VIII. X-RAY DIFFRACTION (XRD) AND FLUORESCENSE (XRF) ANALYSIS OF VANE COATINGS

Fuel	Vane Material	Burner Rig Time (hours)	Burner Rig Temperature (°F)	Leading Edge XRD	Leading Edge XRF	Trailing Edge XRD	Trailing Edge XRF	
JP-4 Fuel	B-1900 coated	75	2000			Tentatively identified as $Ca_2Al_2SiO_7$	Ca Al Si P Cr	Ni Fe Ti Co
Emulsified Fuel C	Inco 713c	75	1700	Fe_3O_4, $CaSO_4$ with unidentified diffraction lines at 1.10Å and 2.69Å	Fe Zn Ca Ni Si	$CaSO_4$ with unidentified diffraction lines at 5.79Å and 5.23Å	Ca Zn S Fe Ni	

TABLE IX. WEIGHT CHANGE DUE TO CORROSION AFTER 75 HOURS TESTING

Material	Condition	JP-4 Fuel 1700°F (grams)	JP-4 Fuel 2000°F (grams)	Emulsified Fuel A 1700°F (grams)	Emulsified Fuel A 2000°F (grams)	Emulsified Fuel B 1700°F (grams)	Emulsified Fuel B 2000°F (grams)	Emulsified Fuel C 1700°F (grams)	Emulsified Fuel C 2000°F (grams)
Wrought U-500	Uncoated	-0.0311	-0.3895	+0.0080	-0.2350	-0.0264	-0.3996	+0.0590	-0.3667
Wrought U-500	Uncoated	-0.0286	-0.4342	+0.0128	-0.2860	-0.0696	-0.3057	+0.0815	-0.5155
W.I. 52	Chromalloy U.C. aluminide coating	+0.0367	+0.0310	+0.0402	+0.0416	+0.0662	-0.7730	+0.0670	+0.1391
W.I. 52	Chromalloy U.C. aluminide coating	+0.0288	+0.0372	+0.0396	+0.0374	+0.0135	-0.6071	+0.0669	+0.0503
Wrought U-700	Uncoated	-0.0103	-0.2911	+0.0141	-0.0888	-0.1151	0.0394*	+0.0642	-0.0659
Wrought U-700	Uncoated	-0.0179	-0.2474	+0.0114	-0.0839	-0.1068	-0.3821	+0.7409	-0.1065
Inco 713C	PWA proprietary aluminide coating	+0.0114	-0.0010	+0.0181	+0.0076	-0.1445	-0.2762	+0.0528	+0.0380
Inco 713C	PWA proprietary aluminide coating	+0.0067	+0.0048	+0.0153	+0.0139	-0.2537	-0.1351	+0.0567	-0.0071
Inco 713C	Uncoated	+0.0075	-0.1430	+0.0013	-0.0366	-0.0568	-0.0407	+0.0537	+0.0517
Inco 713C	Uncoated	+0.0033	-0.0904	+0.0001	-0.0328	-0.4052	-0.0549	+0.0604	-0.0272
B-1900	PWA proprietary aluminide coating	+0.0029	-0.0805	+0.0128	+0.0074	-0.4355	+0.0543	+0.0484	+0.0330
B-1900	PWA proprietary aluminide coating	+0.0041	-0.4001	+0.0116	+0.0052	-0.2769	+0.0322	+0.0496	+0.0294

* 37-Hour exposure

The higher weight gains associated with emulsified fuel C are primarily attributed to the brownish colored scale (Fe_3O_4 and $CaSO_4$) which was observed on the vane surfaces. All vanes exposed to emulsified fuel C generally gained about the same weight, while Chromalloy coated W.I. 52 vanes tested with emulsified fuel A gained considerably more weight (+0.04 gram) at 1700°F than did the other vanes (+0.01 gram).

Weight changes after 1700°F testing with emulsified fuel B showed general weight losses in all vanes except the Chromalloy coated W.I. 52 vanes. The coated W.I. 52 vanes exhibited a weight gain of 0.01 and 0.06 gram. The greatest weight loss occurred in the coated B-1900 vanes (-0.27 and 0.43 gram). Extensive base metal attack was observed on the vane platform of several alloys as a result of an uneven flame pattern which contributed to the overall weight loss.

At 2000°F, a general loss in weight was observed for all vanes tested with JP-4 fuel except for both coated W.I. 52 vanes and one coated Inco 713 vane. All uncoated vanes tested at 2000°F with emulsified fuel A exhibited a loss in weight, while all coated vanes showed slight gain. Except for one uncoated Inco 713 vane, which showed a slight weight gain, all uncoated vanes tested at 2000°F with emulsified fuel C lost weight. Coated vanes showed slight weight gains except for one coated Inco 713 vane. The wrought U-500 vanes showed a relatively higher weight loss (about 0.4 gram) compared with the other five vane alloys. All vanes tested at 2000°F with emulsified fuel B showed a weight loss except coated B-1900, which showed a slight unexplained weight gain.

On a weight loss basis, vanes exposed to both emulsified fuels A and C exhibited equivalent to slightly better oxidation-erosion resistance compared to those exposed to JP-4. This was found to be consistent at both 1700°F and 2000°F. However, vanes exposed to emulsified fuel B exhibited consistently greater weight loss than JP-4 at 1700°F. At 2000°F vanes exposed to emulsified fuel B exhibited a weight loss equivalent to that of vanes exposed to JP-4.

Metallographic examination of transverse airfoil sections through the hot zone was made on each vane material in each set. The location of these sections is illustrated by arrows and dashed lines on the vanes shown in Figures 77 through 84. A detailed discussion of the metallographic examination is contained in Appendix II.

VALIDATION OF DATA

The validity of the flame intensity readings was verified through daily calibrations and spot checks during the period when the flame intensity unit was installed on the burner rig. A post-test check of the complete unit and system showed it to be within 1 percent of its initial setup calibration. Therefore, it was assumed that readings from this instrument were reflections of actual phenomena occurring during the combustion tests.

It is believed that small variations in the data were caused by differences in setting pressure and flow data points. When any large deviations were found these were attributed to errors resulting from unnoticed shifts or from direct human error in reading data, and these data have been discarded in the evaluation of the results.

CONCLUSIONS

The following conclusions have been drawn based on the evaluation of visual and recorded test data and operational experiences:

1. From the standpoint of combustion characteristics at the conditions tested, it is concluded that only minor differences in performance exist between JP-4 and the emulsified fuels tested when using pressure atomizing fuel nozzles. The combustor performance is not compromised with the use of the emulsified fuels tested because the fuel spray distribution and atomization have not been significantly altered relative to JP-4 fuel.

2. Before emulsified fuels, such as those tested, can be successfully used in gas turbine engines, work is required in the area of the fuel system to prevent the plugging of fuel nozzle screens. This plugging was caused primarily by the tendency of the fuels to pick up contaminants, and secondarily, by the apparent decreased thermal stability of the emulsified fuels.

3. Emulsified fuel A had the best overall characteristics from standpoint of corrosive attack, handling, and fuel system plugging and for this reason appeared most suitable for evaluation in experimental full scale engine tests.

4. Near complete breakdown of the emulsion in an emulsified fuel prior to delivery to the gas turbine combustor fuel manifold is considered a desirable feature to insure undeteriorated performance in current gas turbine burner systems.

5. Emulsified fuel A exhibited the least corrosive attack on vane coatings and substrate compared to JP-4 and emulsified fuels B and C.

6. Emulsified fuel B exhibits the most corrosive attack on vane materials and coatings based on weight loss and post-test metallurgical examinations and as such appears unacceptable as a candidate fuel.

7. The test material which best withstands corrosive tests with emulsified fuels is coated W.I. 52, whereas uncoated U-500 is the most affected material.

8. Overall operational characteristics of emulsified fuel A most closely resemble those of JP-4, while emulsified fuel B is most deficient in this respect.

9. More development effort on the air-assist fuel nozzle to improve atomization appears to be warranted on the basis of its potential to tolerate contaminated fuels.

RECOMMENDATIONS

1. This program has revealed a serious problem, i.e., plugging of the fuel nozzle screen to various degrees depending on the type of emulsified fuel used. Examination of the plugged screens (228 microns) has shown that a mat comprised mostly of carbonaceous material covers the surface of the screen. It is reasoned that as this mat builds up it forms a trap for the miscellaneous debris that otherwise would have passed through the fuel nozzle system, since it had already survived a 40-micron filtration prior to the fuel nozzle. It is therefore imperative that work be initiated to investigate the thermal stability characteristics of the emulsified fuels as they are exposed to the entire range of environmental conditions imposed on a gas turbine combustor fuel system.

2. Emulsified fuel A is recommended as the candidate fuel for running engine endurance tests in order to further define the durability or performance problems which may evolve under actual engine environmental conditions.

3. Additional corrosion tests with emulsified fuels should be conducted with rig type apparatus to determine the long term effect (250 hours) on the various turbine materials. It is also recommended that these tests be conducted on all alloys in both cast and wrought fabrication.

4. Should the formulation yield value and breakdown characteristics of advanced emulsified fuels greatly differ from the fuels tested in this program, it is recommended that combustion and spray qualities be further evaluated as a function of breakdown and initial yield value for each new formulation.

5. Fuel nozzle design studies, based on pressure as well as air atomization principle, should be conducted to determine the effect of initial yield value and breakdown characteristics of emulsified fuel on spray distribution, droplet diameter, and spray cone angle. These studies should cover the complete range of flow rates and environmental conditions which could be encountered in gas turbine operation. The results of these studies should be verified by conducting flow tests at simulated engine pressure levels.

6. The experience gained in this program as well as a previous experience with emulsified fuels have identified certain problem areas in addition to those listed above, which will require development effort.

    a. Define the design modifications to fuel control components that will be required to maintain the same fuel system component performance levels that are now attained with liquid fuel over the entire spectrum of flight conditions encountered.

    b. Investigate hot shutdown problems and aborted starts with emulsified fuels.

c. Determine the deleterious effects to fuel system components resulting from extended dormant and dynamic operational periods.

d. Determine the fuel control scheduling revisions necessary because of the reduced heating value associated with emulsified fuels.

APPENDIX I

PERFORMANCE TEST PROCEDURE

The test procedure and performance point settings used to determine stead-state combustion performance are outlined in the steps listed below:

1. Remove and clean plane indicator sight windows before each run (note on operator's comment sheet).

2. Zero all U-tubes before starting air (note on operator's comment sheet).

3. Set rake 55 degrees out of stream.

4. Fully open back-pressure valve and start airflow through rig.

5. For light-off, set airflow (W_a) at approximately 4000 pph and inlet temperature (T_{in}) at approximately 350°F. Then light-off. Raise fuel flow (W_f) no higher than 75 pph.

6. Run performance points 1 through 16 in order. Run one lean blowout (LBO) after point 8. Light-off per step 5; then run one more lean blowout after point 16.

7. Record time of each point on operator's comment sheet with same time recorded on all data sheets.

8. Make several checks during each point and readjust, if necessary, the airflow, fuel flow, inlet temperature, and total inlet pressure (P_t).

9. Record the following data at all performance points:

   a) Time

   b) Orifice

      - Total pressure (P_t)
      - Static pressure (P_s)
      - Temperature

   c) JP-4 Fuel Flow

      - Primary
      - Secondary
      - Total

d) Emulsified Fuel Flow

- Weight before
- Weight after
- Time interval

e) Fuel Nozzle Pressure

- Primary
- Secondary

f) Air-Assist Nozzle

- Air pressure
- Air temperature

g) Fuel Temperature

h) Nozzle Fuel Temperature

i) Barometric Pressure

j) Dew Point

k) Inlet Total Pressure

l) Inlet Static Pressure

m) Inlet Temperature

n) Room Temperature

When running lean blowouts, stop dropping fuel flow at the point where flameout seems imminent and record the data listed in step 10. Then proceed until flameout, and again record fuel flow.

10. Record the following data at the points indicated:

Point	Both Flame Indicators	Smoke Density	Traverse Temperature	Traverse Pressure
1	x			
2	x	x	x	
3	x			
4	x	x	x	
5	x			
6	x	x	x	
7	x			
8	x	x	x	x
LBO	–	–	–	–
9	x			
10	x	x	x	
11	x			
12	x	x	x	
13	x			
14	x	x	x	
15	x			
16	x	x	x	x
LBO	–	–	–	–

Note: Take flame indicator readings with rate set at 55 degrees.

11. Performance Point Settings

Point	Rig Inlet P_t(In. Hg A)	Rig Inlet Temp (^{O}F)	Airflow (PPH)	Pri. Fuel Flow (PPH)	Sec. Fuel Flow (PPH)	Total Fuel Flow (PPH)
1	70	500	8200	80.4	0	80.4
2	70	500	8200	90.2	0	90.2
3	70	500	8200	100.0	0	100.0
4	70	500	8200	109.0	0	109.0
5	70	500	8200	119.8	0	119.8
6	70	500	8200	120.0	9.6	129.6
7	70	500	8200	120.0	19.5	139.5
8	70	500	8200	120.0	30.1	150.1
LBO	70	500	8200	–	0	–
9	70	500	7150	73.8	0	73.8
10	70	500	7150	81.9	0	81.9
11	70	500	7150	91.0	0	91.0
12	70	500	7150	100.1	0	100.1
13	70	500	7150	108.5	0	108.5
14	70	500	7150	118.0	0	118.0
15	70	500	7150	120.0	7.2	127.2
16	70	500	7150	120.0	16.6	136.6
LBO	70	500	7150	–	0	–

Note: When running with the air-assist nozzle, the total fuel flow will pass through the primary only.

APPENDIX II

METALLOGRAPHIC EXAMINATION OF TRANSVERSE AIRFOIL SECTIONS THROUGH THE HOT ZONE

Metallographic examinations of transverse airfoil sections through the hot zone were made on each vane material in each set. In most instances each airfoil section was nickel plated (0.001-0.003 inch thick) to maintain surface scale and configuration.

The microstructures of transverse airfoil sections through the hot zone were examined optically using a research metallograph, with photomicrographs taken at magnifications of either 100 or 500X. A combination of mechanical polish and chemical immersion etching was used for all specimens. Samples were polished with 120 to 600 silicon carbide papers followed by polishing on felt wheels impregnated with 6.0 and 0.25-micron diamond compounds. Final mechanical preparation was accomplished on a wheel with a fine alumina abrasive. All samples were immersed in Kalling's reagent (5 grams $CuCl_2$, 100 ml ethyl alcohol and 100 ml H_2O) from 10 to 30 seconds. After etching, samples were buffed with an abrasive to eliminate the flow layer and were re-etched with the same reagent. Typical specimen sections marked to show the make up or origin of the various layers appearing in the photomicrographs used in this examination are shown in Figure 85.

Specimens from the leading edges of uncoated U-500 vanes exposed for 75 hours at 1700°F to the combustion products of each fuel are shown in Figures 86 and 87. The vanes exposed to JP-4 fuel exhibited considerable surface and subsurface oxidation; vanes exposed to the emulsified fuels also exhibited subsurface oxidation but to a lesser degree. Vanes exposed to emulsified fuel B, in addition, exhibited preferential intergranular attack and nonuniform surface attack along the leading edges.

Sections from uncoated Inco 713 vanes after 75 hours of exposure at 1700°F to each fuel are presented in Figures 88 and 89. Test vanes exposed to fuel B exhibited a thick oxide scale (approximately 0.004 inch thick) and uniform surface attack, while the remaining vanes exhibited less scale (approximately 0.001 inch – 0.002 inch thick) and nonuniform surface attack. All vanes contained a denuded zone along the periphery of the leading edge which was most pronounced in the vanes exposed to emulsified fuels A and C.

Uncoated U-700 vane specimens exposed for 75 hours at 1700°F to each fuel are presented in Figures 90 and 91. All vanes showed a denuded zone along the periphery of the leading edge approximately 0.001 inch – 0.003 inch thick. Surface attack was generally uniform on all vanes with subsurface oxidation prevalent on vanes exposed to emulsified fuel A.

Coated WI. 52 vanes exposed to each fuel for 75 hours at 1700°F are shown in Figures 92 and 93. JP-4 and emulsified fuels A and C caused slight oxidation-erosion of the coating and some internal oxidation of the coating. Emulsified fuel B caused severe degradation of the coating with complete loss of the coating and base metal attack along the leading edge.

Coated Inco 713 vanes exposed for 75 hours at 1700°F to each fuel are presented in Figures 94 and 95. JP 4 and emulsified fuels A and C produced a slight oxide layer along the surface with only minor coating distress observed. Some localized pitting in the coating was evident in vanes exposed to JP-4 and emulsified fuels A and C. Vanes exposed to emulsified fuel B suffered considerable coating distress with complete erosion of the coating occurring at the leading edge.

Coated B-1900 vanes exposed for 75 hours at 1700°F to each fuel are shown in Figures 96 and 97. Vanes exposed to JP-4 and emulsified fuel A exhibited slight oxidation of the leading edge coating with occasional sites of localized pitting in the coating observed along the leading edge. Vanes exposed to emulsified fuel C showed somewhat less coating distress but a somewhat thicker scale along the surface. Vanes exposed to emulsified fuel B showed complete erosion of the coating and base metal attack progressing along the leading edge.

Specimens from uncoated U–500 vanes exposed to each fuel for 75 hours at 2000°F are presented in Figures 98 and 99. Surface attack progressed uniformly along the periphery of all vanes. Evidence of denuded zones and subsurface attack was also apparent on all vanes but was slightly more predominant in the vanes exposed to JP-4 fuel.

Sections from uncoated Inco 713 vanes exposed for 75 hours at 2000°F to each fuel are shown in Figures 100 and 101. All vanes contained a denuded area along the surface extending approximately 0.002 inch – 0.005 inch into the base metal. Attack was generally uniform along the surface except for the vanes exposed to emulsified fuel B which appeared to suffer more severe attack occurring nonuniformly along the leading edge.

Uncoated U–700 vane specimens exposed for 75 hours at 2000°F to each fuel are presented in Figures 102 and 103. Surface attack occurred uniformly on all vanes with only a slight oxide scale left after the test. Denuded zones were apparent on all vanes but were less predominant on vanes exposed to emulsified fuel B. Preferential subsurface intergranular attack was also noted on vanes exposed to emulsified fuel C.

Coated W.I. 52 vanes exposed to each fuel for 75 hours at 2000°F are shown in Figures 104 and 105. Vanes exposed to JP-4 and emulsified fuel A were similar in appearance with moderate to heavy attack of the coating observed along the leading edge. Attack occurred uniformly along the surface; however, the coating thickness was reduced to about 0.001 inch – 0.002 inch. Vanes exposed to emulsified fuel C suffered complete loss of the coating and surface and subsurface attack of the base metal along the leading edge. Vanes exposed to emulsified fuel B suffered the most extensive damage. The coating along with considerable base metal was eroded with deposits of melted coating present at the midchord section of the vane. The severe erosion and melting of the coating indicated the leading edge temperature was at least 2200°F.

Coated Inco 713 vanes exposed for 75 hours at 2000°F to each fuel are shown in Figures 106 and 107. Vanes exposed to JP-4 suffered complete loss of the coating at the leading edge and about 50 percent of the coating at the midchord location. Deposits of melted

coating were also evident adjacent to the leading edge and at the midchord location indicating temperatures in excess of 2200°F may have been experienced. Coated Inco 713 vanes exposed to emulsified fuel B also suffered complete loss of the coating with preferential intergranular attack of the base metal observed along the leading edge. Inco 713 vanes exposed to emulsified fuels A and C were generally similar in appearance. Attack was generally uniform along the surface and some coating distress was evident.

Coated B-1900 vanes exposed for 75 hours at 2000°F to each fuel are presented in Figures 108 and 109. Vanes exposed to emulsified fuel B suffered complete erosion of the coating but only minor base metal attack. Vanes exposed to emulsified fuels A and C suffered moderate coating distress, however, attack progressed uniformly along the surface and no base metal distress was observed. Vanes exposed to JP-4 fuel suffered complete erosion of the coating and severe base metal attack.

In summary, most vanes experienced only minor amounts of attack during the various 75 hour tests. It was apparent, however, that coated WI. 52 vanes exhibited the best overall resistance to attack while uncoated U–500 vanes exhibited the poorest resistance. Since cobalt-base superalloys are known to possess generally superior oxidation resistance at elevated temperatures than nickel-base superalloys, it is not surprising that the WI.52 alloy was found to exhibit the best resistance to attack in these tests. The Chromalloy pack coating on the WI.52 cobalt base alloy further increases its oxidation resistance over Pratt & Whitney Aircraft aluminide coated nickel-base alloys. Dynamic oxidation testing at Pratt & Whitney Aircraft of uncoated nickel-base alloys has also shown U–500 to possess inferior elevated temperature oxidation resistance to U-700 and Inco 713.

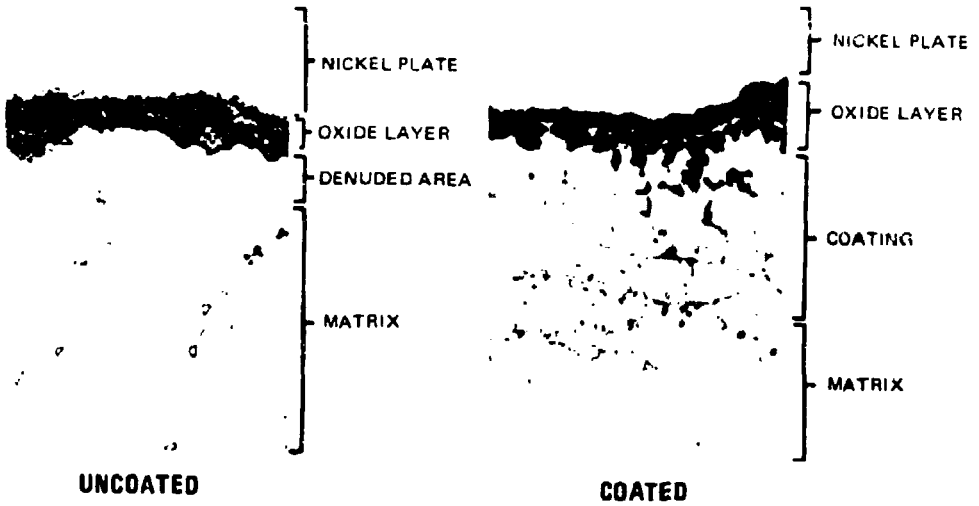

Figure 85. Typical Photomicrographs of Uncoated and Coated Leading Edge Specimens Labeled to Indicate Significance of Specific Areas. (Nickel Plate at Top was added Before Sectioning to Preserve Integrity of Surface Layer. Mag. 500X.)

JP-4 FUEL

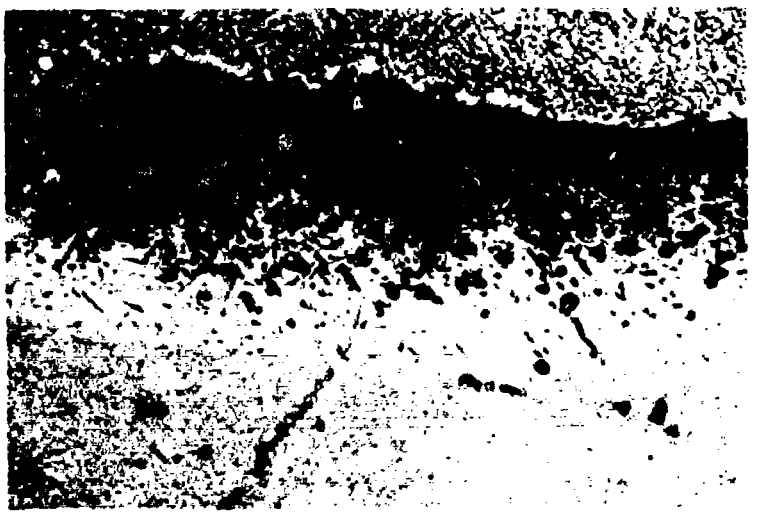

FUEL A

Figure 86. Microstructure of Uncoated U-500 Vane Leading Edge Specimens After 75 Hours of Rig Testing at 1700°F with JP-4 and Emulsified Fuel A. (Brackets Show Surface Oxidation; Arrows Show Subsurface Oxidation. Mag. 500X.)

FUEL B

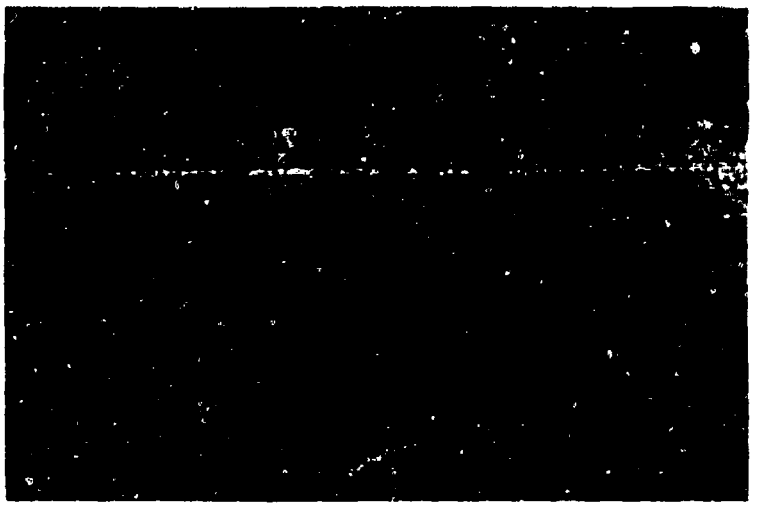

FUEL C

Figure 87. Microstructure of Uncoated U-500 Vane Leading Edge Specimens After 75 Hours of Rig Testing at 1700°F with Emulsified Fuels B and C. (Arrows Show Intergranular Attack. Mag. 500X.)

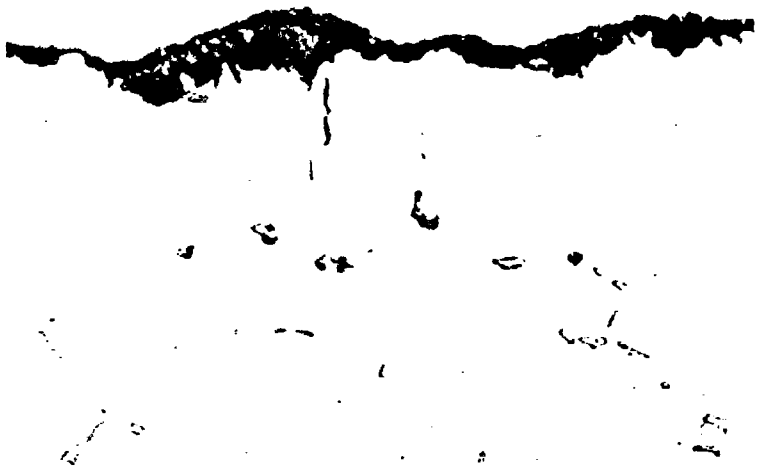

JP-4 FUEL

FUEL A

Figure 88. Microstructure of Uncoated Inco 713 Vane Leading Edge Specimens After 75 Hours of Rig Testing at 1700°F with JP-4 and Emulsified Fuel A. (Brackets Show Denuded Zone. Mag. 500X.)

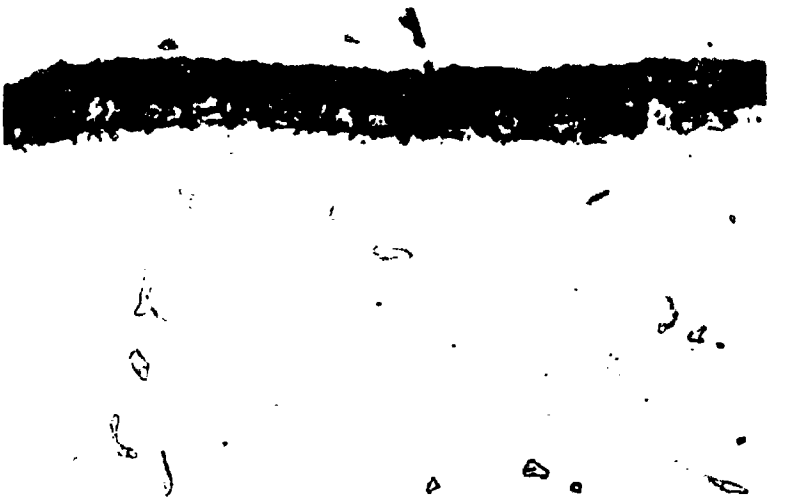

FUEL B

FUEL C

Figure 89. Microstructure of Uncoated Inco 713 Vane Leading Edge Specimens After 75 Hours of Rig Testing at 1700°F with Emulsified Fuels B and C. (Bracket Shows Denuded Zone. Mag. 500X.)

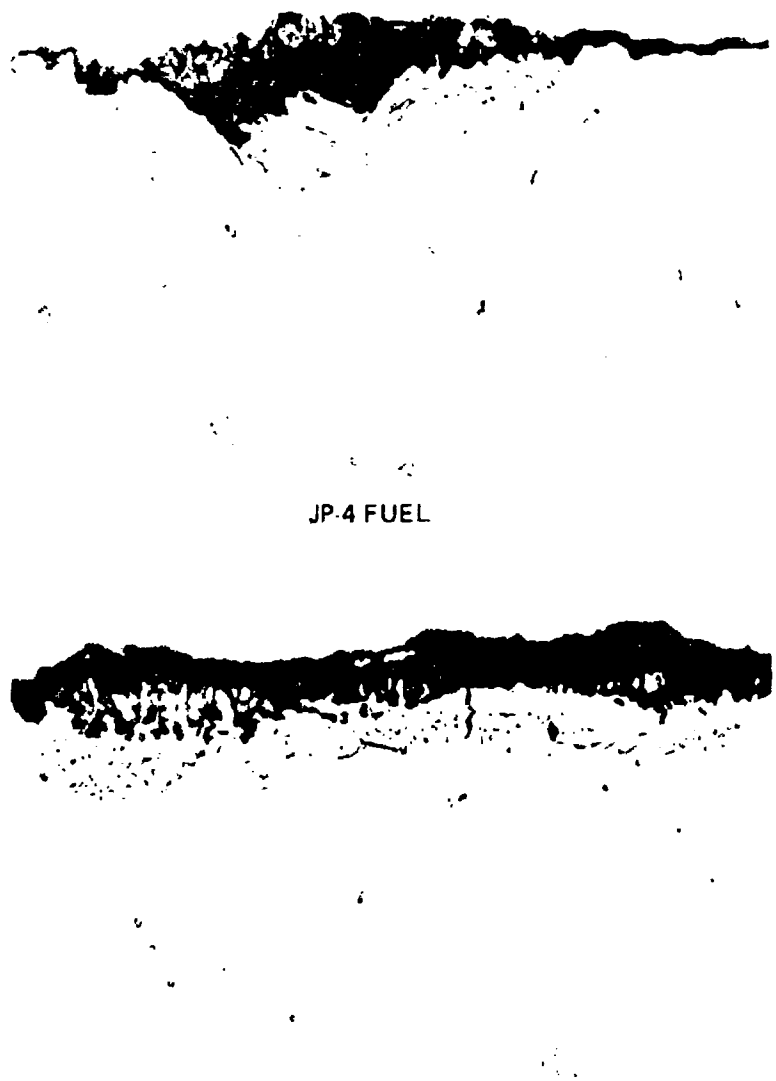

Figure 90. Microstructure of Uncoated Wrought U-700 Vane Leading Edge Specimens After 75 Hours of Rig Testing at 1700°F with JP-4 and Emulsified Fuel A. (Bracket Shows Denuded Zone. Mag. 500X.)

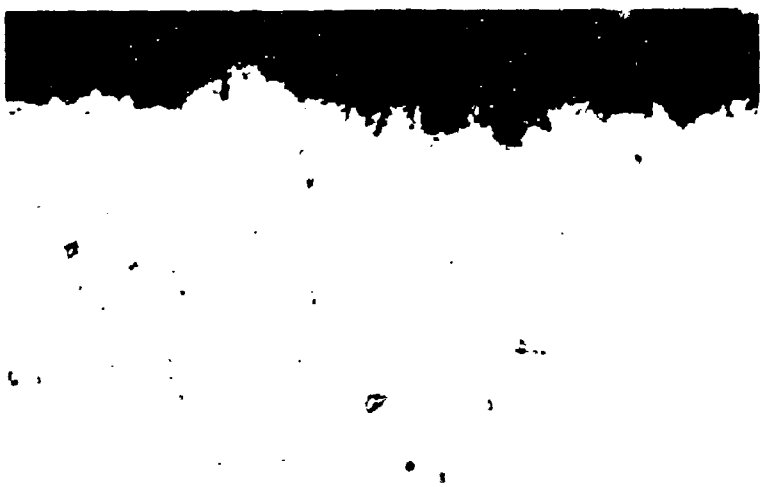

FUEL B

FUEL C

Figure 91. Microstructure of Uncoated Wrought U-700 Vane Leading Edge Specimens After 75 Hours of Rig Testing at 1700°F with Emulsified Fuels B and C. (Bracket Shows Denuded Zone. Mag. 500X.)

JP-4 FUEL

FUEL A

Figure 92. Microstructure of Coated W.I. 52 Vane Leading Edge Specimens After 75 Hours of Rig Testing at 1700°F with JP-4 and Emulsified Fuel A. (Mag. 500X.)

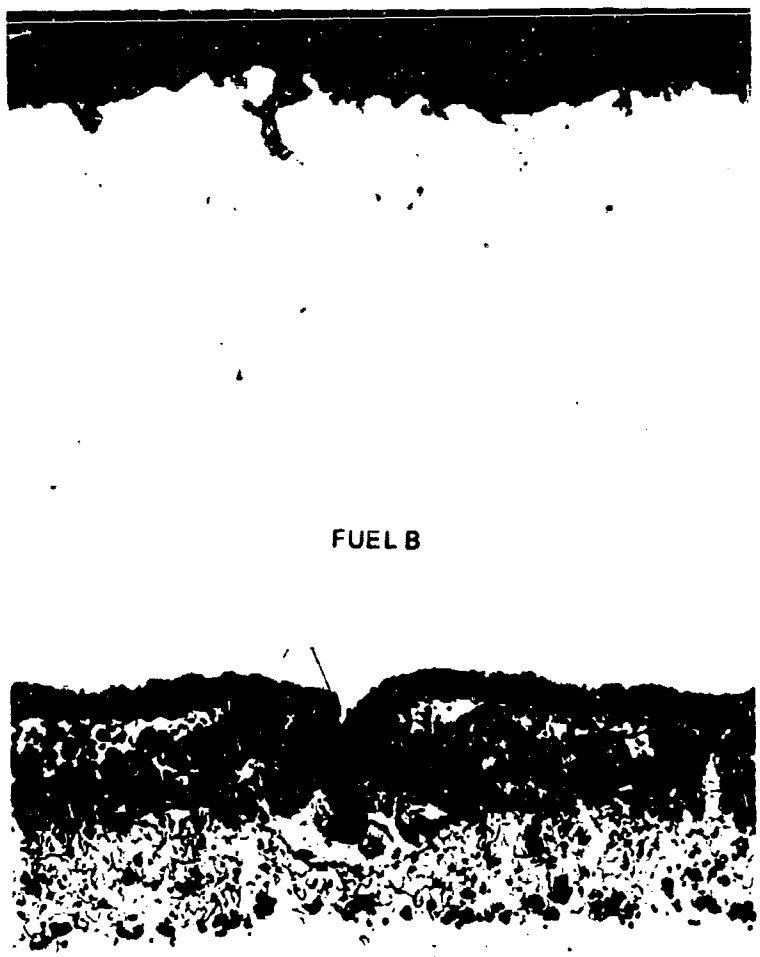

Figure 93. Microstructure of Coated W.I. 52 Vane Leading Edge Specimens After 75 Hours of Rig Testing at 1700°F with Emulsified Fuels B and C. (Mag. 500X.)

JP-4 FUEL

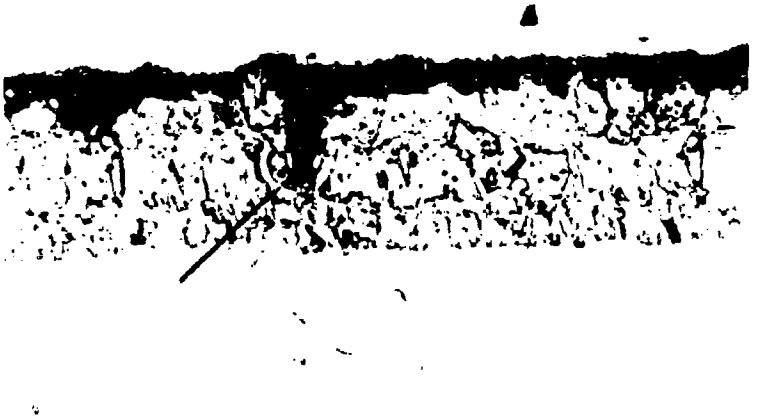

FUEL A

Figure 94. Microstructure of Coated Inco 713 Vane Leading Edge Specimens After 75 Hours of Rig Testing at 1700°F with JP-4 and Emulsified Fuel A. (Arrows Show Pitting. Mag. 500X.)

FUEL B

FUEL C

Figure 95. Microstructure of Coated Inco 713 Vane Leading Edge Specimens After 75 Hours of Rig Testing at 1700°F with Emulsified Fuels B and C. (Arrow Shows Pitting. Mag. 500X.)

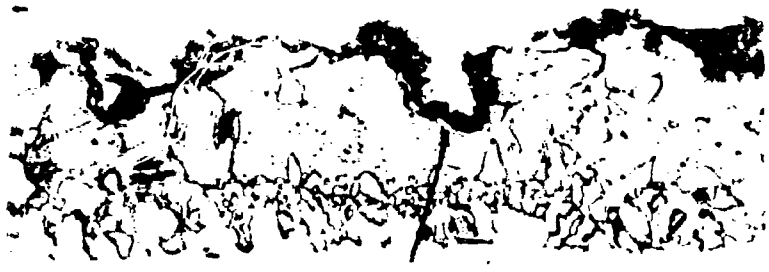

JP-4 FUEL

FUEL A

Figure 96. Microstructure of Coated B-1900 Vane Leading Edge Specimens After 75 Hours of Rig Testing at 1700°F with JP-4 and Emulsified Fuel A. (Arrows Show Pitting. Mag. 500X.)

FUEL B

FUEL C

Figure 97. Microstructure of Coated B-1900 Vane Leading Edge Specimens After 75 Hours of Rig Testing at 1700°F with Emulsified Fuels B and C. (Brackets Show Scale. Mag. 500X.)

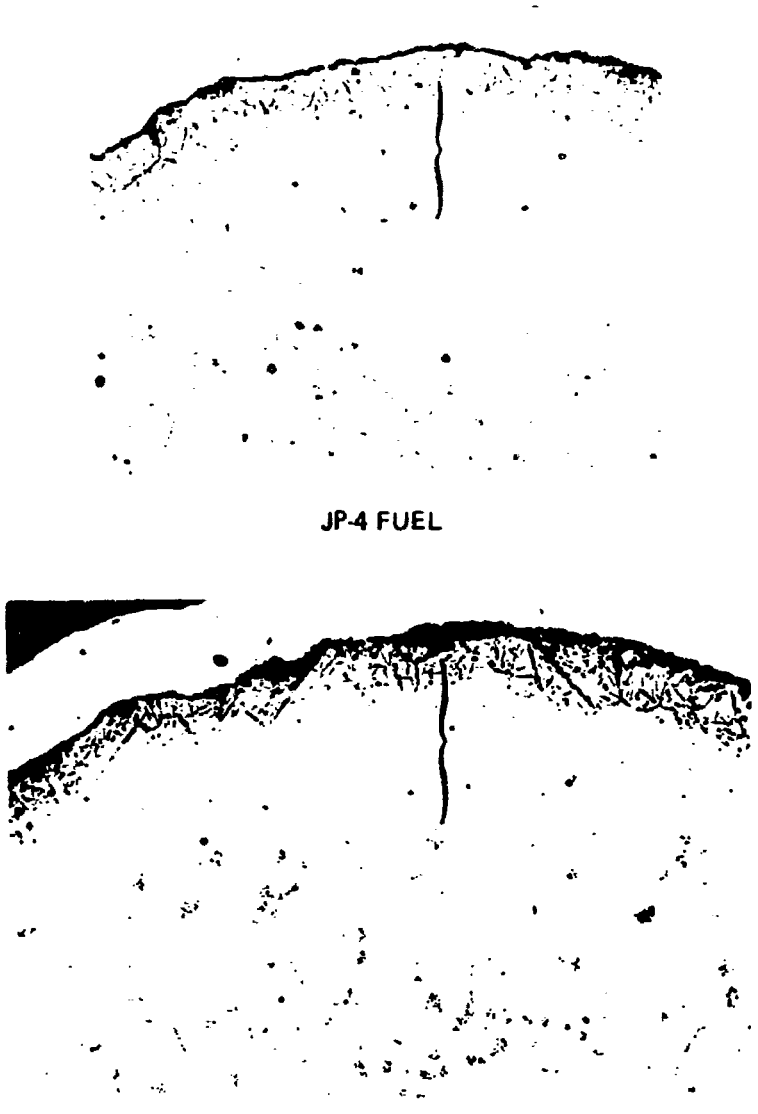

Figure 98. Microstructure of Uncoated U-500 Vane Leading Edge Specimens After 75 Hours of Rig Testing at 2000°F With JP-4 and Emulsified Fuel A. (Bracket Shows Denuded Area. Mag. 100X.)

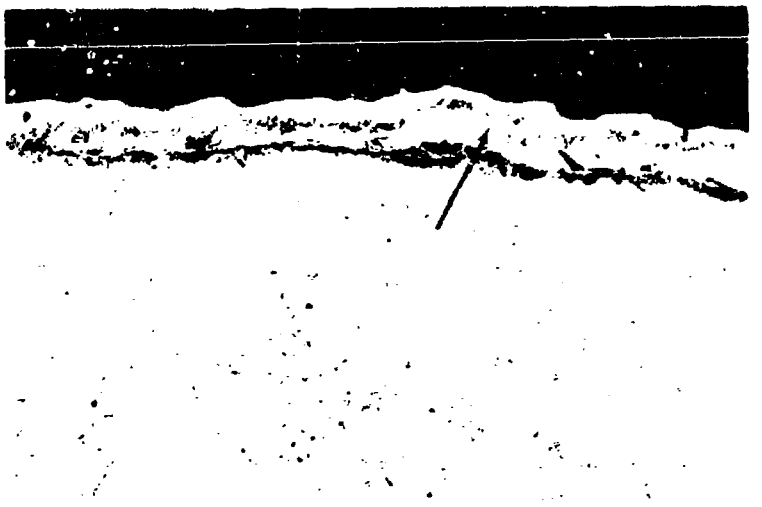

FUEL B

FUEL C

Figure 99. Microstructure of Uncoated U-500 Vane Leading Edge Specimens After 75 Hours of Rig Testing at 2000°F With Emulsified Fuels B and C. (Arrow Shows Nickel Plating. Mag. 100X)

JP-4 FUEL

FUEL A

Figure 100. Microstructure of Uncoated Inco 713 Vane Leading Edge Specimens After 75 Hours of Rig Testing at 2000°F with JP-4 and Emulsified Fuel A. (Mag. 100X.)

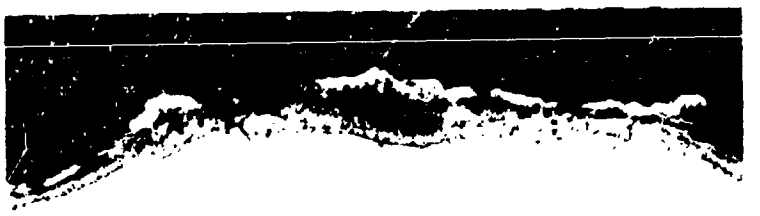

FUEL B

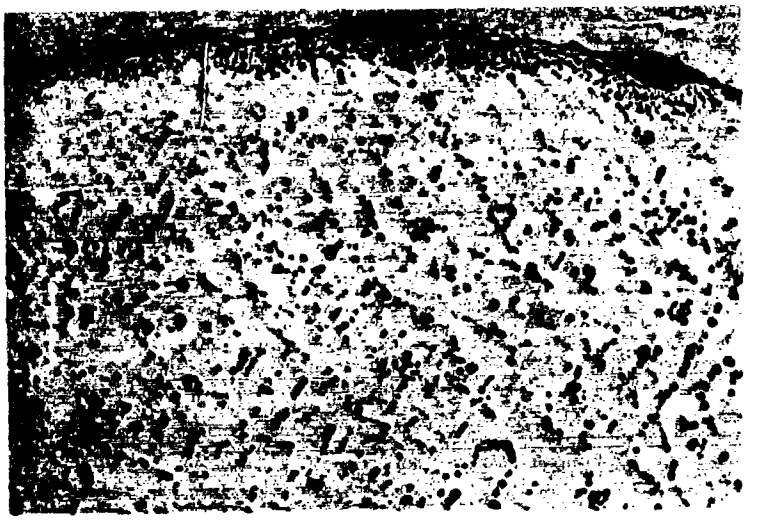

FUEL C

Figure 101. Microstructure of Uncoated Inco 713 Vane Leading Edge Specimens After 75 Hours of Rig Testing at 2000°F With Emulsified Fuels B and C. (Mag. 100X.)

JP-4 FUEL

FUEL A

Figure 102. Microstructure of Uncoated Wrought U-700 Vane Leading Edge Specimens After 75 Hours of Rig Testing at 2000°F With JP-4 and Emulsified Fuel A. (Bracket Shows Denuded Zone. Mag. 100X.)

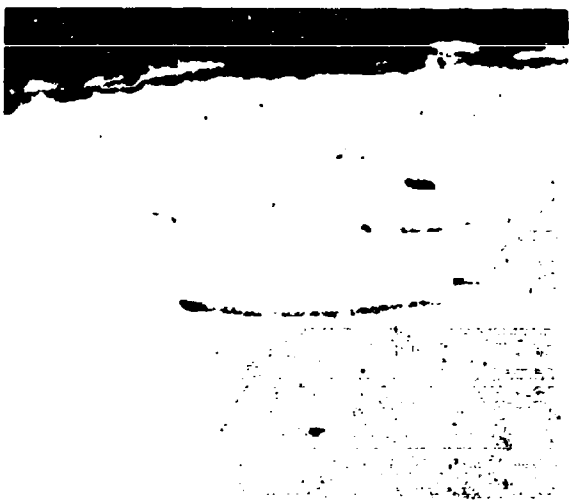

FUEL B

FUEL C

Figure 103. Microstructure of Uncoated Wrought U-700 Vane Leading Edge Specimens After 75 Hours of Rig Testing at 2000°F with Emulsified Fuels B and C. (Arrows Show Intergranular Attack. Mag. 100X.)

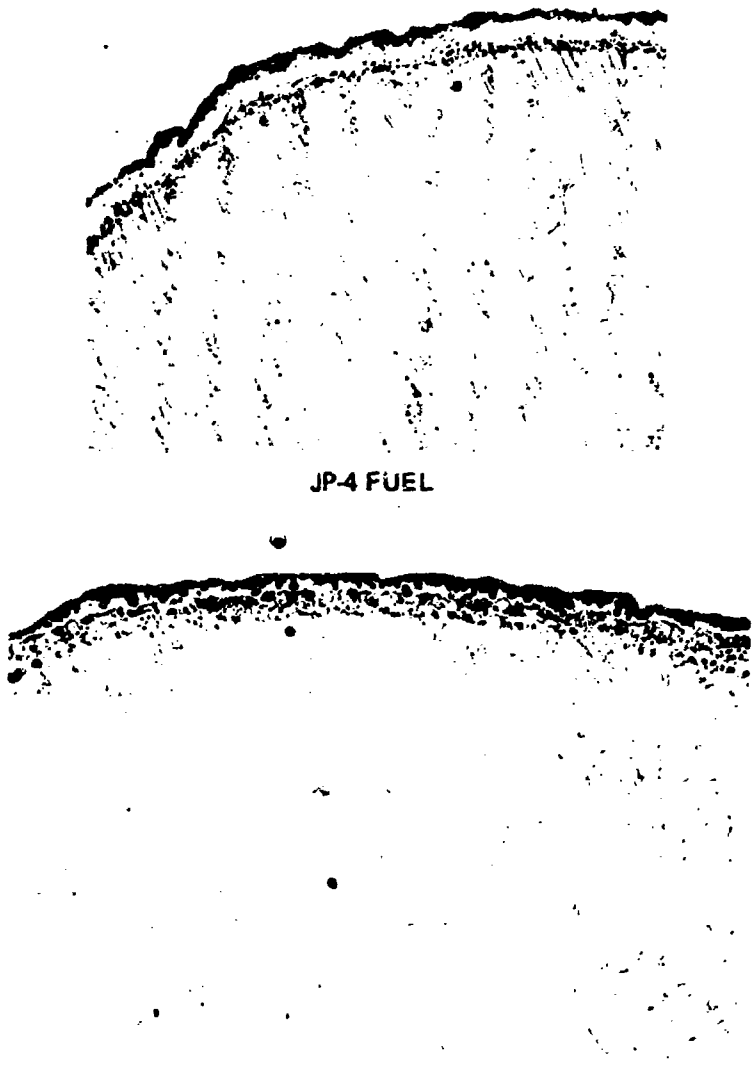

Figure 104. Microstructure of Coated W.I. 52 Vane Leading Edge Specimens After 75 Hours of Rig Testing at 2000°F With JP-4 and Emulsified Fuel A. (Mag. 100X.)

FUEL B

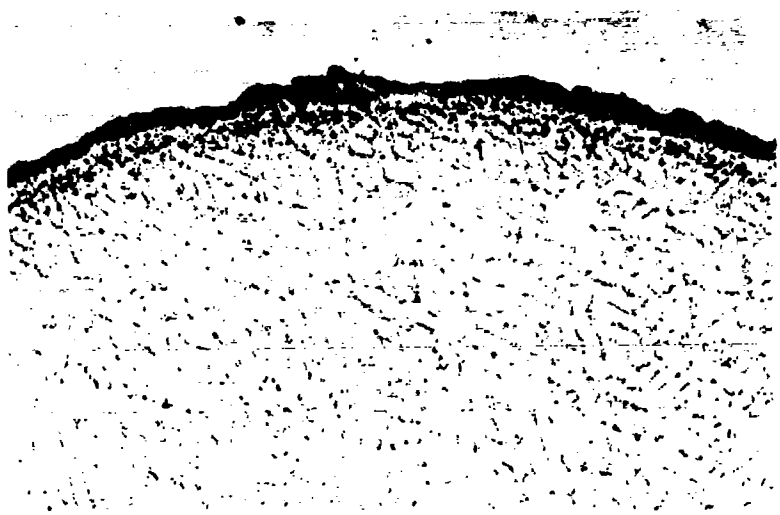

FUEL C

Figure 105. Microstructure of Coated W.I. 52 Vane Leading Edge Specimens After 75 Hours of Rig Testing at 2000°F with Emulsified Fuels B and C. (Arrow Shows Nickel Plate Coating Applied Before Sectioning, Mag. 100X.)

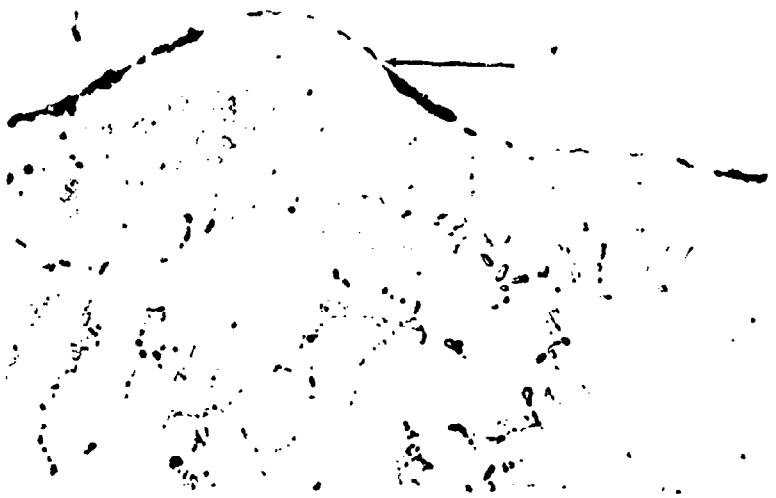

JP-4 FUEL

FUEL A

Figure 106. Microstructure of Coated Inco 713 Vane Leading Edge Specimens After 75 Hours of Rig Testing at 2000°F with JP-4 and Emulsified Fuel A. (Arrow Shows Redeposit of Melted Coating. Mag. 100X.)

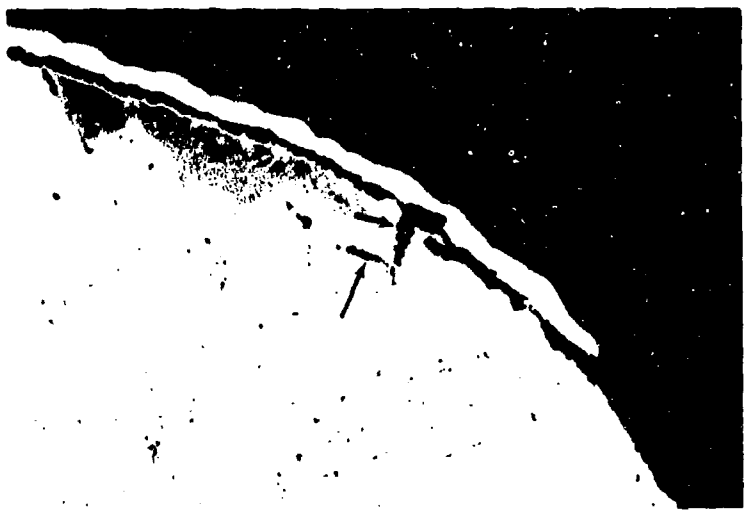

FUEL B

FUEL C

Figure 107. Microstructure of Coated Inco 713 Vane Leading Edge Specimens After 75 Hours of Rig Testing at 2000°F With Emulsified Fuels B and C. (Arrows Show Intergranular Attack, Mag. 100X.)

JP-4 FUEL

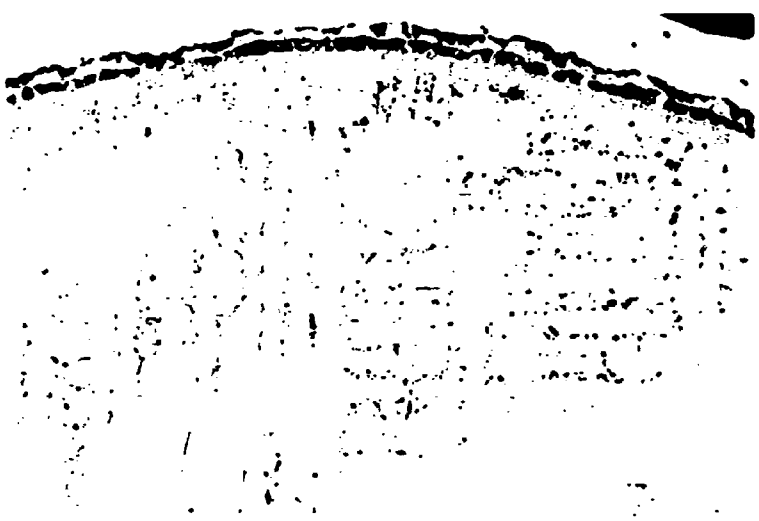

FUEL A

Figure 108. Microstructure of Coated B-1900 Vane Leading Edge Specimens After 75 Hours of Rig Testing at 2000°F With JP-4 and Emulsified Fuel A. (Mag. 100X.)

FUEL B

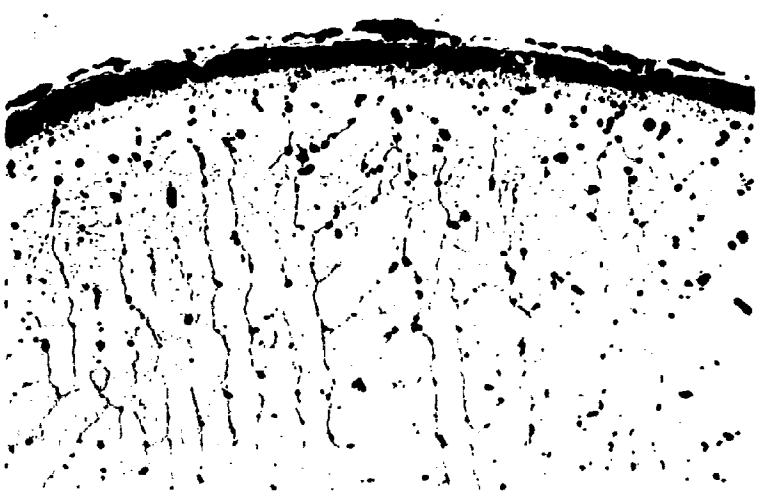

FUEL C

Figure 109. Microstructure of Coated B-1900 Vane Leading Edge Specimens After 75 Hours of Rig Testing at 2000°F with Emulsified Fuels B and C. (Mag. 100X.)

Unclassified

Security Classification

DOCUMENT CONTROL DATA R & D

(Security classification of title, body of abstract and indexing annotation must be entered when the overall report is classified)

1. ORIGINATING ACTIVITY (Corporate author)	2a. REPORT SECURITY CLASSIFICATION
Pratt & Whitney Aircraft Division of United Aircraft Corporation East Hartford, Connecticut	Unclassified 2b. GROUP

3. REPORT TITLE

EMULSIFIED FUELS COMBUSTION STUDY

4. DESCRIPTIVE NOTES (Type of report and inclusive dates)

Final Technical Report (29 June 1967 through 28 September 1968)

5. AUTHOR(S) (First name, middle initial, last name)

Theodore R. Koblish — Robert E. Gordon
Roger A. Roberts — Earle A. Ault
Henry R. Schwartz

6. REPORT DATE	7a. TOTAL NO. OF PAGES	7b. NO. OF REFS
February 1969	138	1

8a. CONTRACT OR GRANT NO.	9a. ORIGINATOR'S REPORT NUMBER(S)
DAAJ02-67-C-0094 b. PROJECT NO. 1F612203A15003 c. d.	USAAVLABS Technical Report 69-4 9b. OTHER REPORT NO(S) (Any other numbers that may be assigned this report) PWA-3515

10. DISTRIBUTION STATEMENT

This document has been approved for public release and sale; its distribution is unlimited.

11. SUPPLEMENTARY NOTES	12. SPONSORING MILITARY ACTIVITY
	U.S. Army Aviation Materiel Laboratories Fort Eustis, Virginia

13. ABSTRACT

This report describes a research program conducted to determine the cold flow, combustion, and corrosion characteristics of three different Government selected and supplied emulsified JP-4 fuels and to compare them to liquid JP-4 fuel. The program consisted of a study of the emulsified fuel flow and spray characteristics, an evaluation of the combustion and altitude relight capabilities of emulsified fuels relative to JP-4 fuel using a can-type burner rig that simulates a gas turbine environment, and an evaluation of the corrosion characteristics of the emulsified fuels relative to liquid JP-4 on several coated and uncoated turbine materials when operating at 1700°F and 2000°F average combustor exit temperatures for 75 hours each. The cold flow test results show that, except for individual deviations due to formulation differences, the flow behavior of two out of the three emulsified fuels through a typical gas turbine fuel system is nearly identical to the flow of liquid JP-4 fuel. The spray characteristics of these emulsified fuels flowing through a pressure atomizing fuel nozzle were found to be essentially identical to liquid JP-4. The results indicated that only minor differences in combustor performance exist between JP-4 and emulsified fuel under the steady-state conditions tested. The same was found to be true for light-off transient and altitude relight conditions. The steady-state corrosion tests have shown some minor distress in the turbine materials caused by two of the emulsified fuels, whereas major distress was associated with the third emulsified fuel. Based on the test results, it was concluded that emulsified JP-4 fuel could be effectively utilized in a conventional gas turbine combustion system as long as the spray characteristics are not compromised relative to JP-4 fuel, and the tendency for emulsified fuels to plug the nozzle screen is eliminated. Of the three emulsified formulations tested, it is concluded that emulsified fuel A shows superior overall performance relative to the other emulsified fuels.

DD FORM 1 NOV 68 1473 REPLACES DD FORM 1473, 1 JAN 64, WHICH IS OBSOLETE FOR ARMY USE.

Unclassified

Security Classification

14 KEY WORDS	LINK A		LINK B		LINK C	
	ROLE	WT	ROLE	WT	ROLE	WT
Cold Flow Characteristics Combustion Combustion Characteristics Corrosion Characteristics Emulsified Fuel Gas Turbine Fuels Low Volatility Aviation Fuels Turbine Materials						